US Army Corps of Engineers

(12)

TECHNICAL REPORT SL-85-5

EFFECTS OF REINFORCEMENT CONFIGURATION ON RESERVE CAPACITY OF CONCRETE SLABS

by

S. C. Woodson, S. B. Garner

Structures Laboratory

DEPARTMENT OF THE ARMY
Waterways Experiment Station, Corps of Engineers
PO Box 631, Vicksburg, Mississippi 39180-0631

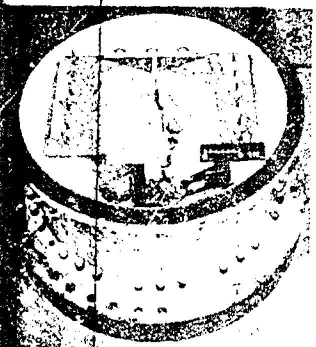

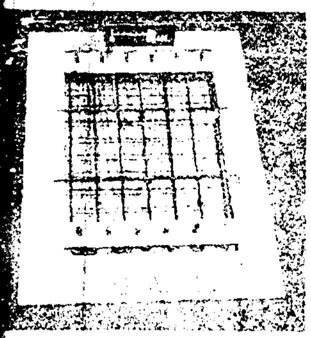

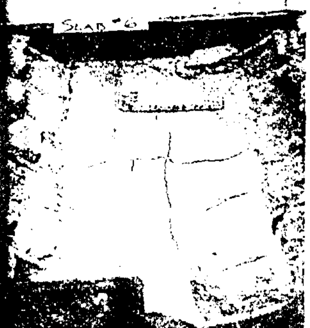

AD-A162 155

US ARMY ENGINEER WATERWAYS EXPERIMENT STATION

August 1985

Final Report

Approved For Public Release; Distribution Unlimited

DTIC ELECTE
DEC 9 1985
B

DTIC FILE COPY

STRUCTURES LABORATORY

Prepared for

Federal Emergency Management Agency
Washington, DC 20472

85 12 -9 072

Destroy this report when no longer needed. Do not return it to the originator.

The findings in this report are not to be construed as an official Department of the Army position unless so designated by other authorized documents.

The contents of this report are not to be used for advertising, publication, or promotional purposes. Citation of trade names does not constitute an official endorsement or approval of the use of such commercial products.

TECHNICAL REPORT SL-85-5

EFFECTS OF REINFORCEMENT CONFIGURATION ON RESERVE CAPACITY OF CONCRETE SLABS

by

S. C. Woodson, S. B. Garner

Structures Laboratory

DEPARTMENT OF THE ARMY
Waterways Experiment Station, Corps of Engineers
PO Box 631, Vicksburg, Mississippi 39180-0631

August 1985

Final Report

Approved For Public Release; Distribution Unlimited

This report has been reviewed in the Federal Emergency Management Agency and approved for publication. Approval does not signify that the contents necessarily reflect the views and policies of the Federal Emergency Management Agency.

Prepared for

Federal Emergency Management Agency
Washington, DC 20472

Unclassified

SECURITY CLASSIFICATION OF THIS PAGE (When Data Entered)

REPORT DOCUMENTATION PAGE

READ INSTRUCTIONS BEFORE COMPLETING FORM

1. REPORT NUMBER
Technical Report SL-85-5

2. GOVT ACCESSION NO.
AD-A1[illegible]155

3. RECIPIENT'S CATALOG NUMBER

4. TITLE (and Subtitle)
EFFECTS OF REINFORCEMENT CONFIGURATION ON RESERVE CAPACITY OF CONCRETE SLABS

5. TYPE OF REPORT & PERIOD COVERED
Final report

6. PERFORMING ORG. REPORT NUMBER

7. AUTHOR(s)
S. C. Woodson
S. B. Garner

8. CONTRACT OR GRANT NUMBER(s)

9. PERFORMING ORGANIZATION NAME AND ADDRESS
US Army Engineer Waterways Experiment Station
Structures Laboratory
PO Box 631, Vicksburg, Mississippi 39180-0631

10. PROGRAM ELEMENT, PROJECT, TASK AREA & WORK UNIT NUMBERS

11. CONTROLLING OFFICE NAME AND ADDRESS
Federal Emergency Management Agency
Washington, DC 20472

12. REPORT DATE
August 1985

13. NUMBER OF PAGES
116

14. MONITORING AGENCY NAME & ADDRESS (if different from Controlling Office)

15. SECURITY CLASS. (of this report)
Unclassified

15a. DECLASSIFICATION/DOWNGRADING SCHEDULE

16. DISTRIBUTION STATEMENT (of this Report)
Approved for public release; distribution unlimited.

17. DISTRIBUTION STATEMENT (of the abstract entered in Block 20, if different from Report)

18. SUPPLEMENTARY NOTES
Available from National Technical Information Service, 5285 Port Royal Road, Springfield, Virginia 22161.
S. back

19. KEY WORDS (Continue on reverse side if necessary and identify by block number)

Beam-column action,	Compressive membrane,	Slabs,
Blast shelters,	Reinforced concrete,	Tensile membrane.
Buried shelters,	Shelters,	
Civil defense,	Slab capacity,	

20. ABSTRACT (Continue on reverse side if necessary and identify by block number)

Fifteen one-way reinforced concrete slabs were statically tested under uniform surface pressure either to failure, or to deflections that exceeded 17 to 24 percent of slab clear span. The main objective was to determine principal reinforcement configurations that would enhance tensile membrane behavior at large deflections. Each slab had a clear span of 24 inches and was 2-5/16 inches thick. Grade-60 reinforcement and 4,000-psi concrete were used. The total amount of principal reinforcement was about the same in every test,

(Continued)

DD FORM 1 JAN 73 1473 EDITION OF 1 NOV 65 IS OBSOLETE

Unclassified

SECURITY CLASSIFICATION OF THIS PAGE (When Data Entered)

20. ABSTRACT (Continued).

but the percentages of reinforcement in tension and compression zones were varied. The slabs were supported in a reaction structure and restrained at the supports.

A modified three-hinged mechanism was formed, and rupture of reinforcement prohibited the development of pure tensile membrane behavior in most of the slabs. Posttest analysis applying tensile membrane theory agreed with the experimental tensile membrane slope, when the area of ruptured reinforcement was deleted. Based on these test results, principal reinforcement details were recommended for a blast shelter roof slab design. Keywords

PREFACE

The research reported herein was sponsored by the Federal Emergency Management Agency (FEMA) through the US Army Engineer Huntsville Division (HND).

Construction and testing were conducted by personnel of the Structures Laboratory (SL), US Army Engineer Waterways Experiment Station (WES), under the general supervision of Mr. Bryant Mather, Chief, SL and Mr. J. T. Ballard, Assistant Chief, SL. Chief of the Structural Mechanics Division (SMD) during this investigation was Dr. J. P. Balsara. The project was managed by Dr. S. A. Kiger, and Mr. S. C. Woodson supervised the experiments. This report was prepared by Mr. Woodson and Ms. S. B. Garner.

COL Tilford C. Creel, CE, and COL Robert C. Lee, CE, were Commanders and Directors of WES during the conduct of the study. COL Allen F. Grum, USA, was Director of WES during the preparation and publication of this report. Mr Fred R. Brown and Dr. Robert W. Whalin were Technical Directors.

Accession For
NTIS
DTIC
By
Distribution/
Availability Codes
Avail and/or
Dist Special
A-1

CONTENTS

LIST OF ILLUSTRATIONS

LIST OF TABLES

CONVERSION FACTORS, NON-SI TO SI (METRIC) UNITS OF MEASUREMENT

Non-SI units of measurement used in this report can be converted to SI (metric) units as follows:

Multiply	By	To Obtain
degrees (angle)	0.01745	radians
feet	0.3048	metres
pounds force · feet	1.355818	newton metres
inches	25.4	millimetres
kips per square inch	6.894757	megapascals
megatons (nuclear equivalent of TNT)	4,184	terajoules
microinches per inch	1.0	millionths
pounds (force) per square inch	0.00689475	megapascals

EFFECTS OF REINFORCEMENT CONFIGURATION ON RESERVE CAPACITY OF CONCRETE SLABS

CHAPTER 1

INTRODUCTION

1.1 BACKGROUND

At the initiation of this study civil defense planning called for the evacuation of nonessential personnel to safe (lower-risk) host areas during a time of crisis, requiring the construction of shelters to protect the key-workers remaining in the high-risk areas. Both expedient (20-person capacity) and deliberate (100- to 400-person capacity) shelters are planned. The shelters will be designed to resist blast, radiation, and associated weapon effects at the 50-psi[1] peak overpressure level for a 1-MT nuclear weapon. The Federal Emergency Management Agency (FEMA) tasked the US Army Engineer Huntsville Division (HND) to design the shelters. The research reported herein is in support of the HND design effort.

With the anticipated construction of many shelters, economic design factors as well as load-response requirements assume added significance. A preliminary structural design for the deliberate shelters was developed by HND based on computational procedures developed by Kiger, Slawson, and Hyde (Reference 1) in the Shallow Buried Structures Research Program at the US Army Engineer Waterways Experiment Station (WES). Using a roof slab thickness of 10 inches, a span of 11.33 feet, and limiting the midspan deflection to 7 inches, the principal tension ratio (ρ) and compression steel ratio (ρ') were determined to be approximately 0.007 using the procedures in Reference 1. Six static tests and twelve dynamic tests were performed on approximately 1/4-scale structural models of sections of the keyworker blast shelter and reported by Slawson and others (Reference 2). As discussed in Reference 2, the roof slab was determined to be capable of resisting a 1-MT weapon at 150 psi with only light damage. However, no increase in roof slab resistance was observed with deflections greater than about the roof thickness.

---

[1]A table of factors for converting non-SI units of measurement used in this report to SI (metric) units is presented on page 5.

Slabs having an increase in load resistance at large deflections have a significant reserve capacity and fail by excessive deflection rather than sudden collapse. Park and Gamble (Reference 3) discuss the resistance increase known as tensile membrane behavior. After ultimate load resistance has been reached in a reinforced concrete slab, the supported load decreases rapidly with further deflections. Eventually, membrane forces in the central region of the slab change from compression to tension and the slab boundary restraints begin resisting inward movement. Cracks in the central region penetrate the whole thickness of the concrete and yielding of the steel spreads throughout the region. The reinforcement may begin acting as a tensile membrane with load-carrying capacity increasing with further deflection until the reinforcement fractures. Park and Gamble believe that knowledge of the tensile membrane region is important because as soon as the ultimate load of the slab is reached in the case of gravity loading (which remains unchanged as the slab deflects), the load will drop suddenly through the slab unless the tensile membrane strength is great enough to "catch" the load.

Tests by Park (Reference 4) indicated that pure tensile membrane action did not occur in lightly reinforced two-way slabs, since the cracking present at the end of the tests was little more than the cracking which developed with the yield-line pattern at the ultimate flexural load. Therefore, the load was carried by combined bending and tensile membrane action. Heavily reinforced slabs cracked over much of their area and therefore approached pure tensile membrane action.

Keenan and others (Reference 5) state that for support rotations greater than 2 degrees, the design of reinforced concrete members without lacing reinforcement depends on their capacity to act as a tensile membrane. If lateral restraint does not exist at the supports, tensile membrane action does not develop and the member reaches incipient collapse at between 2 and 4 degrees rotation at the supports. However, if lateral restraint exists, deflection of the member induces membrane action and the in-plane forces provide the means for the member to continue resisting substantial load to maximum rotation exceeding 12 degrees at supports.

Woodson (Reference 6) investigated the effects of shear stirrup details on the ultimate capacity and tensile membrane behavior of uniformly loaded one-way reinforced concrete slabs. It was found that under-reinforced slabs ($\rho < \rho_b$) with a large number of closely spaced (spacing $\leq d/2$) single-leg stirrups exhibit increasing load resistance at large deflections. Large midspan deflections were defined to be those greater than the effective depth of the tensile reinforcement. Rotations between 13 and 21 degrees were experienced at the supports. The principal steel details in the slabs were similar to those of the keyworker blast shelter models tested by Slawson and others (Reference 2). The use of a large number of closely spaced stirrups to achieve increased resistance at large deflections significantly increases the cost of prototype construction.

The tests conducted by Woodson indicated that the load-response behavior of the slabs in the tensile membrane region is enhanced when the transverse or temperature steel is placed outside the principal reinforcement. Recommendations included the development of other construction details (including modification of principal reinforcement patterns) to provide a secondary resistance.

1.2 OBJECTIVES

The main objective of this investigation was to determine principal reinforcement configurations which would provide maximum reserve capacity for a given total area of steel and depth of tensile reinforcement in the FEMA keyworker shelter roof slab. A secondary objective was to evaluate the effect of these reinforcement details on the ultimate load capacity and secondary response of the slabs. Additional objectives included evaluating the effects of stirrup spacing and exterior temperature steel placement on the response of the predicted "best" design.

Another objective was to relate the behavior of the clamped, surface-flush slabs of this series to that of a buried reinforced concrete box structure tested by Getchell and Kiger (Reference 7). The roof of the buried box structure was a one-way slab. The correlation was intended to provide insight into the behavior of the slabs in this series when buried and supported at reinforced concrete roof-wall connections.

1.3 SCOPE

The approach taken for this study was to modify the principal reinforcement designs used in the investigation reported in References 2 and 6. In general, the modifications consisted of varying the areas of tension and compression steel, while keeping the total area of principal reinforcement constant.

Variations of the reinforcement included:

1. Placing equal areas of top face and bottom face reinforcement, as described in References 2 and 3.

2. Placing 25 percent of the reinforcement as top steel and 75 percent as bottom steel.

3. Bending all principal reinforcement such that only initial tension zones were reinforced and compression zones were not.

4. Bending 50 percent of the principal reinforcement into the tension zones and dividing the remaining 50 percent equally among the top and bottom faces.

5. Cutting 50 percent of the principal reinforcement and placing it in the tension zones while dividing the remaining 50 percent equally among the top and bottom faces.

6. Placing stirrups at spacings of approximately 0.4 and 1.7 times the tensile reinforcement effective depth in combination with variation No. 4 above.

7. Placing the temperature reinforcement exterior to the principal reinforcement in combination with variation No. 6 above.

Four of the fifteen slabs tested included variations which altered the total amount of reinforcement. Slabs 4 and 5 were constructed with dowels extending from the supports to simulate the extension of wall reinforcement into the slab in the prototype keyworker blast shelter. Slab 15 was constructed with the removal of one-half of the bent steel used in variation No. 4, thereby reducing the total area of principal reinforcement. Slab 14 modeled the roof slab of the reinforced concrete box discussed in Reference 7.

CHAPTER 2

EXPERIMENTS

2.1 GENERAL DESCRIPTION

Fifteen one-way slabs with clear spans of 24 inches and span-to-effective-depth ratios (L/d) from 10.0 to 13.2 were built and statically tested under uniform water pressure. The slabs were restrained against rotation and longitudinal expansion. Plan details for the slabs are shown in Figure 2.1.

2.2 CONSTRUCTION DETAILS

All slabs were 24 inches wide by 36 inches long. Slab 14 represented the roof slab of a previously tested shallow-buried structure (Reference 7) and was 2.9 inches thick. All other slabs were 2-5/16 inches thick. The slabs were reinforced with deformed wire and small-diameter rebar. Area of total principal reinforcing for all slabs except 1, 14, and 15 was 1.58 percent of net concrete area. Total temperature reinforcing was approximately 0.37 percent. Effective depth, d, was 1-13/16 inches for all slabs except 1 and 14. Reinforcing details of the slabs, bottom-side-up, are shown in Figures 2.2 through 2.16.

Slab 1 represented the HND design discussed in Reference 2. Slab 2 was a modification of Slab 1 to allow equal concrete covers on compression and tension steel. Principal reinforcing was distributed evenly between top and bottom mats, resulting in $\rho = \rho' = 0.0079$ for Slab 2 and $\rho = \rho' = 0.0074$ for Slab 1. (Effective depth for Slab 1 was 1-15/16 inches.)

Approximately three-fourths of the total principal reinforcing in Slabs 3, 4, and 5 was placed at the bottom face and one-fourth at the top face, resulting in $\rho = 0.0114$ and $\rho' = 0.004$ at midspan and $\rho' = 0.0114$ and $\rho = 0.004$ at the supports. Dowels were added over the supports in Slabs 4 and 5 to simulate the extension of wall reinforcing into the roof. The dowels in Slab 4 modeled the HND design, and the dowels in Slab 5 were extended further to the point of contraflexure (zero moment under uniform loading) of the roof.

Reinforcing in Slab 6 was bent such that all principal reinforcing fell in the tension zone, and $\rho = 0.0158$ at midspan and supports.

Slabs 7 through 12 represented the predicted "best design" for tensile membrane behavior. Pairs of bent and straight bars were alternated as shown in Figure 2.1, with $\rho = 0.0113$ and $\rho' = 0.0045$. Single-leg stirrups were added to Slabs 8 through 12. Stirrup spacing was 3 inches for Slab 8 and 3/4 inch for Slabs 9 through 12. Stirrup details and spacing for Slabs 9 through 12 are shown in Figure 2.17. Slabs 9 through 11 were identically reinforced. Temperature reinforcing was placed outside the principal reinforcing in Slab 12.

Slab 13 was reinforced with alternate pairs of full-length and cut straight bars. The percentage of reinforcing was the same as for Slabs 7 through 12. Slab 13 did not have stirrups.

The effective depth for Slab 14 was 2.4 inches, and principal reinforcement was equally distributed between top and bottom faces with $\rho = \rho' = 0.0102$. Total temperature reinforcement was increased to 1.23 percent of net concrete area, and 1/4-inch-diameter deformed wire stirrups were placed at 1.6 inches center-to-center.

Slab 15 was similar to Slab 7 except that single bent bars were alternated with pairs of straight bars.

A summary of parameters for each slab is included in Table 2.1.

2.3 REACTION STRUCTURE

The reaction structure used in the test series is shown in Figure 2.18. After being placed in the reaction structure, slabs were clamped to prevent rotation and translation with 1/2- by 6- by 24-inch steel plates bolted into place at each end with 1/2-inch-diameter bolts. Clear span between supports was 24 inches.

A removable door was provided in the reaction structure to allow access and placement of a camera for photography during testing.

2.4 LOADING DEVICE

Slabs were tested in the 4-foot-diameter Small Blast Load Generator (SBLG) (Reference 8). The SBLG (Figure 2.19) consists of a series of stacked rings with a 3-foot 10-3/4-inch inside diameter and an elliptical dome top called a "bonnet". The rings are bolted together to allow variations in depth of the test specimen. Static pressures of up to 500 psi can be generated by forcing water into the bonnet to load the test specimen.

2.5 INSTRUMENTATION

Each slab was instrumented for strain, displacement, and pressure measurement. Figure 2.20 shows a typical instrumentation layout.

2.5.1 Deflection Measurements

Two Celesco PT-101 displacement transducers were used in each test, one at one-quarter span (D1) and one at midspan (D2). The transducers had a maximum allowable working range of 10 inches.

2.5.2 Pressure Measurements

One Kulite HKMS-375, 500-psi-range pressure gage was mounted in the bonnet of the test chamber to measure water pressure applied to the slab.

2.5.3 Strain Measurements

An example strain gage layout is shown in Figure 2.21. When possible, principal reinforcement strain gages were placed in pairs, with one gage on a top bar and one on a corresponding bottom bar. Gages were located at midspan, at quarter span, and near supports. Single gages were used at bent or cutoff bars, dowels, and stirrups. Pairs of gages were installed on the top and bottom temperature reinforcement of Slabs 9 and 12.

2.6 TEST PROCEDURES

The reaction structure was placed in the test chamber and surrounded with compacted sand. The slab to be tested was then placed in the reaction structure and covered with 3/32-inch-thick neoprene membrane to prevent loss of pressure through and around the slab. To ensure watertightness, Aqua-seal putty was placed on the rubber membrane at the bolts. The 1/2- by 6- by 24-inch steel plates were then bolted into place. Bolts were torqued to approximately 50 ft-lb. The pressure bonnet was bolted to the top ring flange, sealing the SBLG and securing the edge of the neoprene diaphragm.

Immediately before applying pressure, calibration steps for the instrumentation transducers were recorded. The bonnet was then filled with water from a commercial waterline. When required water pressure exceeded line pressure (approximately 70 psi), a pneumatic water pump was used.

After draining and removing the bonnet, posttest photographs and measurements of the slab were taken. The slab was removed and the reaction structure was prepared for the next specimen.

Table 2.1. Slab details.

Slab No.	Slab Dimensions Width in	Span, L in	h in	d in	d' in	l/h	Concrete Cylinder Strength 28 Day psi	Appropriate Test Day psi	Reinforcing Yield Strength ksi	Reinforcing Ratio Midspan ρ, %	ρ', %	Supports ρ, %	ρ', %	Stirrup Spacing in
1	24	24	2-5/16	1-15/16	5/8	10.4	4,610	4,470	66	0.74	0.74	0.74	0.74	None
2	24	24	2-5/16	1-13/16	1/2	10.4	4,610	4,470	66	0.79	0.79	0.79	0.79	None
3	24	24	2-5/16	1-13/16	1/2	10.4	4,610	4,470	63-63.5	1.14	0.40	0.40	1.14	None
4	24	24	2-5/16	1-13/16	1/2	10.4	4,610	4,490	63-63.5	1.14	0.40	1.19	1.14	None
5	24	24	2-5/16	1-13/16	1/2	10.4	4,610	4,490	63-63.5	1.14	0.40	1.19	1.14	None
6	24	24	2-5/16	1-13/16	1/2	10.4	4,610	4,490	66	1.58	0	1.58	0	None
7	24	24	2-5/16	1-13/16	1/2	10.4	4,610	4,270	66	1.13	0.45	1.13	0.45	None
8	24	24	2-5/16	1-13/16	1/2	10.4	4,610	4,270	66	1.13	0.45	1.13	0.45	3
9	24	24	2-5/16	1-13/16	1/2	10.4	3,430	4,030	66	1.13	0.45	1.13	0.45	3/4
10	24	24	2-5/16	1-13/16	1/2	10.4	3,430	4,030	66	1.13	0.45	1.13	0.45	3/4
11	24	24	2-5/16	1-13/16	1/2	10.4	3,430	4,160	66	1.13	0.45	1.13	0.45	3/4
12	24	24	2-5/16	1-13/16	1/2	10.4	3,430	4,160	66	1.13	0.45	1.13	0.45	3/4
13	24	24	2-5/16	1-13/16	1/2	10.4	3,430	4,160	66	1.13	0.45	1.13	0.45	None
14	24	24	2.9	2.4	1/2	8.3	3,430	3,560	60.3	1.02	1.02	1.02	1.02	1.6
15	24	24	2-5/16	1-13/16	1/2	10.4	3,430	3,560	66	0.79	0.45	0.79	0.45	None

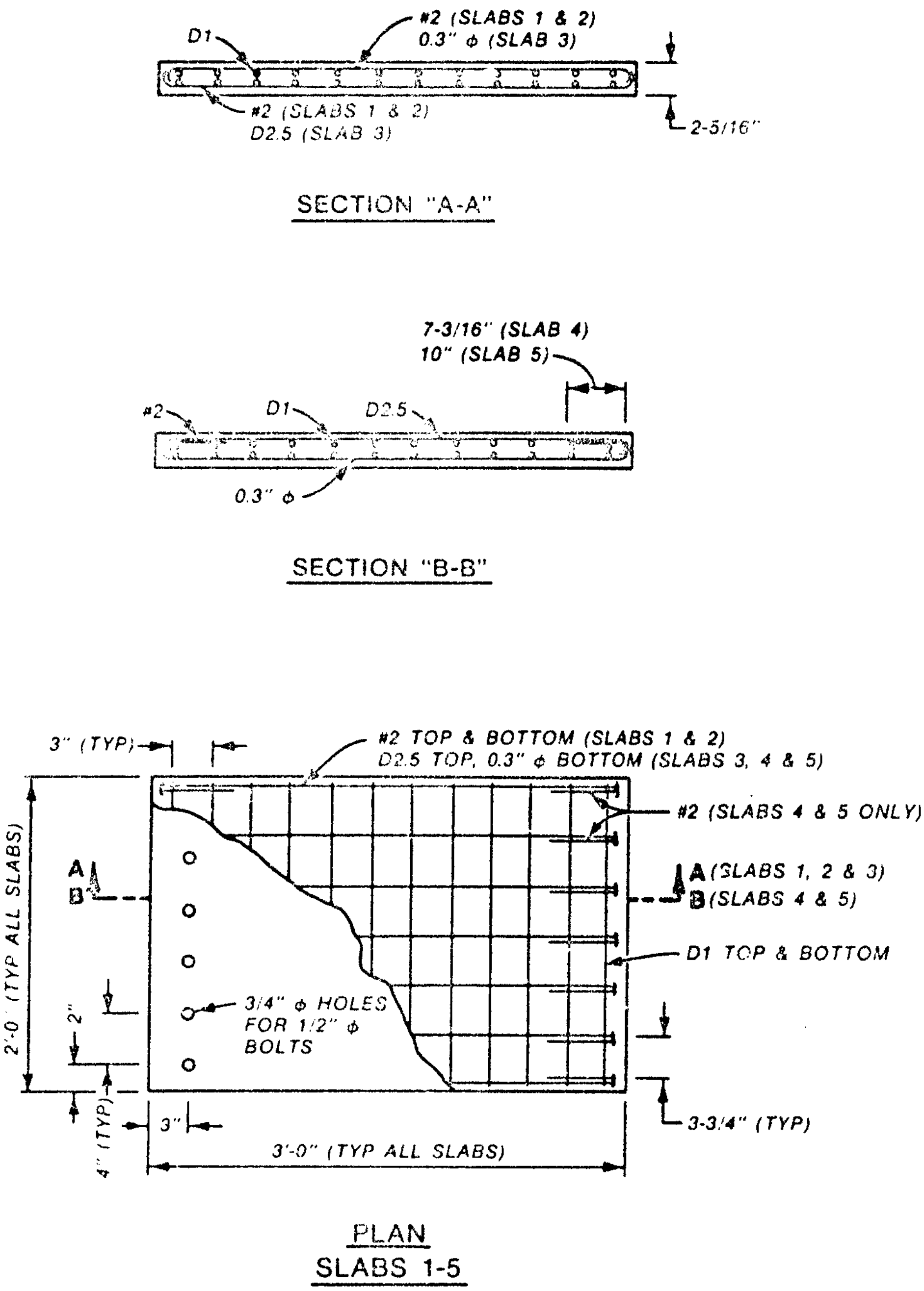

Figure 2.1. Plan details for roof slabs (Sheet 1 of 4).

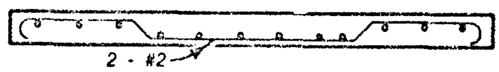

SECTION "C-C"

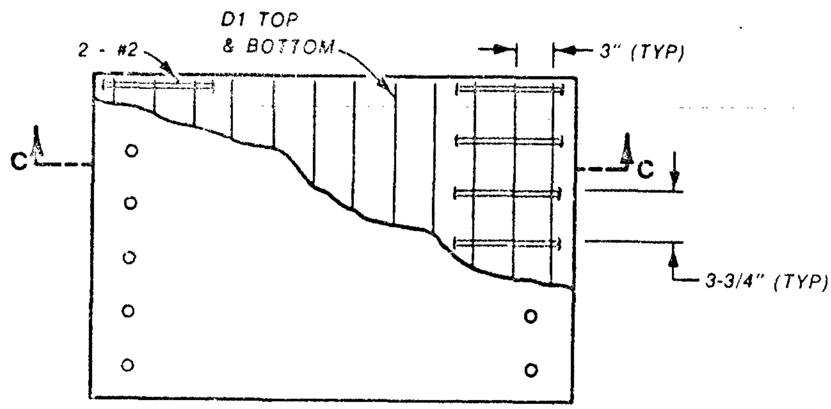

PLAN
SLAB 6

Figure 2.1. (Sheet 2 of 4).

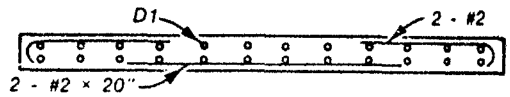

SECTION "F-F"

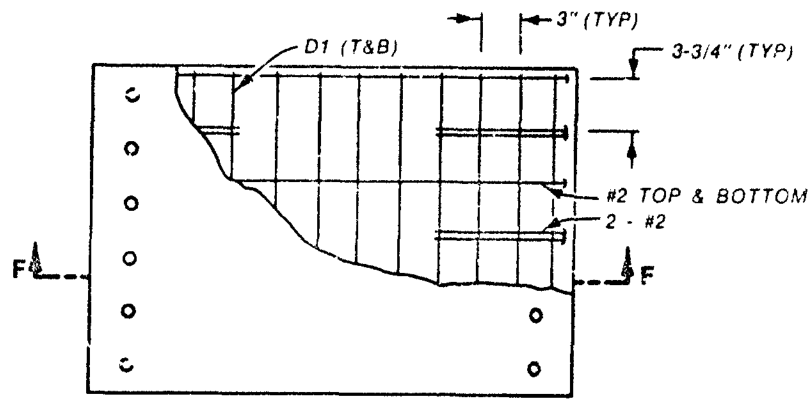

PLAN
SLAB 13

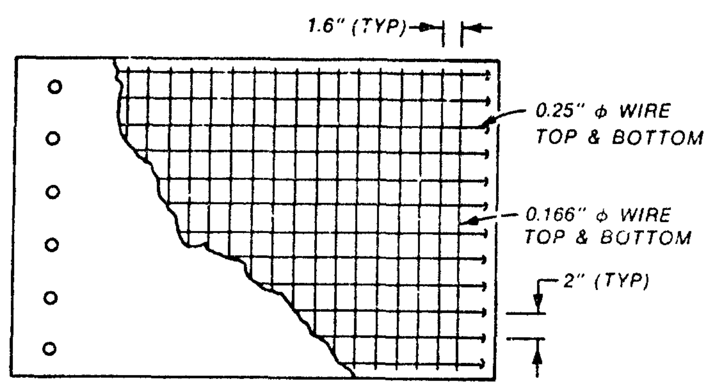

NOTE: STIRRUPS OMITTED FOR CLARITY, SLABS 13 & 14

PLAN
SLAB 14

Figure 2.1. (Sheet 3 of 4).

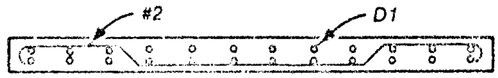

SECTION "D-D"

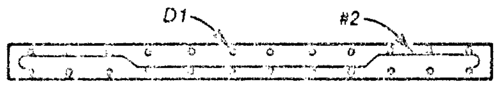

SECTION "E-E"

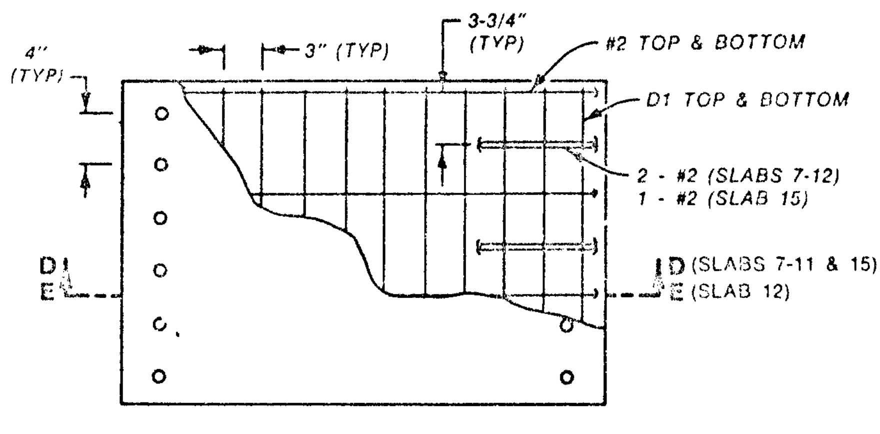

PLAN
SLABS 7-12 & 15

NOTE. STIRRUPS OMITTED FOR CLARITY

Figure 2.1. (Sheet 4 of 4).

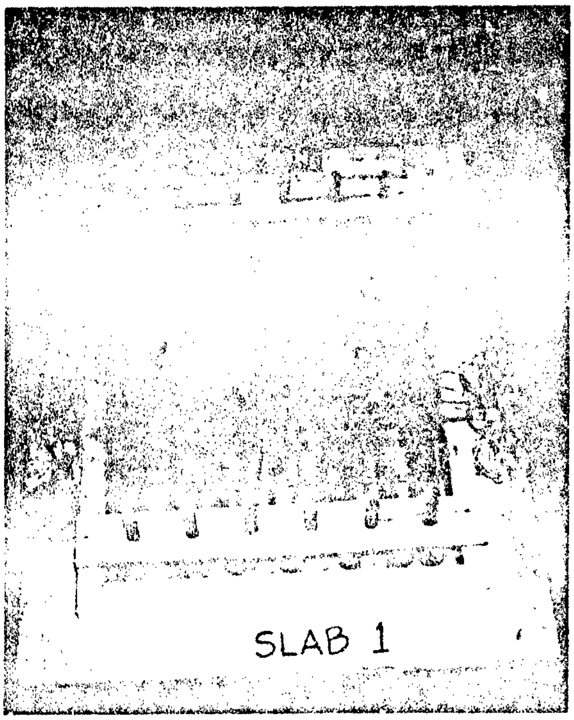

Figure 2.2. Slab 1 construction details.

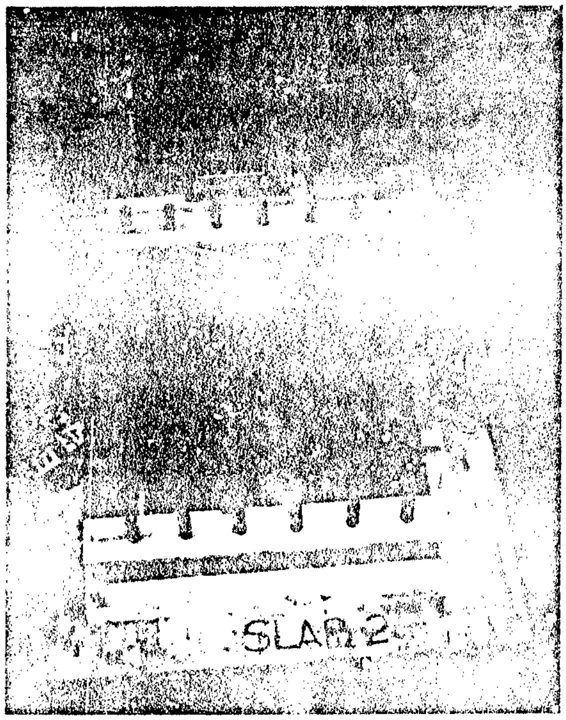

Figure 2.3. Slab 2 construction details.

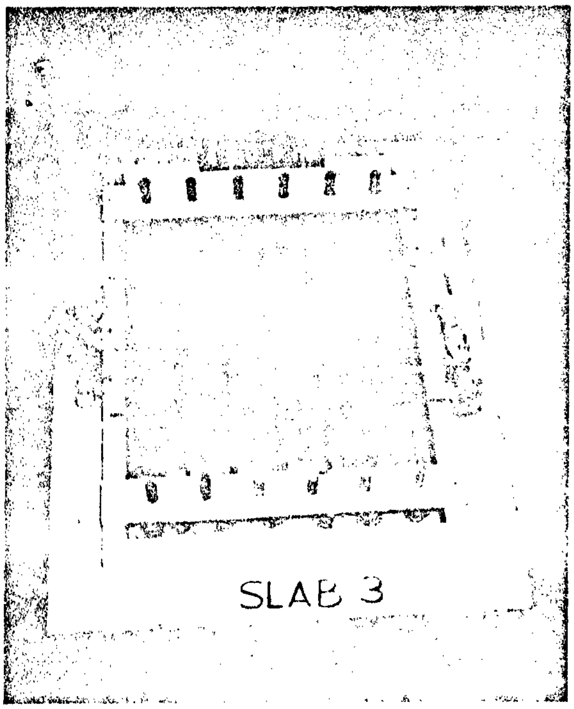

Figure 2.4. Slab 3 construction details.

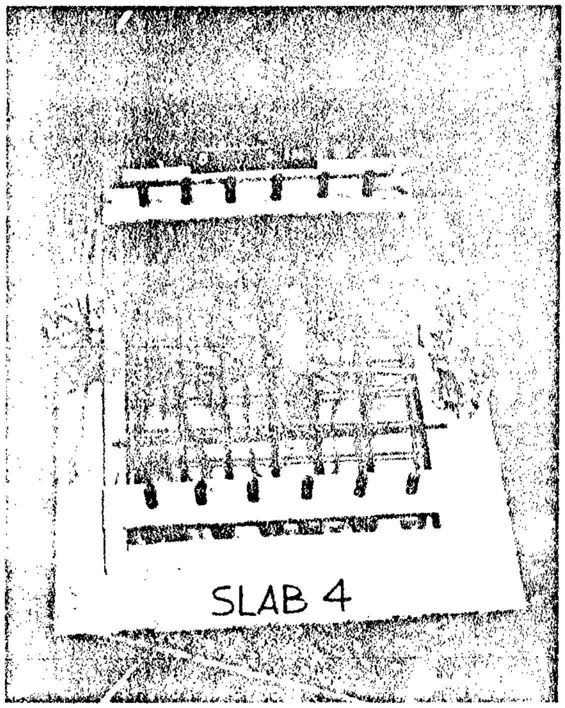

Figure 2.5. Slab 4 construction details.

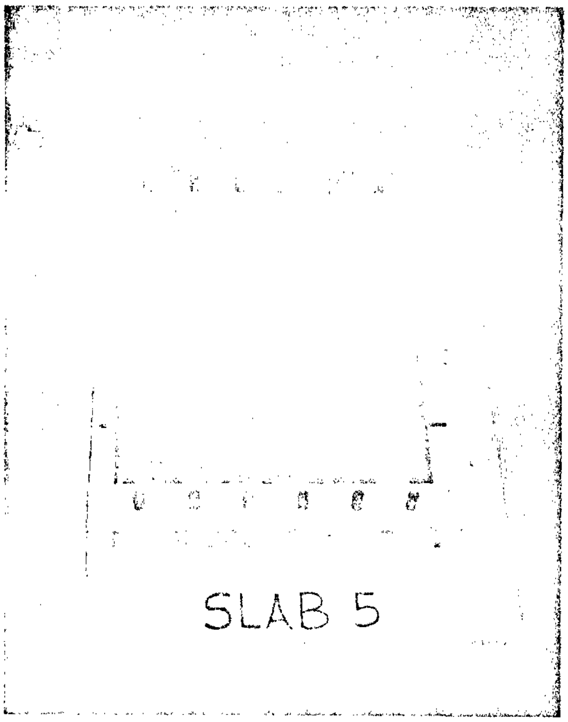

Figure 2.6. Slab 5 construction details.

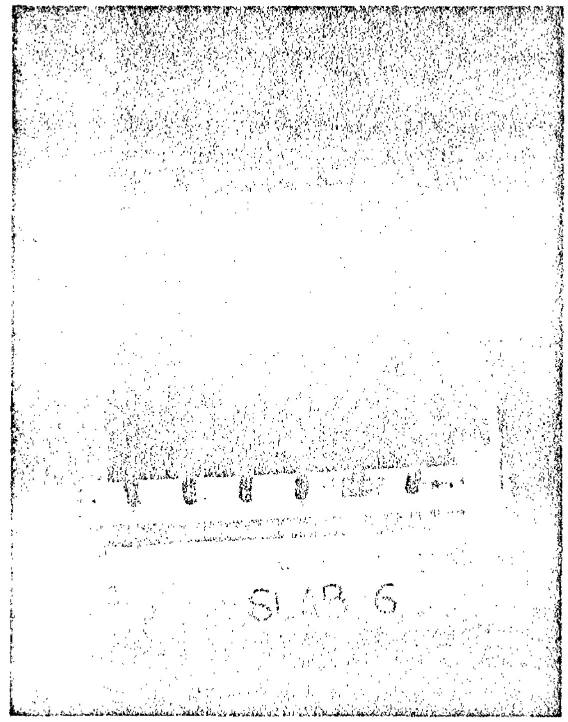

Figure 2.7. Slab 6 construction details.

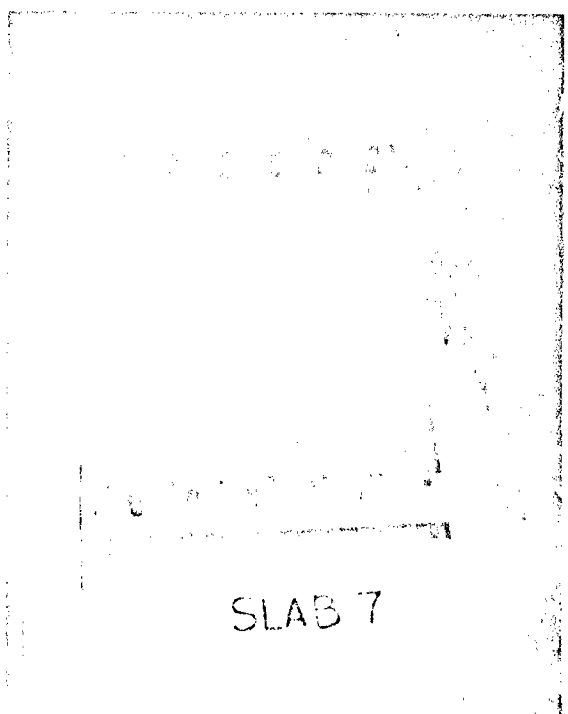

Figure 2.8. Slab 7 construction details.

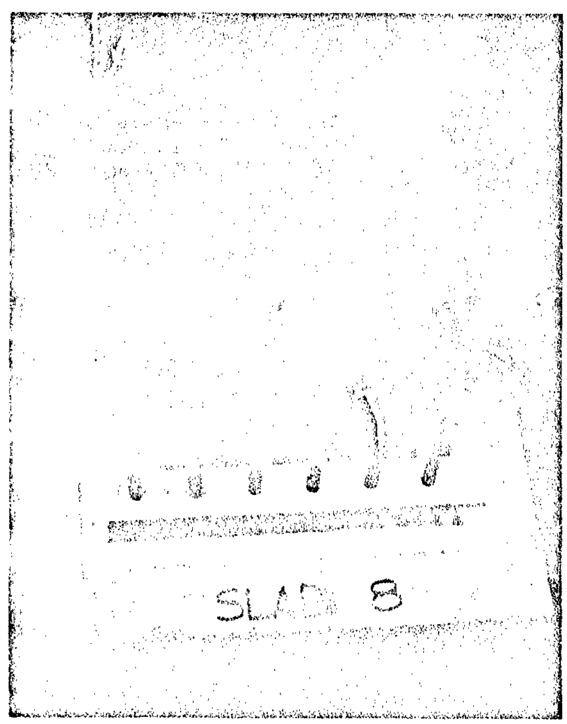

Figure 2.9. Slab 8 construction details.

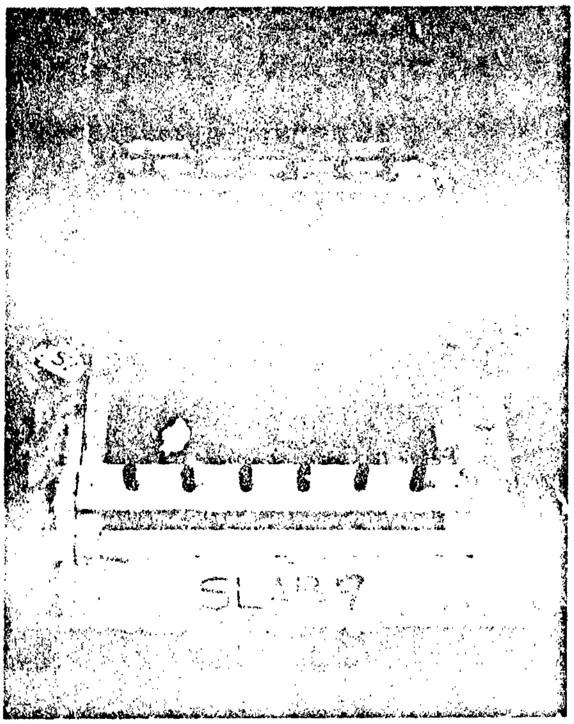

Figure 2.10. Slab 9 construction details.

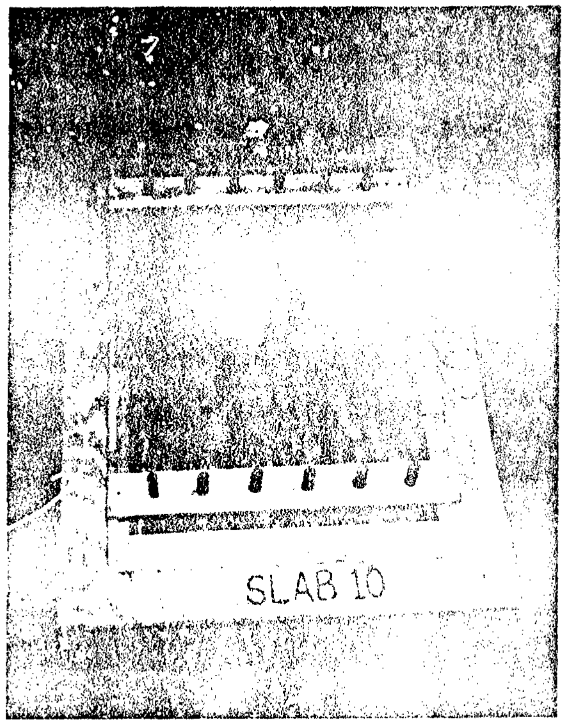

Figure 2.11. Slab 10 construction details.

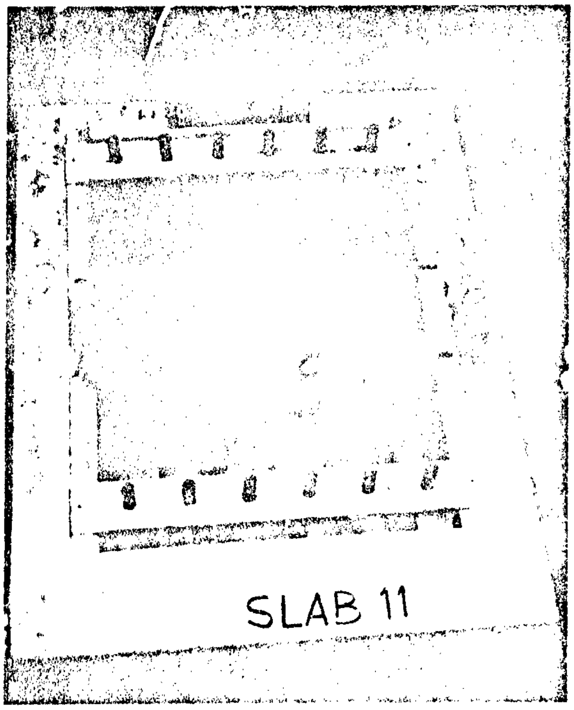

Figure 2.12. Slab 11 construction details.

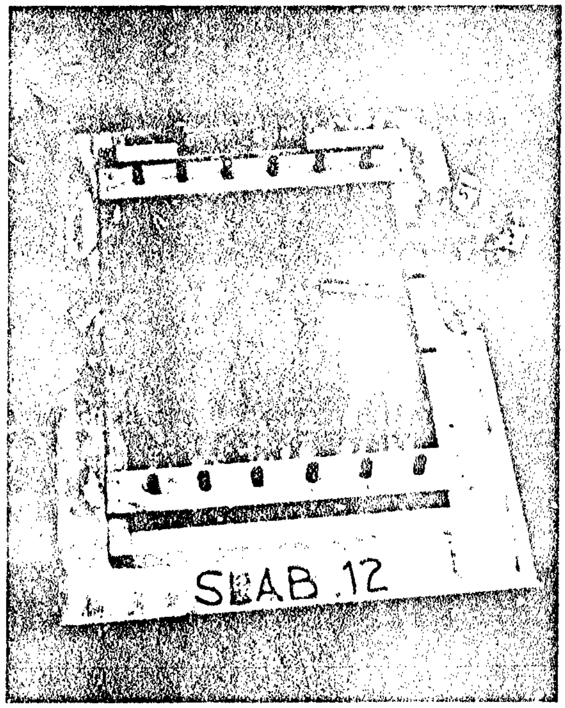

Figure 2.13. Slab 12 construction details.

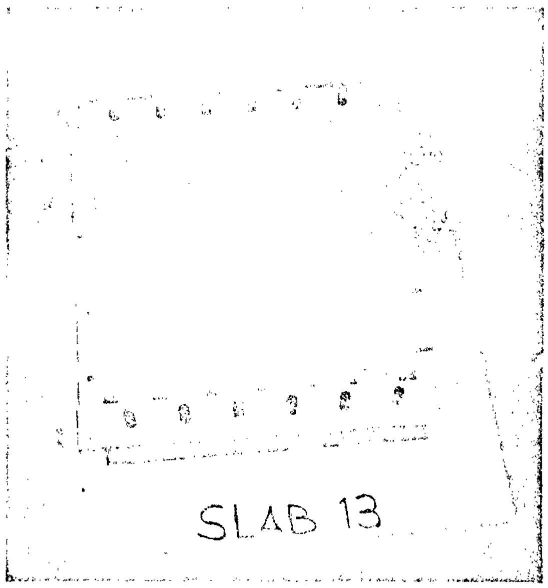

Figure 2.14. Slab 13 construction details.

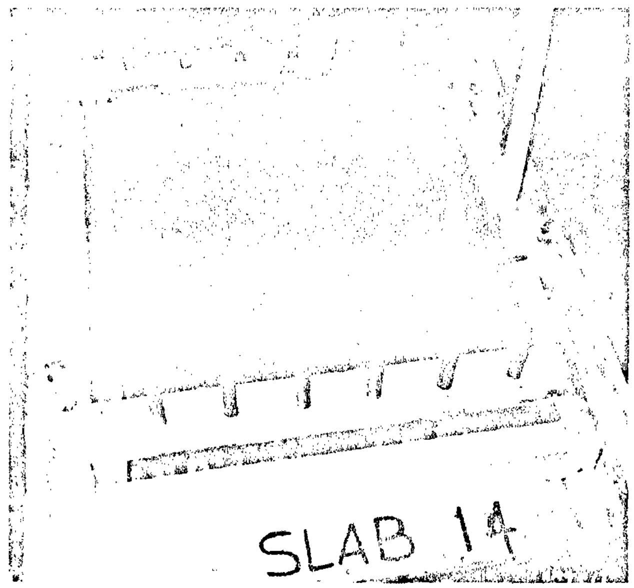

Figure 2.15. Slab 14 construction details.

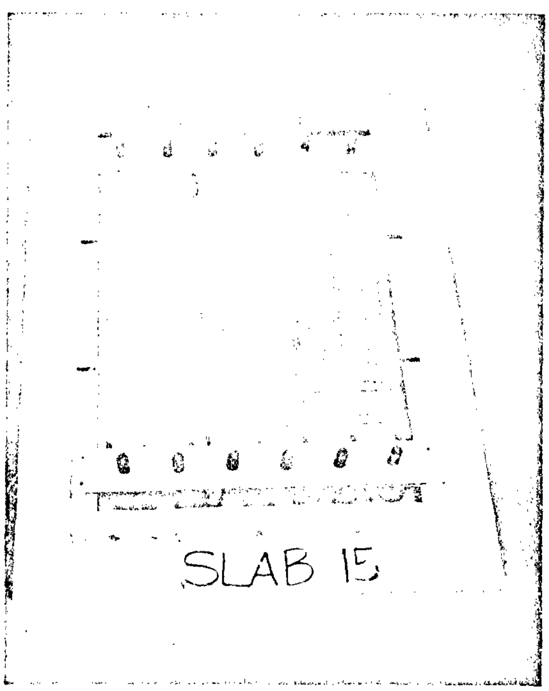

Figure 2.16. Slab 15 construction details.

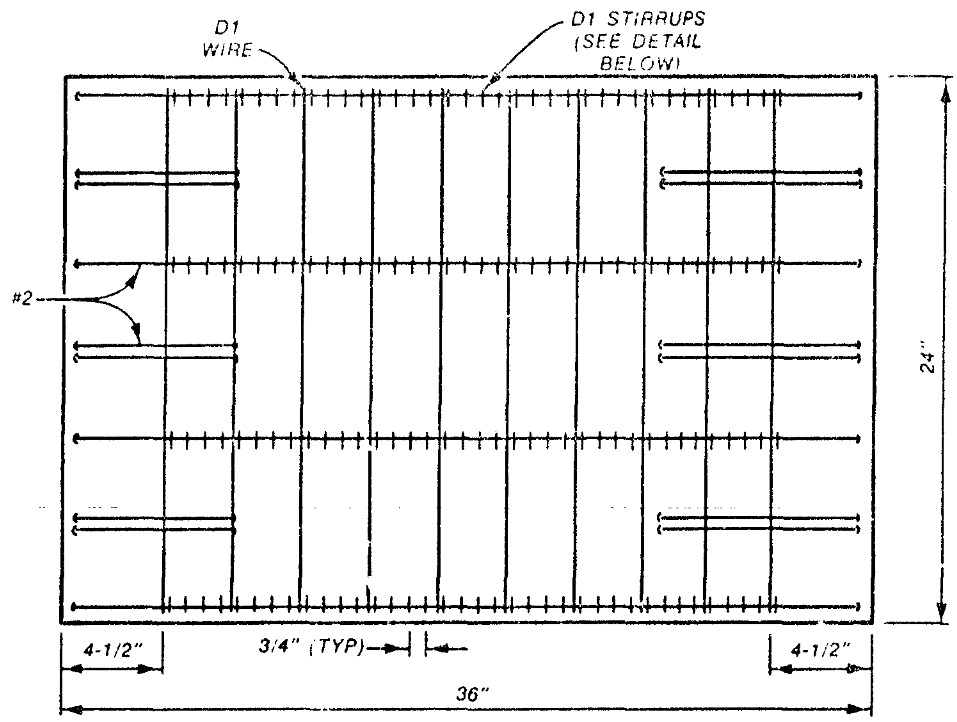

SLABS 9 THROUGH 12
STIRRUP LOCATIONS

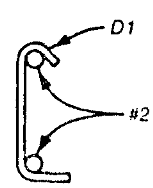

STIRRUP DETAIL

Figure 2.17. Stirrup details, Slabs 9-12.

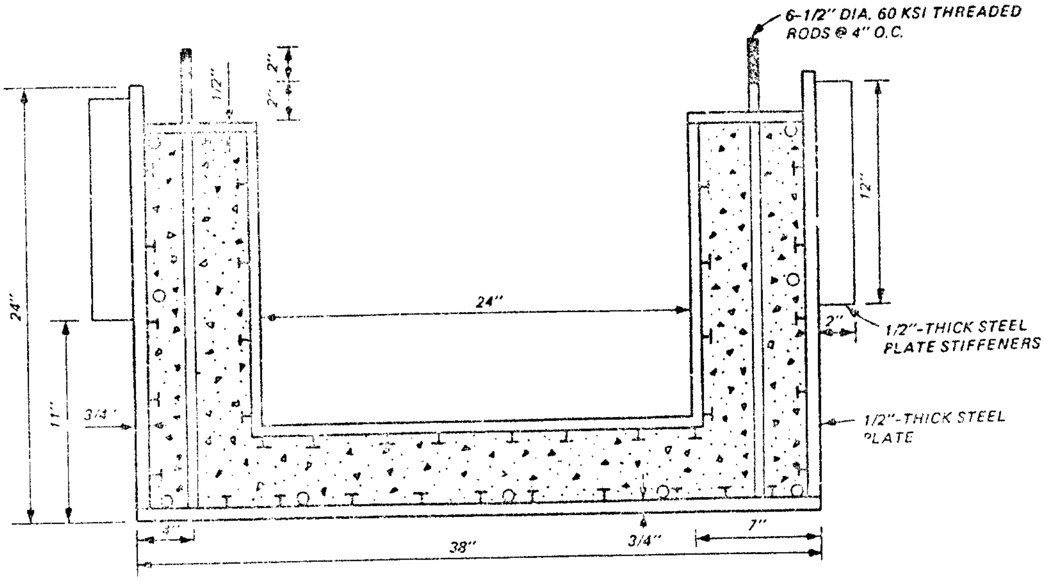

Figure 2.18. Cross section of reaction structure.

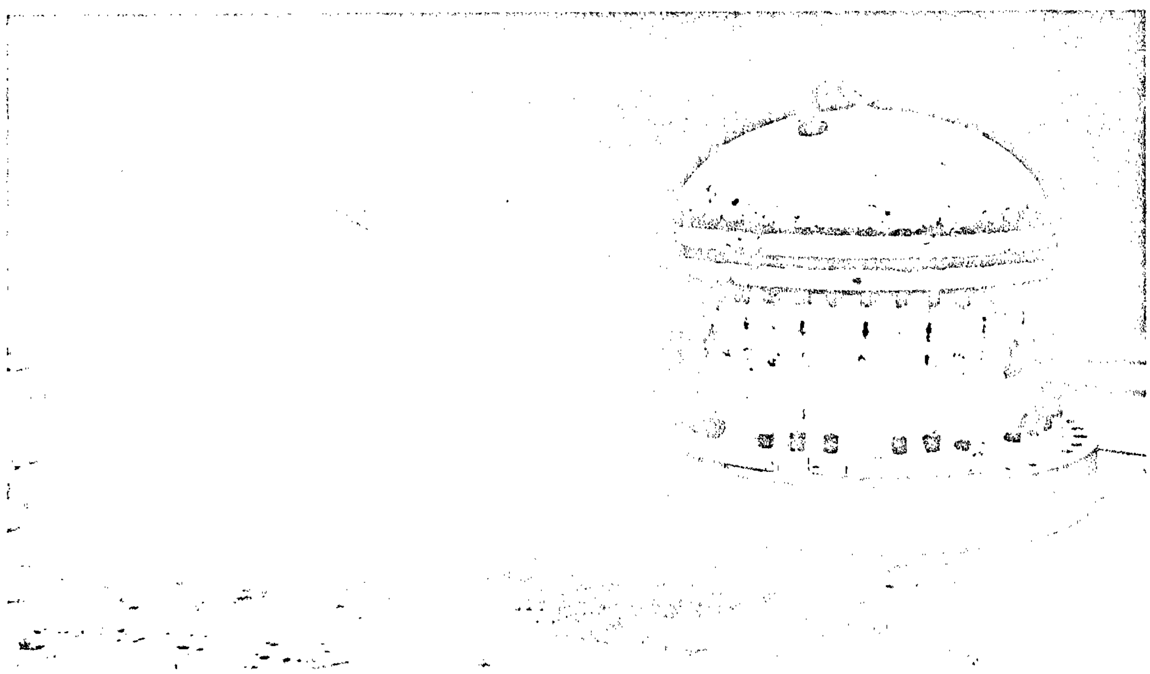

Figure 2.19. Four-foot-diameter blast load generator.

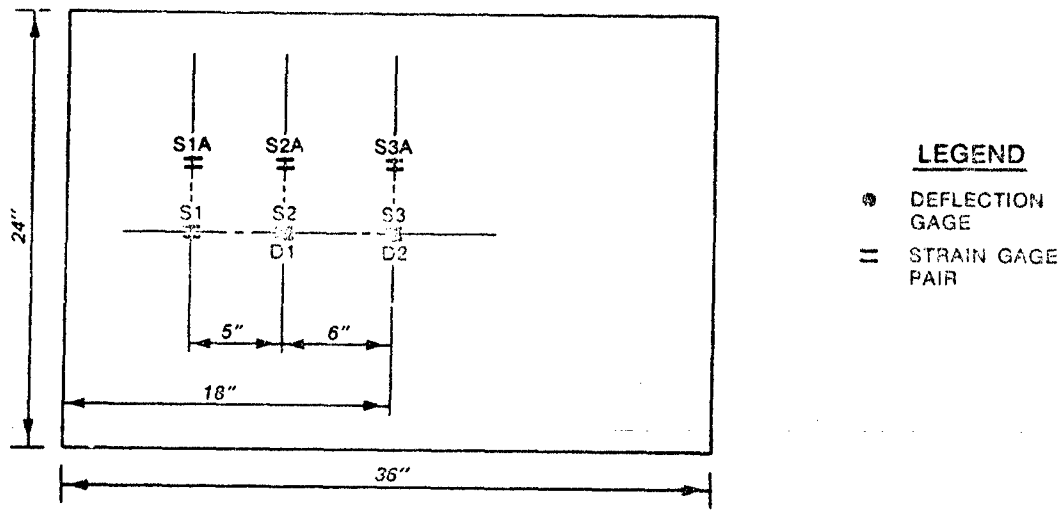

Figure 2.20. Typical instrumentation layout.

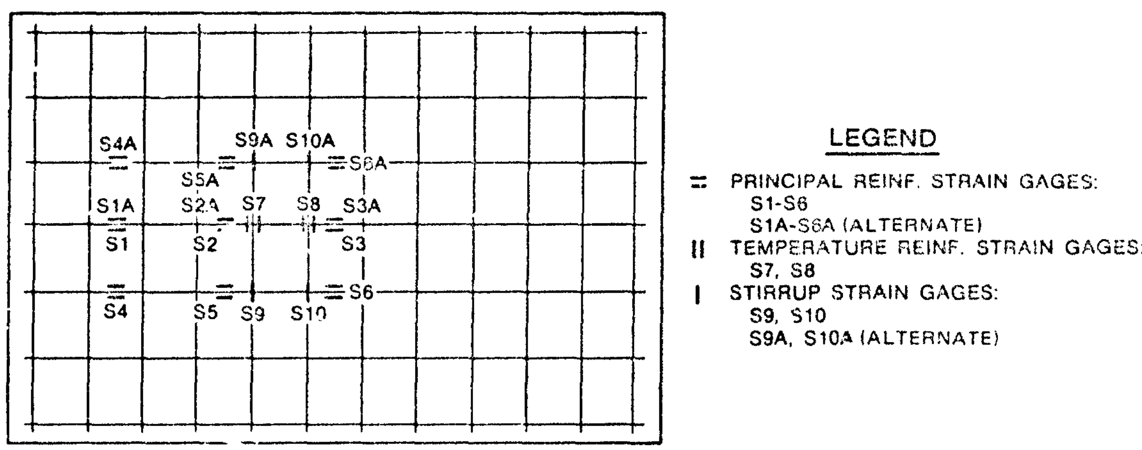

Figure 2.21. Example strain gage layout.

CHAPTER 3

MATERIAL PROPERTIES

3.1 CONCRETE

The concrete used in this test series was designed to have a 28-day compressive strength of 4,000 psi. The mix was prepared at the Structures Laboratory, WES, using a Type I portland cement. Slabs 1 through 8 were poured from batch one, from which fifteen 6- by 12-inch cylinders were cast. The remaining slabs and 16 test cylinders were cast from Batch 2. Average 28-day compressive strength was 4,610 psi for Batch 1 and 3,430 psi for Batch 2. Average 60-day compressive strength was 4,270 psi for Batch 1 and 4,030 psi for Batch 2. Compressive test results are given in Table 3.1.

3.2 REINFORCING STEEL

Principal flexural reinforcing was No. 2 rebar, 0.3-inch-diameter rebar, and D2.5 and 0.25-inch-diameter deformed wire. Stirrups and temperature steel were D1 deformed wire except in Slab 14. Stirrups and temperature steel in Slab 14 were 0.25-inch-diameter deformed wire. Grade-60 reinforcement was used. Results of tensile tests are presented in Table 3.2.

Table 3.1. Compressive test results for concrete test cylinders.

Batch	Slab No.	28-Day Strength psi	60-Day Strength psi	Approximate Test-Day Strength psi
1	1-8	4,440 4,780	4,050 4,490	
	1			4,470
	2			4,470
	3			4,470
	4			4,490
	5			4,490
	6			4,490
	7			4,270
	8			4,270
2	9-15	3,500 3,360	4,400 3,660	
	9			4,030
	10			4,030
	11			4,160
	12			4,160
	13			4,160
	14			3,560
	15			3,560

Table 3.2. Results of static tensile tests of reinforcing.

Specimen	Yield Stress ksi	Ultimate Stress ksi
D1 wire	72.56	74.34
	67.69	71.24
	51.32	56.64
	52.21	56.64
D2.5 wire	62.0	72.73
	62.2	75.91
	64.78	76.71
0.25-inch-diameter wire	73.9	78.9
	73.7	78.7
	51.1	61.9
No. 2 rebar	59.94	--
	58.43	75.0
	62.53	78.3
0.3-inch-diameter rebar	63.4	81.47
	64.35	82.03
	63.65	80.62
	62.66	80.02

CHAPTER 4

RESULTS

4.1 GENERAL

Test results are presented in this chapter and in Appendix A. A general description of the data produced and of the performance of each specimen and accompanying instrumentation is presented herein. Further discussion and analyses are presented in Chapter 5.

4.2 GAGE MEASUREMENTS

The flexural strength of a restrained slab is enhanced by compressive membrane forces, causing the ultimate load to be greater than that calculated using yield-line theory. Ultimate pressure considering compressive membrane forces is represented by Point B of Figure 4.1. At the end of compressive membrane action, center cracks penetrate the entire thickness of the slab, and the reinforcing bars act as a tensile membrane to support the load. In Figure 4.1 the tensile membrane region extends from Point C to Point D, which represents incipient collapse.

Ultimate pressure for Slabs 1 through 13 varied from 64 to 77 psi, with an average for the 13 slabs of about 68.8 psi. With the exception of Slab 6, deflection at ultimate pressure varied from 0.75 inch to 1.2 inches with an average of about 0.9 inch. The average ratio of deflection at ultimate pressure-to-slab thickness for all slabs except 6 and 4 was 0.40. The average for all slabs was 0.37.

The maximum pressure in the tensile membrane region did not necessarily represent pressure at incipient collapse. Decline in pressure readings may have been due to membrane rupture or to deflections exceeding maximum gage settings. End-of-test pressures for Slabs 1 through 13 varied from a high of 122 psi for the second test of Slab 6 to a low of 36 psi for Slab 15. Tensile membrane capacities were generally greater for Slabs 7 through 12 than for other reinforcing patterns. Excluding Slabs 6 and 14, average maximum pressure in the tensile membrane region was 58 psi. Average maximum pressure in the tensile membrane region for Slabs 7 through 12 was 63.3 psi. An unusually low value of 54 psi was recorded for Slab 11.

Ultimate pressure for Slab 14 was 125 psi at a deflection of 0.8 inch.

End-of-test pressure was 92 psi at 5.0 inches of deflection.

Ultimate pressure for Slab 15 was 52 psi, and end-of-test pressure was 36 psi. These were the lowest values for all slabs tested.

Experimental pressure-versus-deflection at ultimate pressure and at maximum pressure in the tensile membrane region are given in Table 4.1. Ultimate pressures at an assumed deflection of 0.5 times the slab thickness were calculated using Park and Gamble's method (Reference 3) and are listed for comparison.

Data recorded from the slab tests are presented in Appendix A.

4.3 STRUCTURAL DAMAGE

The following three failure modes were observed and are shown in Figure 4.2.

1. A three-hinge mechanism, with deep cracks over the supports, crushing of concrete in the center and, with the exception of Slab 3, 100 percent of midspan bottom reinforcing broken.

2. A modified three-hinge mechanism, with cracking at the supports extending in an almost circular pattern from the center of the support to the center of the unsupported edges and a central hinge occurring over a large (and often not clearly defined) area. Although badly bent and elongated, some midspan bottom reinforcing remained unbroken.

3. A four-hinge mechanism with no reinforcing broken, but considerable crushing of concrete. The four-hinge failure mechanism is shown in detail in Figure 4.3.

Slabs are grouped below according to mode of failure.

Posttest observations are summarized in Table 4.1 and posttest views of Slabs 1-15 are contained in Figures 4.4 through 4.32.

4.3.1 Three-Hinge Failure Mechanism

4.3.1.1 Slabs 1 and 2. Complete midspan cracking and crushing through the slab thickness occurred over about one-fourth of the width in Slab 1 (Figures 4.4 and 4.5) and throughout the entire width in Slab 2 (Figures 4.6 and 4.7). Very little cracking occurred outside of the hinge areas.

4.3.1.2 Slab 3. The edge bottom reinforcing bars did not rupture at midspan, and there was some cracking above the edge bars throughout the length of the slab (Figures 4.8 and 4.9). The concrete was cracked and crushed at midspan through the entire thickness of the slab. Most top reinforcing at the supports was broken.

4.3.1.3 Slab 11. The concrete was completely crushed throughout the center, but few cracks occurred outside of the hinge areas (Figures 4.24 and 4.25). Much of the top reinforcing was broken, both at midspan and over the supports.

4.3.1.4 Slab 14. Slab 14 failed in a classic three-hinge mechanism, with 100 percent of tensile reinforcing broken and almost no cracking between hinges (Figure 4.29). There were small gaps in the concrete at midspan where crushing occurred throughout the slab thickness.

4.3.1.5 Slab 15. The slab was totally crushed at midspan, with all bottom reinforcing bars broken and top reinforcing pulled free of the concrete (Figures 4.30 and 4.31). Much of the tensile reinforcing at the supports was broken.

4.3.2 Modified Three-Hinge Failure Mechanism

4.3.2.1 Slabs 4 and 5 (Figures 4.10-4.13). Reinforcement was similar to Slab 3, except that dowels were added in the tensile region over the supports. Both slabs were crushed throughout the thickness at midspan. Few top reinforcing bars were broken at the supports, and no top reinforcing was broken at midspan. Much of the bottom steel was broken at midspan.

4.3.2.2 Slabs 7-10, 12, and 13. The same percentage of top and bottom reinforcing was used in all six slabs and in Slab 11. See Chapter 2 for variations in stirrups and principal reinforcing configurations.

Slabs 7 (Figure 4.17) and 8 (Figures 4.18 and 4.19) behaved similarly, with few top bars broken at the supports, 40 to 60 percent of bottom reinforcing broken at midspan, and no compressive steel broken. Failure was clearly by Mode 2.

Slabs 9 (Figures 4.20 and 4.21) and 12 (Figures 4.26 and 4.27) had areas of crushing outside the central hinge, suggesting that at some points an additional hinge was formed. Slabs 9 and 12 were more heavily instrumented with strain gages and accompanying wiring than Slabs 10 or 11, perhaps affecting the cracking pattern.

The failure mode for Slab 10 (Figure 4.22) closely resembled a three-hinge mechanism. One large crack formed at each end, with very little additional cracking at the supports. The slab was totally crushed through the width at midspan (Figure 4.23). Slab 10 was the only slab in this group with top reinforcing broken at midspan.

Slab 13 was badly cracked throughout the length of the span (Figure 4.28)

4.3.3 Four-Hinge Failure Mechanism

4.3.3.1 Slab 6. Hinges occurred at supports and approximately at centers of reinforcing band locations (Figure 4.3). No reinforcing bars were ruptured, but concrete was badly crushed at the hinges (Figure 4.14). After the second test, much of the bottom concrete at one end had spalled off (Figure 4.15) Except at slab edges, only a few hairline cracks appeared at midspan (Figure 4.16).

Table 4.1. Summary of test results.

Slab No.	Compressive Membrane Region: Experimental P_B psi	Δ_B in	Δ_B/h	Theoretical P_B[a] for $\Delta_B/h = 0.5$ psi	Tensile Membrane Region: Experimental Pressure, P_D psi	Δ_D in	Total Deflection in	Permanent Deflection in	Midspan Reinforcement Rupture, % Top	Midspan Reinforcement Rupture, % Bottom	Support Reinforcement Rupture, % Top	Support Reinforcement Rupture, % Bottom	Type of Mechanism (See Figure 4.2)
1	66	1.0	0.43	46.3	45	4.1	4.1	3.75	0	100	7	0	3-hinge
2	64	0.8	0.35	45.7	55	4.3	4.3	3.9	0	100	14	0	3-hinge
3	68	1.2	0.52	43.6	58	4.6	4.6	4.2	0	71	86	0	3-hinge
4	68	1.1	0.48	43.6	60	4.5	4.55	4.2	0	43	7	0	Modified 3-hinge
5	77	1.0	0.43	59.3	55	4.4	5.1	5.0	29	71	14	0	Modified 3-hinge
6	68	0.25	0.11	86.5	100	3.05	3.1	2.7	0	0	0	0	4-hinge
6B					122	4.13^b	4.93^b	4.45^b					
7	67	1.0	0.45	57.7	63	5.7	5.7	5.45	0	40	10	0	Modified 3-hinge
8	68	0.8	0.35	57.7	70	5.0	5.2	5.0	0	60	20	0	Modified 3-hinge
9	67	0.8	0.35	57.7	71	5.3	5.3	5.3	0	80	20	0	Modified 3-hinge
10	73	0.9	0.39	57.7	62	5.2	5.2	5.05	25	60	45	0	Modified 3-hinge
11	73	0.95	0.41	57.7	54	4.2	--	--	50	100	45	0	3-hinge
12	71	0.8	0.35	57.7	76	4.12	5.5	5.5	0	50	25	0	Modified 3-hinge
13	64	0.75	0.32	57.7	47	5.4	5.4	--	0	40	15	0	Modified 3-hinge
14	126	0.8	0.28	100.7	96	5.0	5.0	4.7	0	100	100	0	3-hinge
15	52	1.0	0.43	45.1	36	5.2	5.4	--	0	100	57	0	3-hinge

[a] Using Park's equations (Reference 3) with $\beta = 0.5$.
[b] Deflection from Test 6B added to 2.7 inches permanent deflection from Test 6.

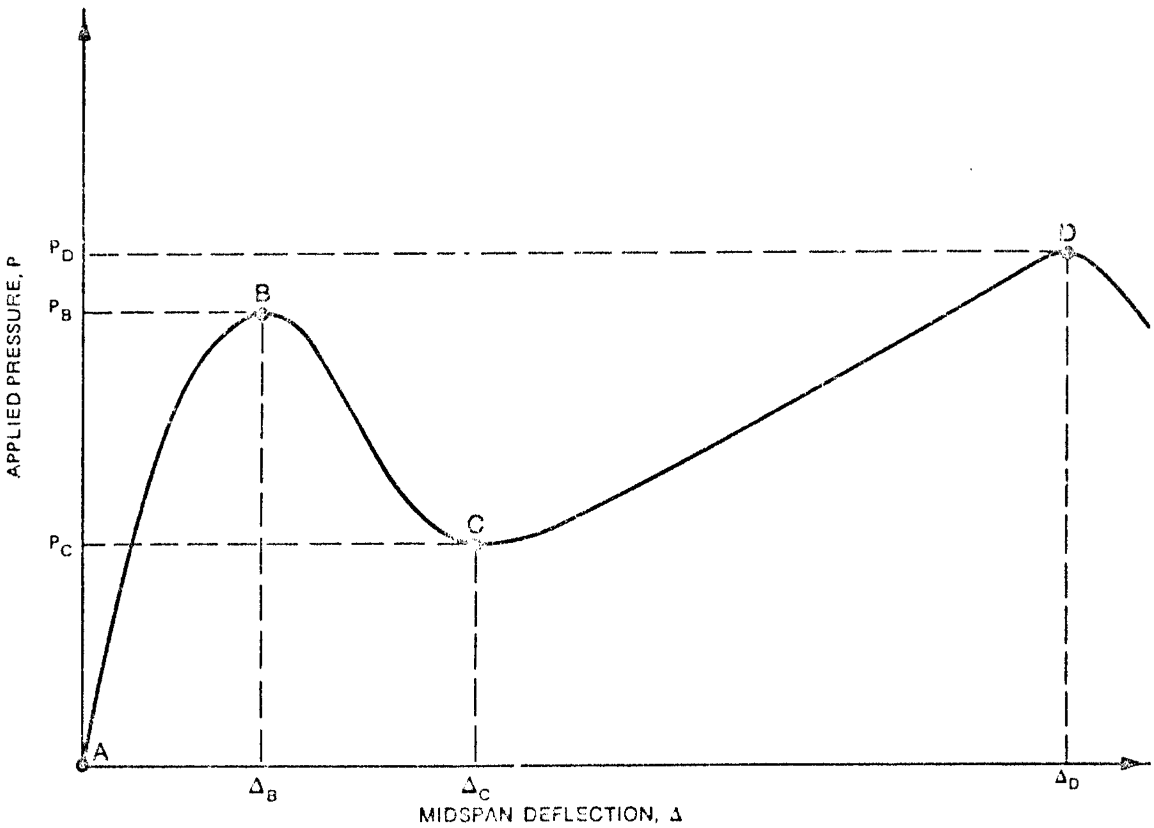

Figure 4.1. Load-deflection relationship for one-way slabs with restrained ends.

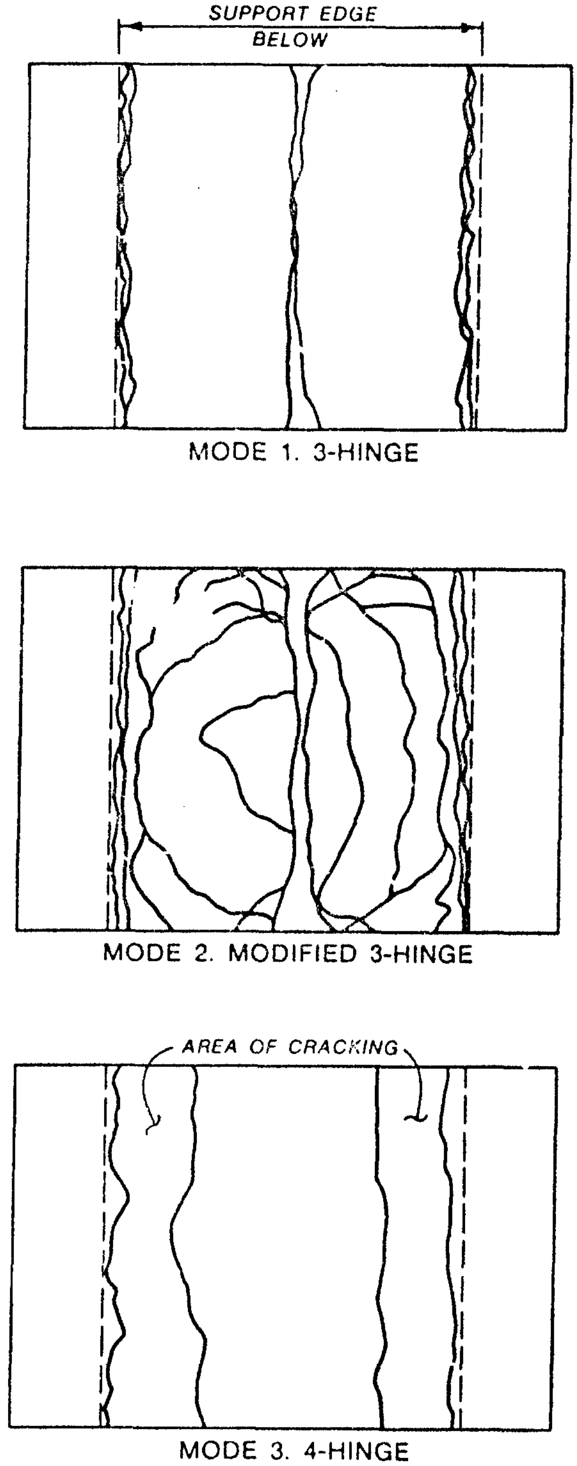

Figure 4.2. Failure modes.

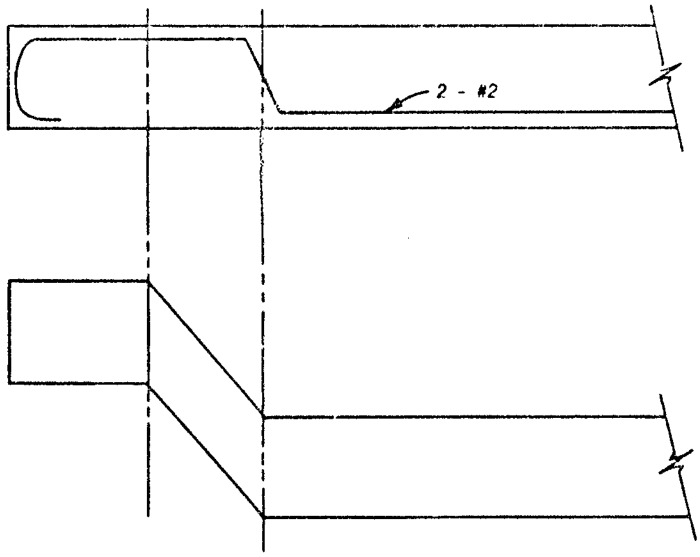

Figure 4.3. Four-hinge failure mechanism.

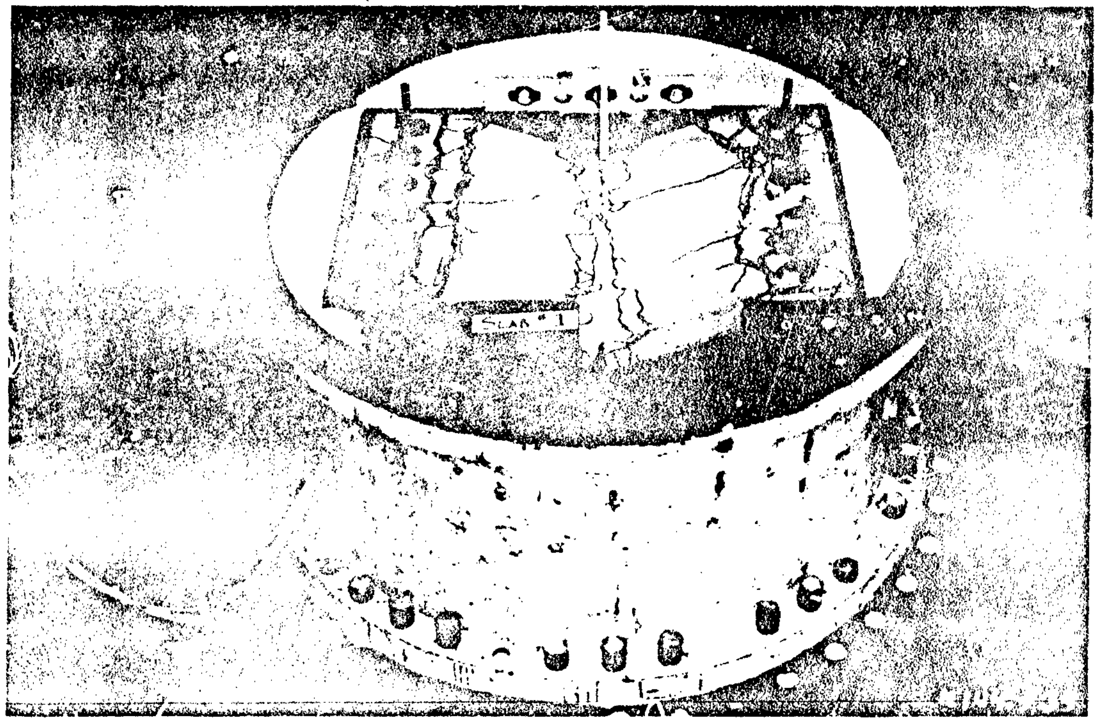

Figure 4.4. Slab 1, posttest.

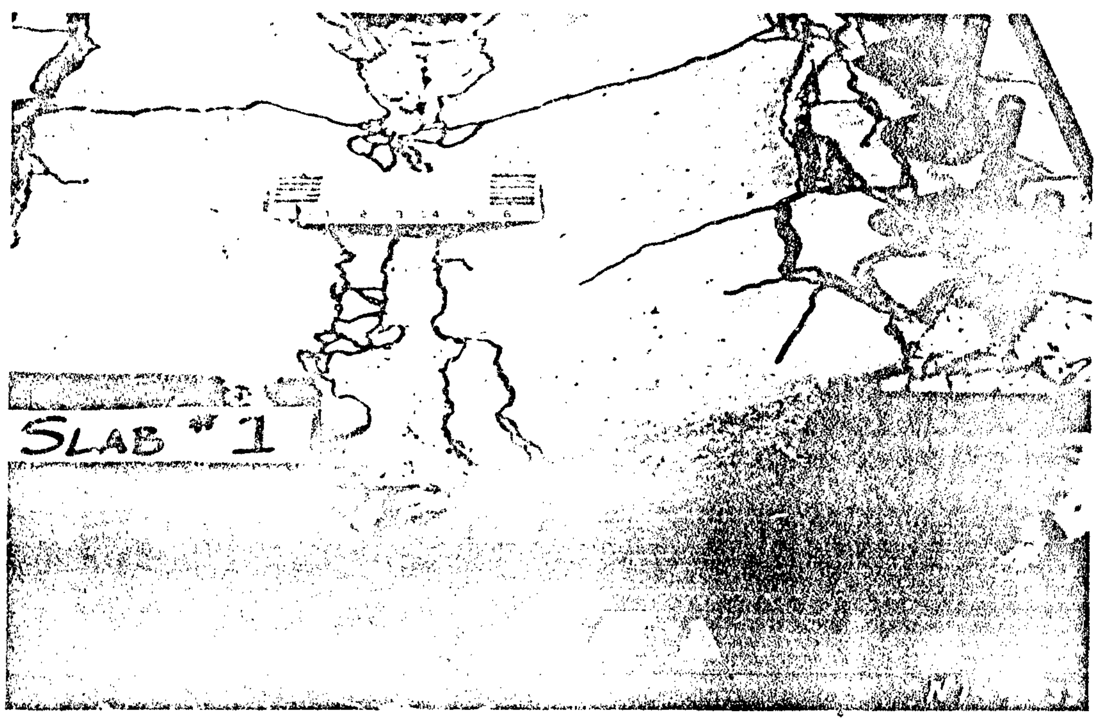

Figure 4.5. Closeup view of Slab 1, posttest.

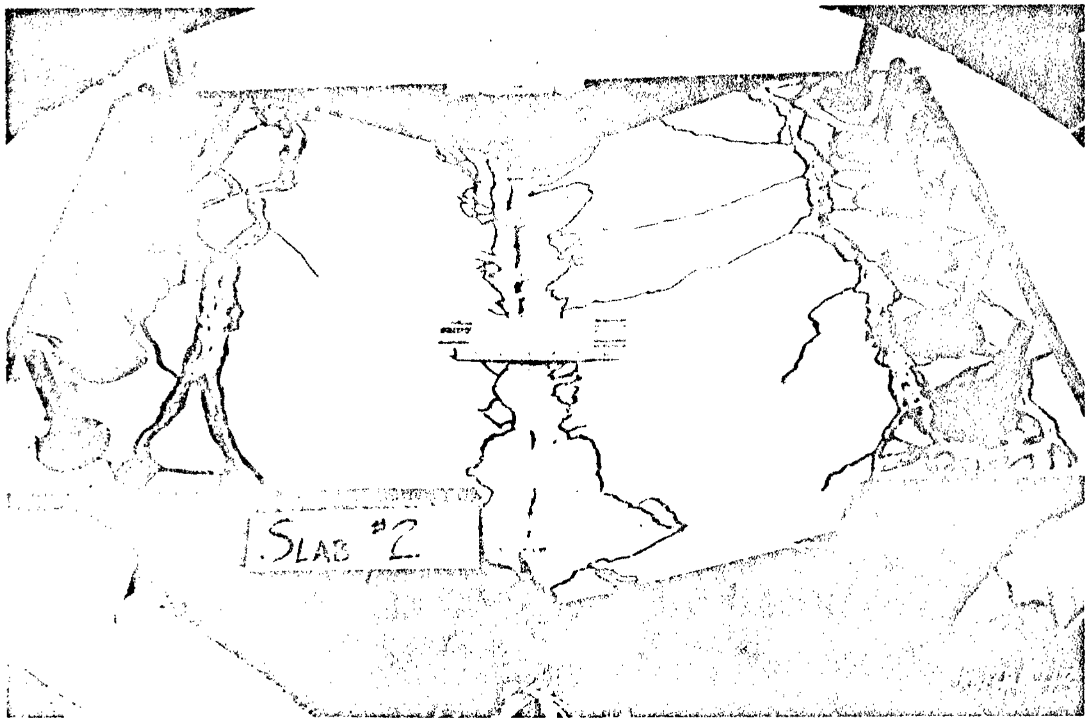

Figure 4.6. Slab 2, posttest.

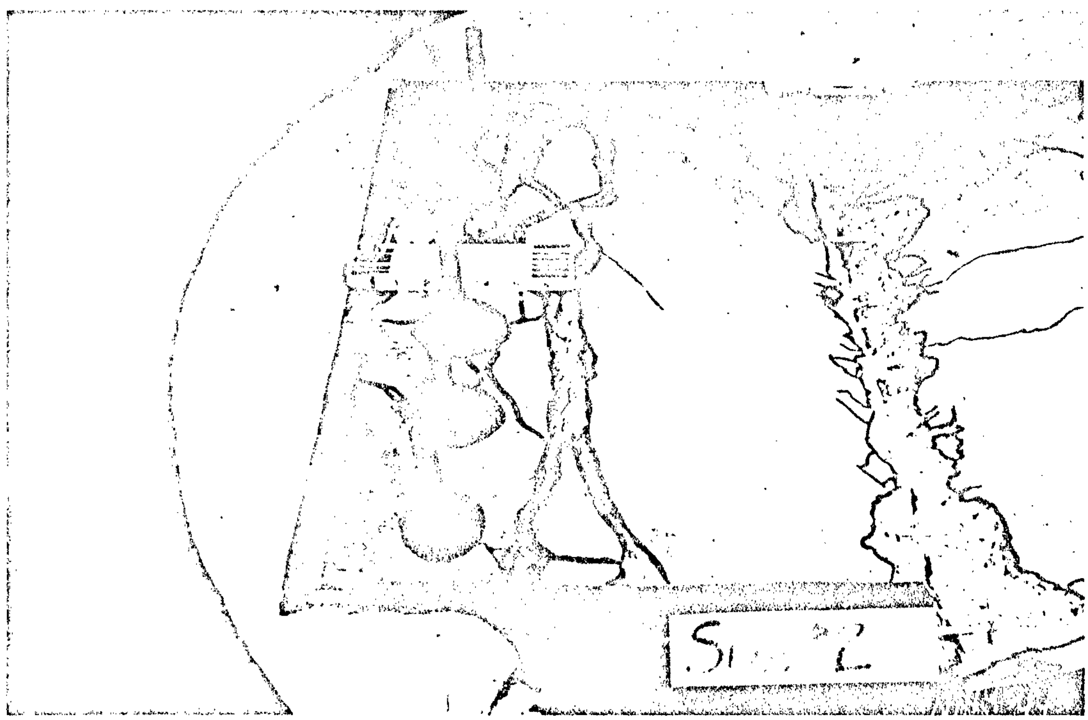

Figure 4.7. Closeup view of Slab 2, posttest.

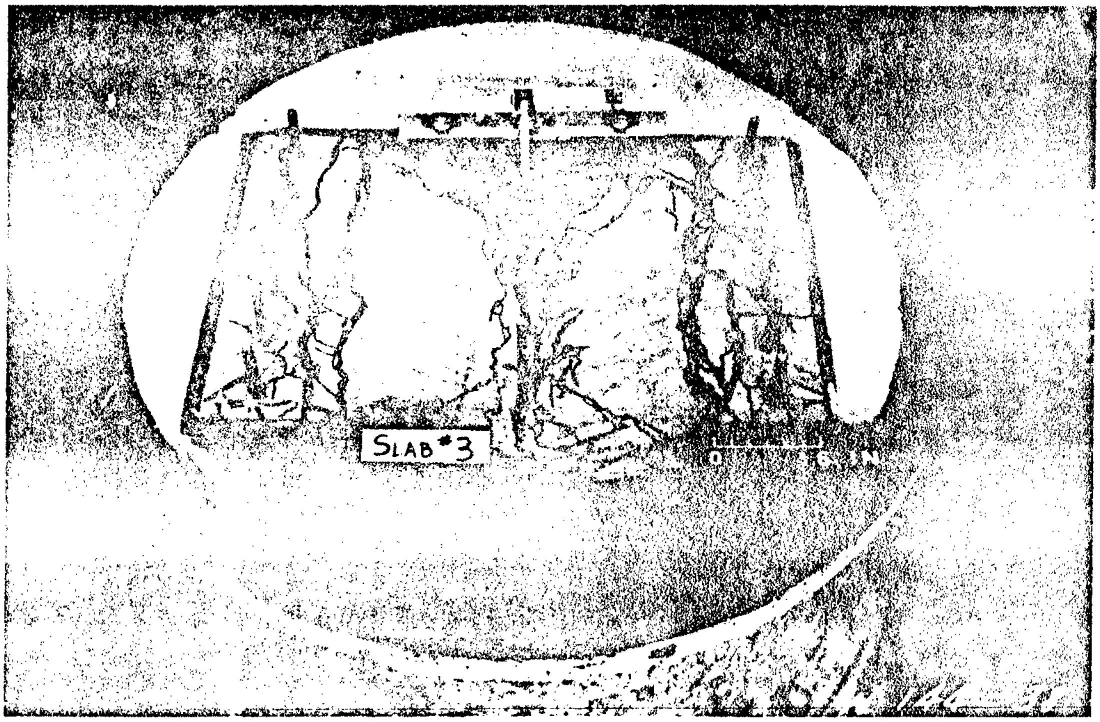

Figure 4.8. Slab 3, posttest.

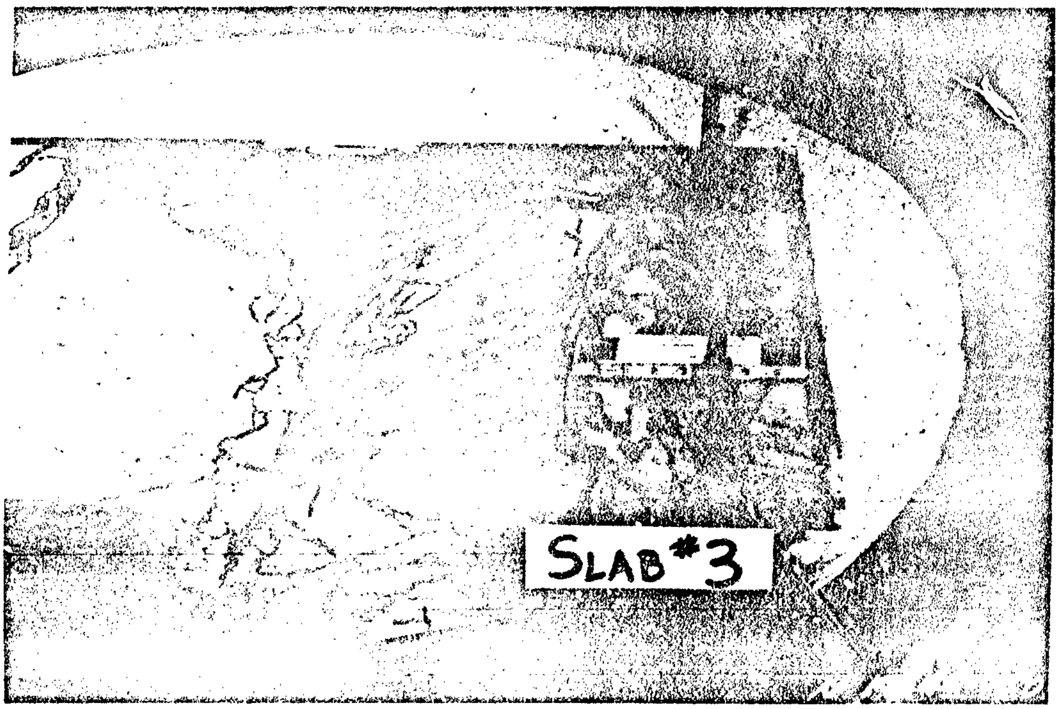

Figure 4.9. Closeup view of Slab 3, posttest.

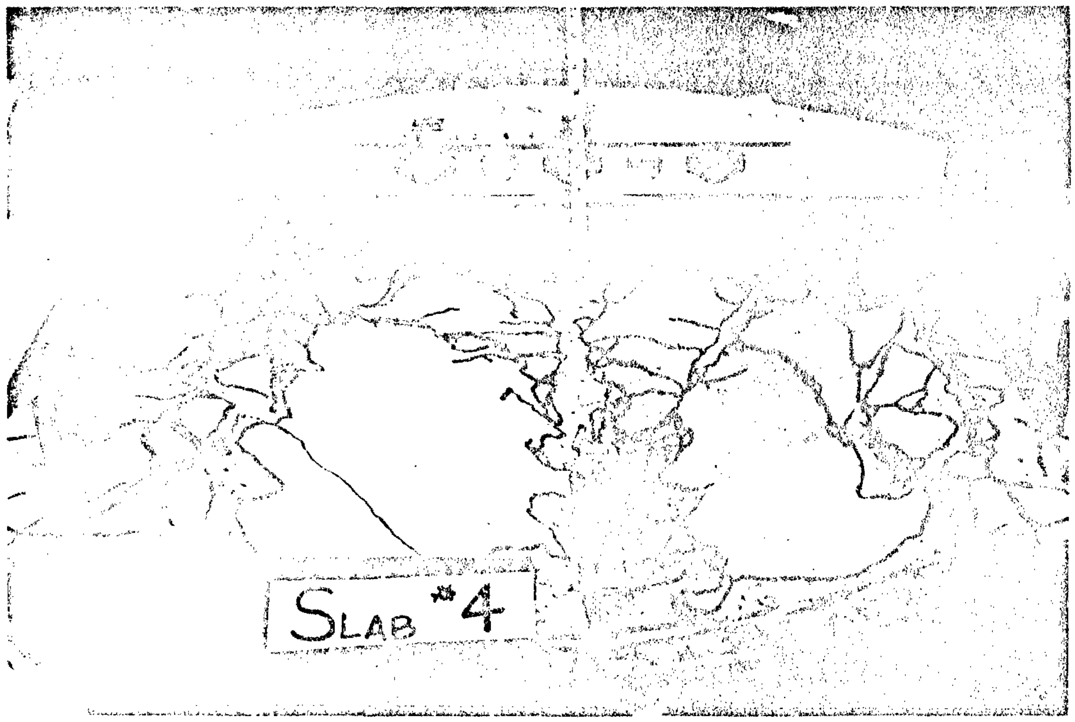

Figure 4.10. Slab 4, posttest.

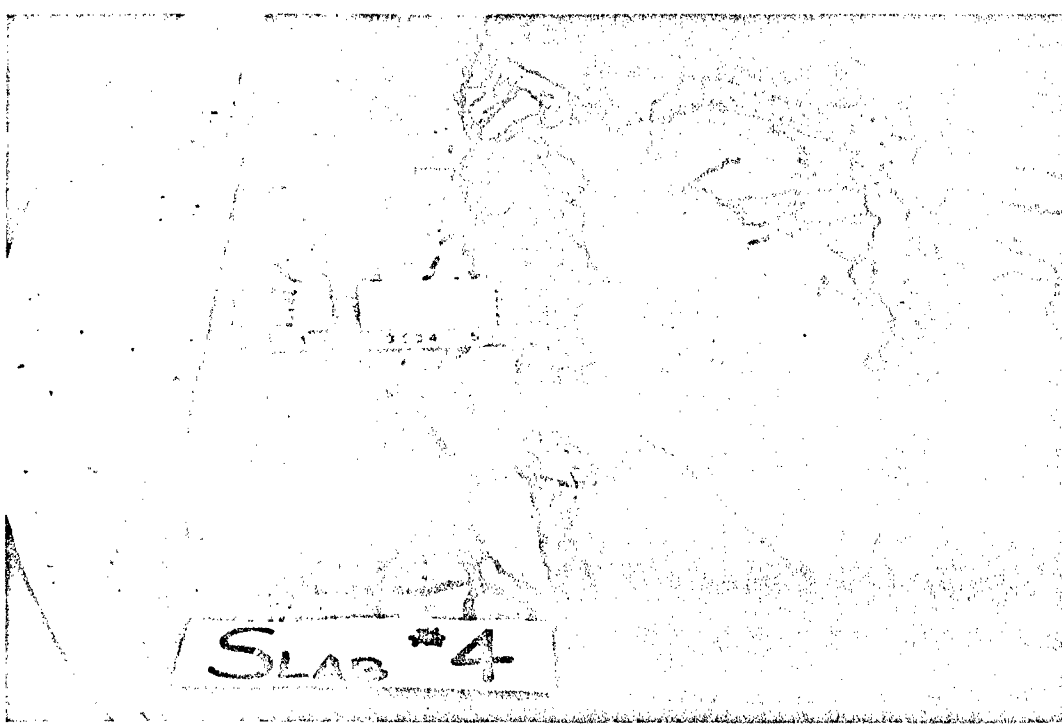

Figure 4.11. Closeup view of Slab 4, posttest.

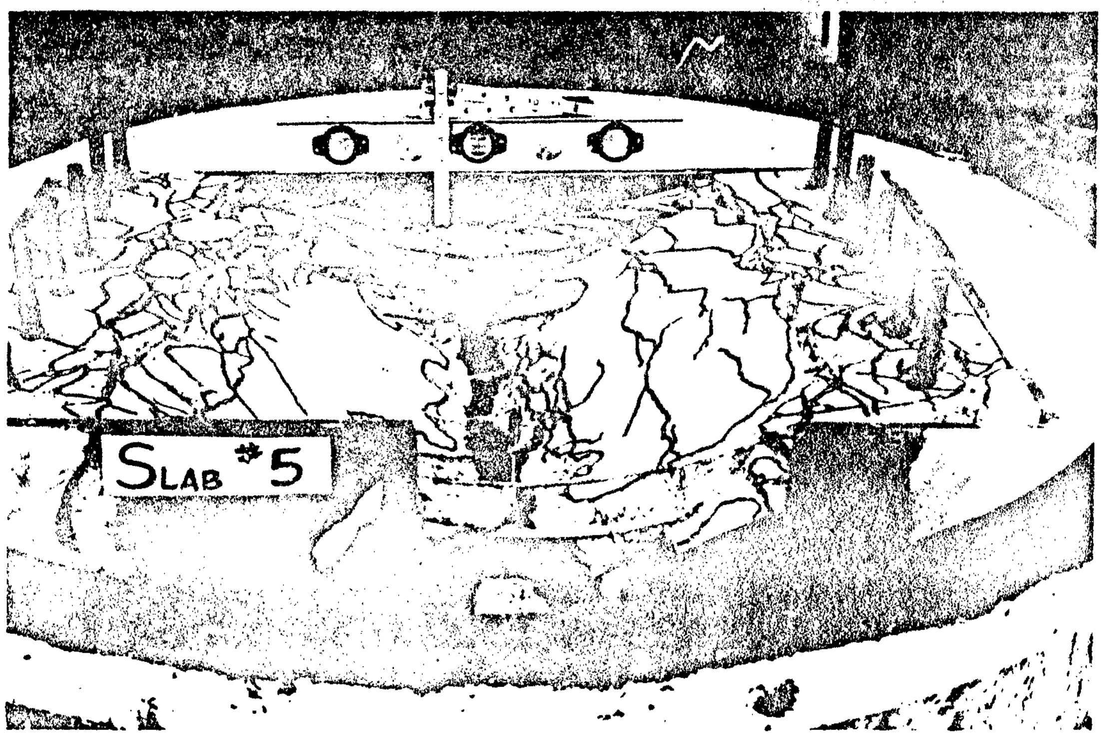

Figure 4.12. Slab 5, posttest.

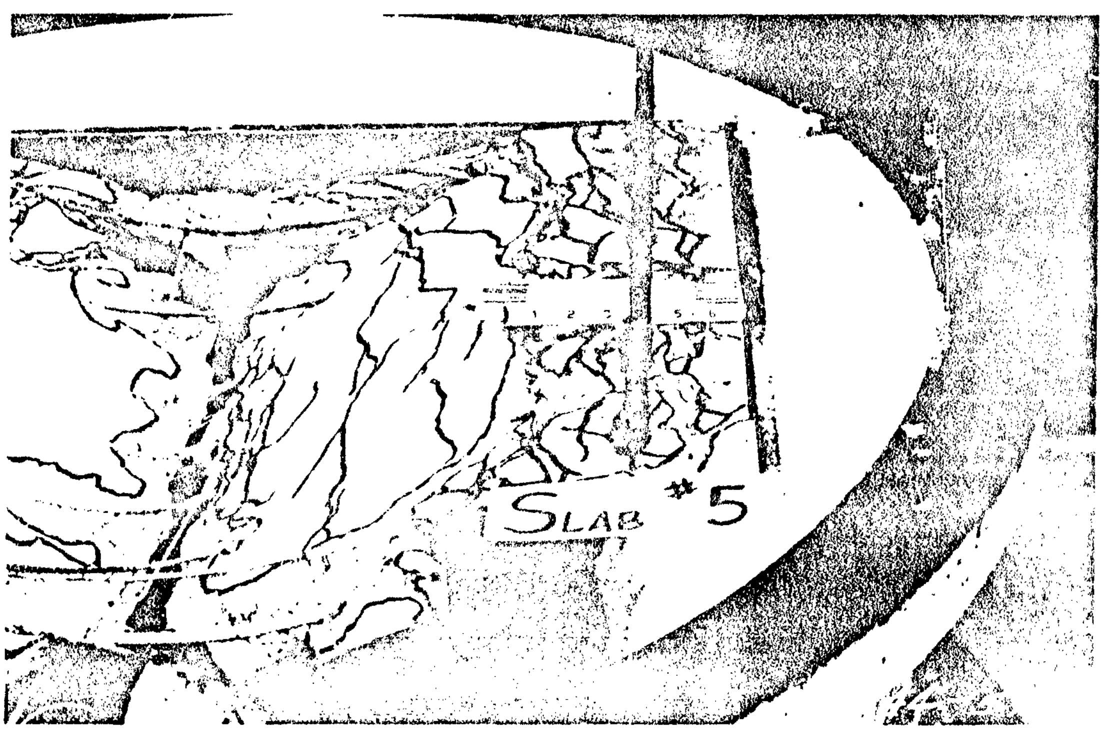

Figure 4.13. Closeup view of Slab 5, posttest.

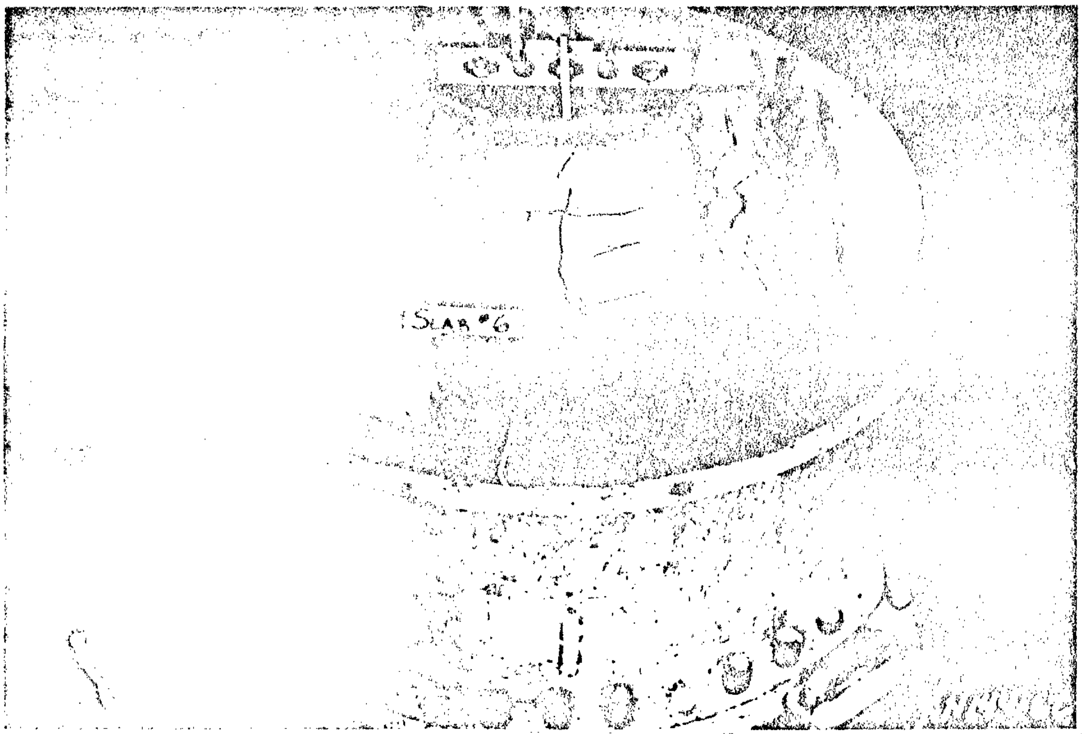

Figure 4.14. Slab 6 following initial test.

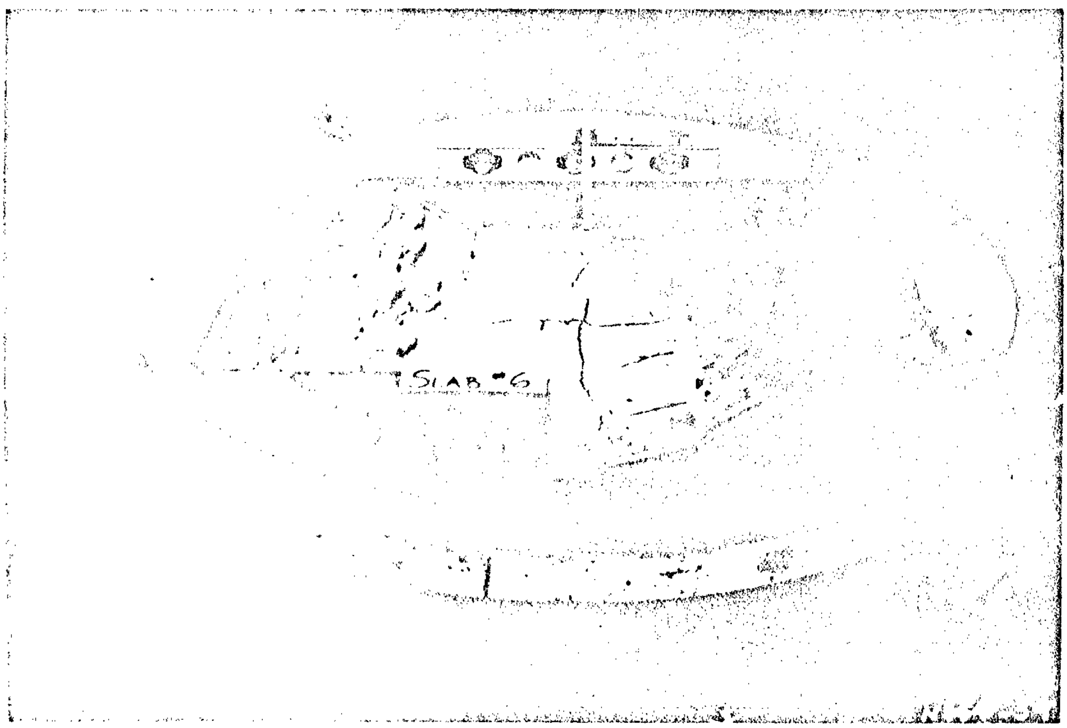

Figure 4.15. Slab 6 following retest.

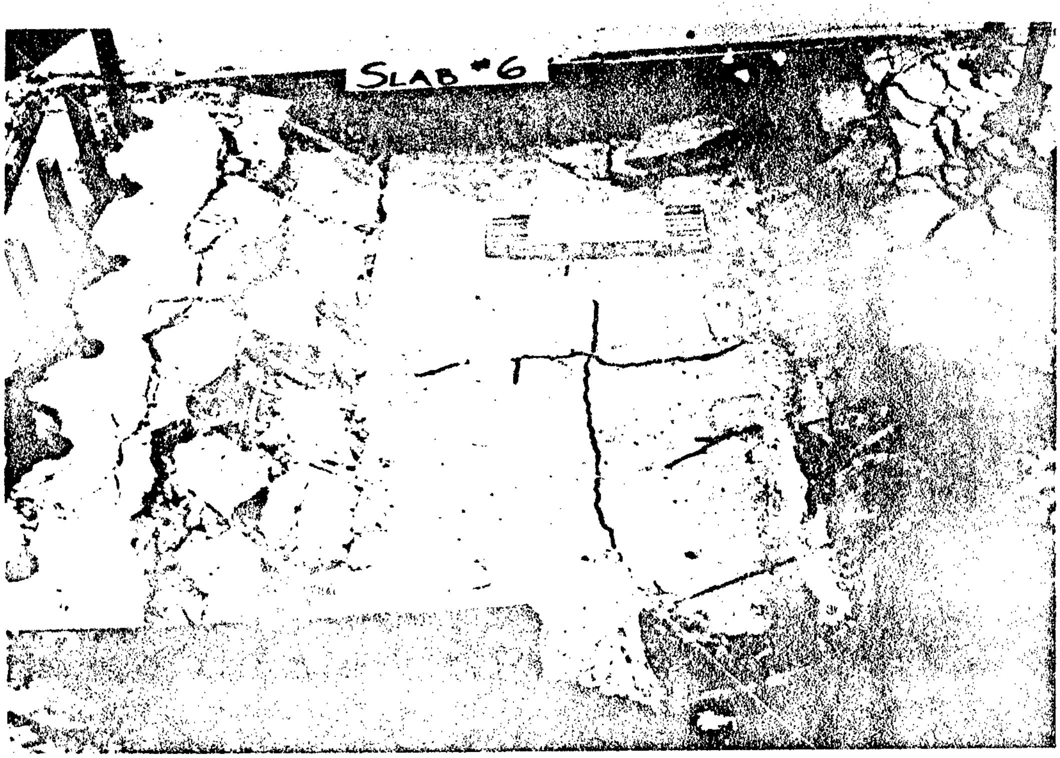

Figure 4.16. Closeup view of Slab 6 following retest.

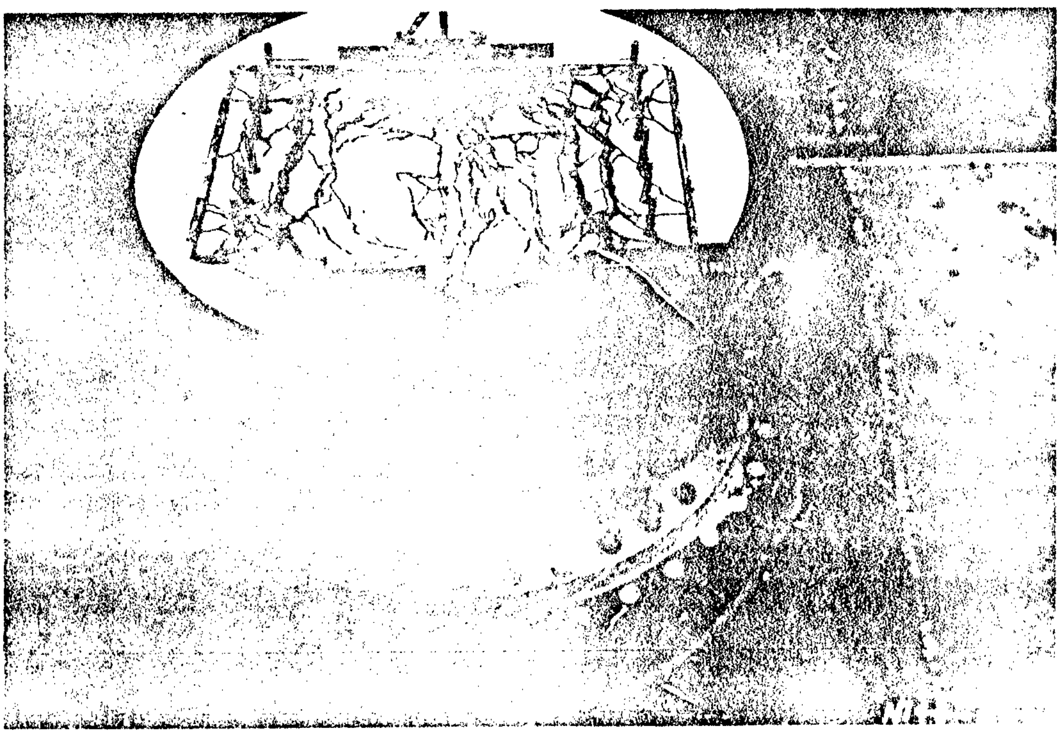

Figure 4.17. Slab 7, posttest.

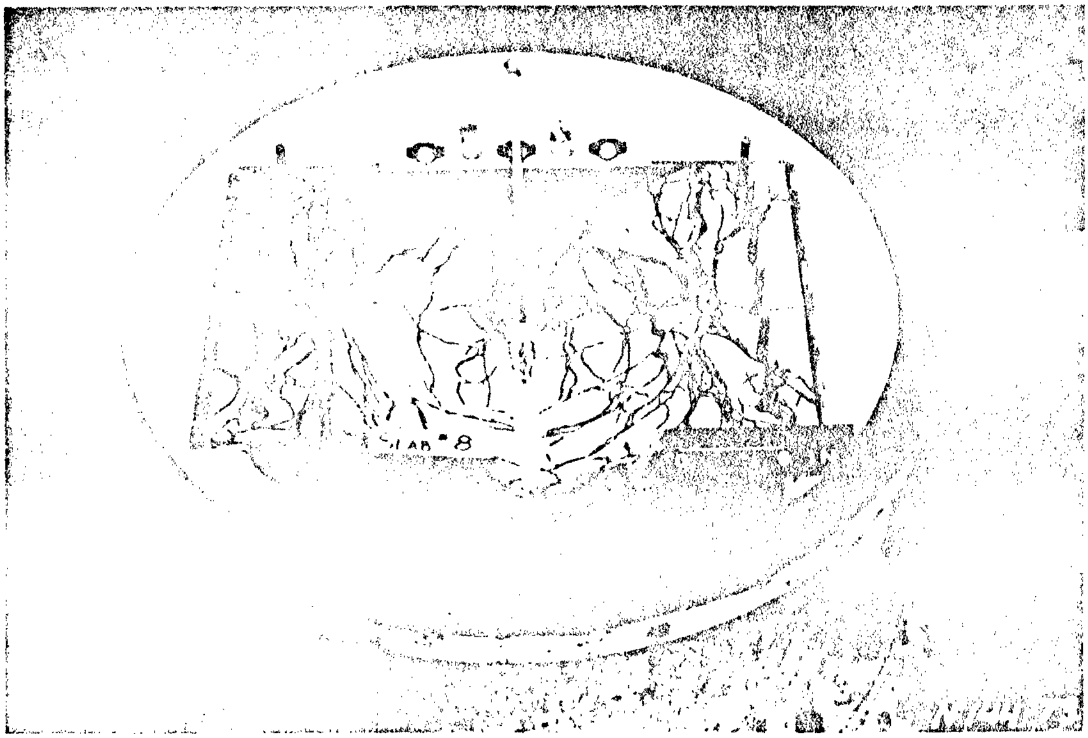

Figure 4.18. Slab 8, posttest.

Figure 4.19. Closeup view of Slab 8, posttest.

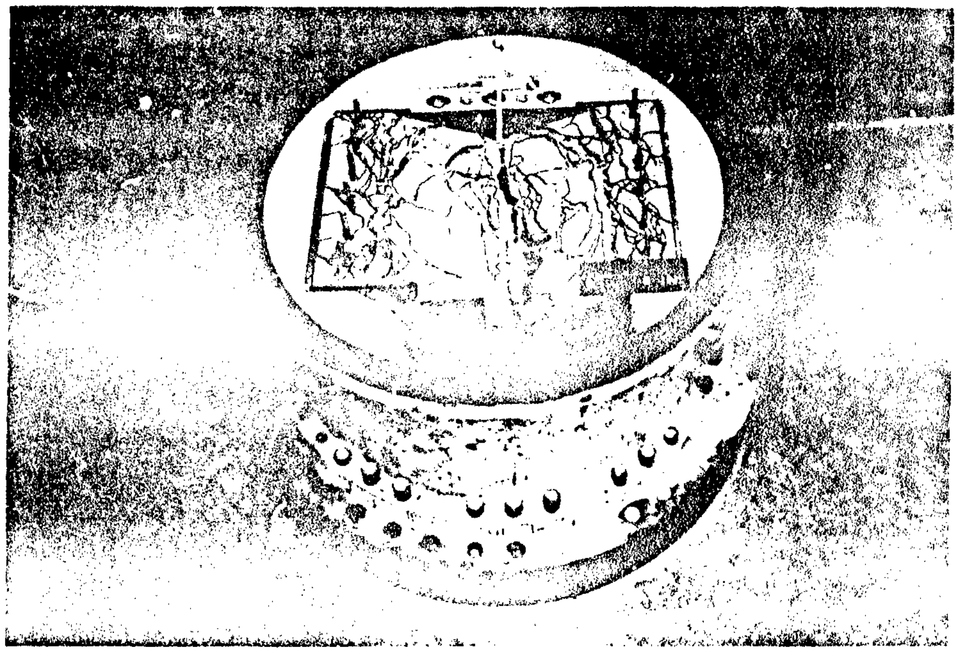

Figure 4.20. Slab 9, posttest.

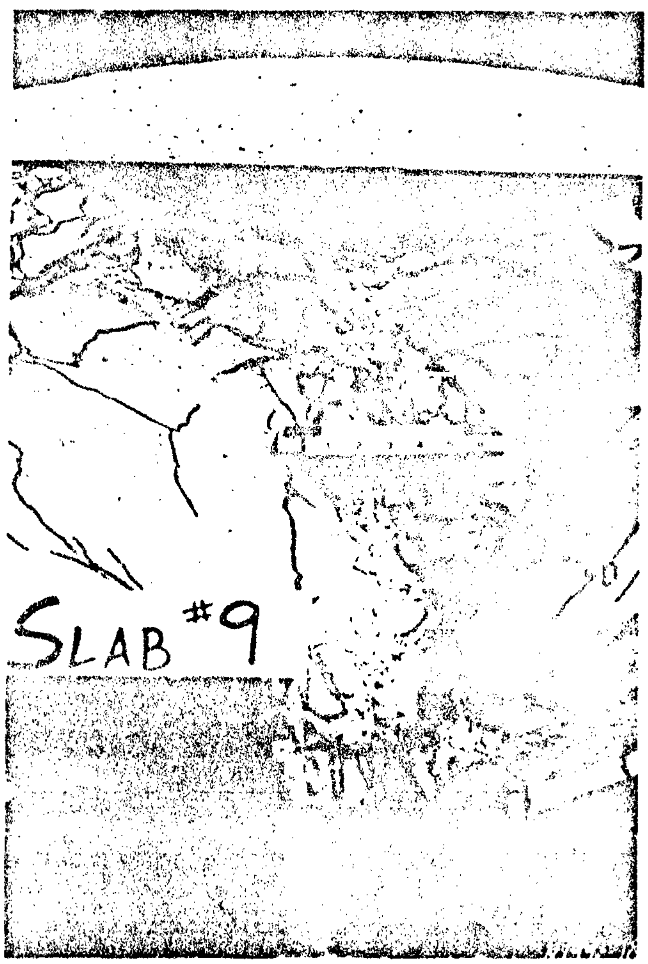

Figure 4.21. Closeup view of Slab 9, posttest.

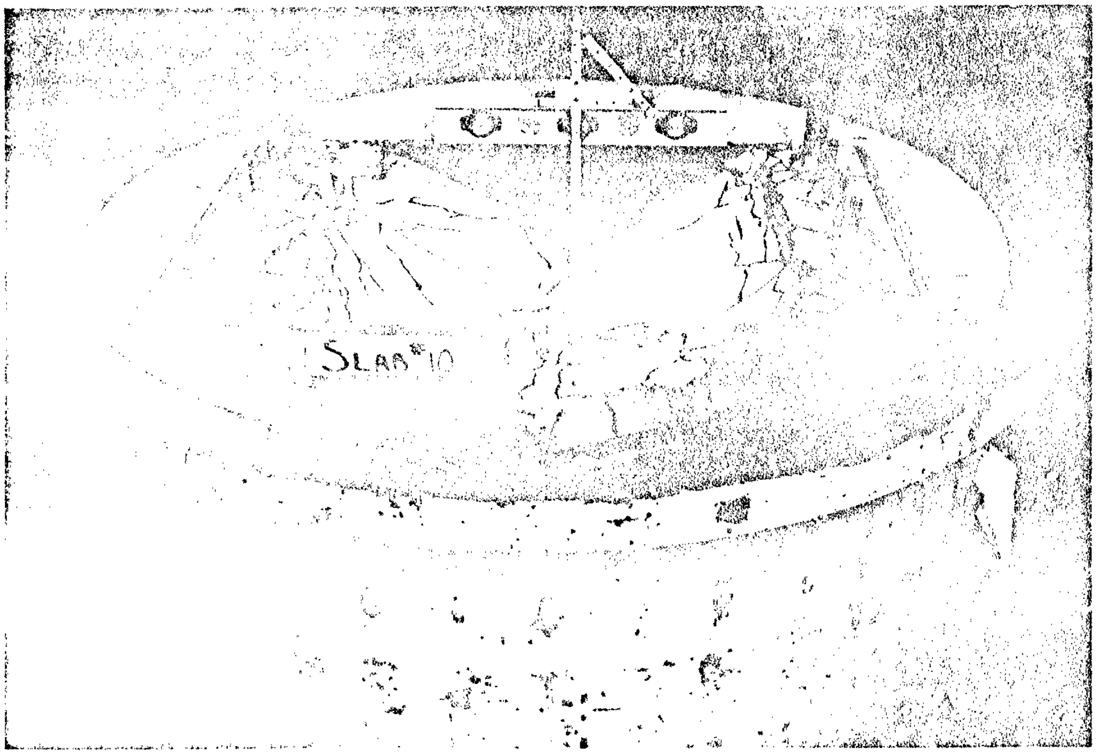

Figure 4.22. Slab 10, posttest.

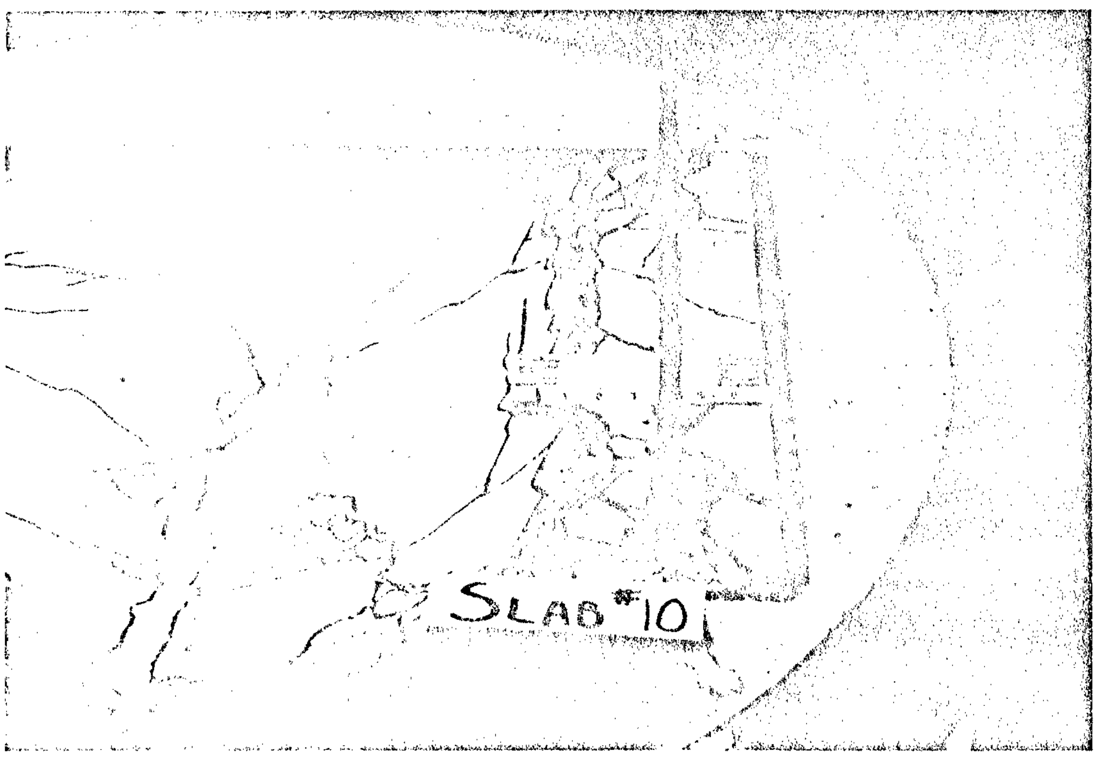

Figure 4.23. Closeup view of Slab 10, posttest.

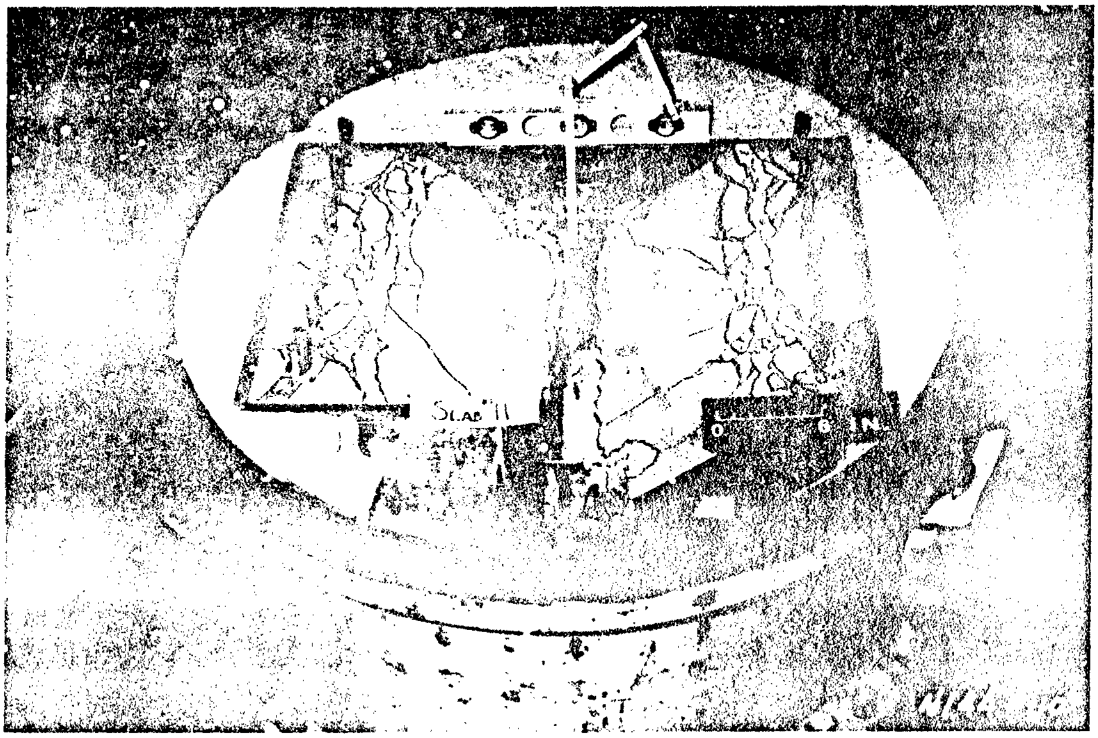

Figure 4.24. Slab 11, posttest.

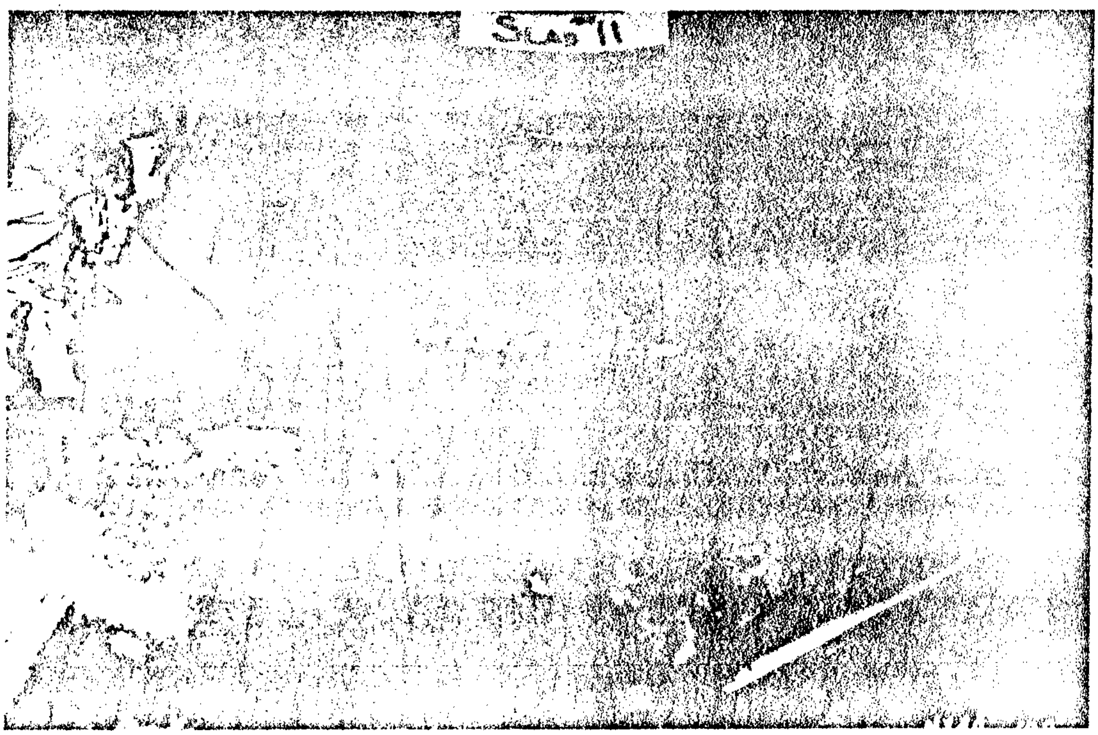

Figure 4.25. Closeup view of Slab 11, posttest.

Figure 4.26. Slab 12, posttest.

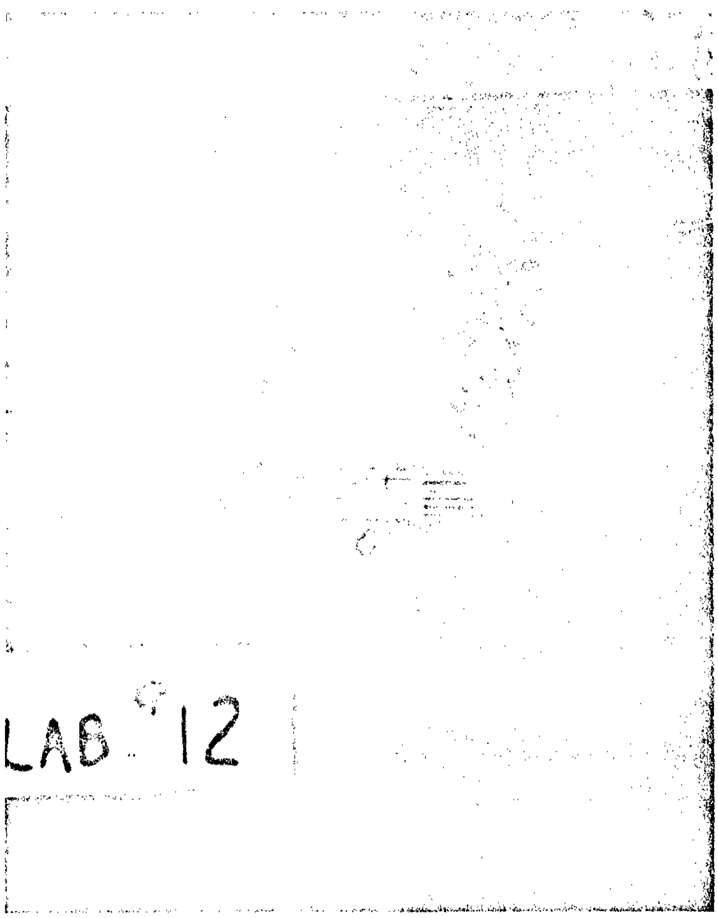

Figure 4.27. Closeup view of Slab 12, posttest.

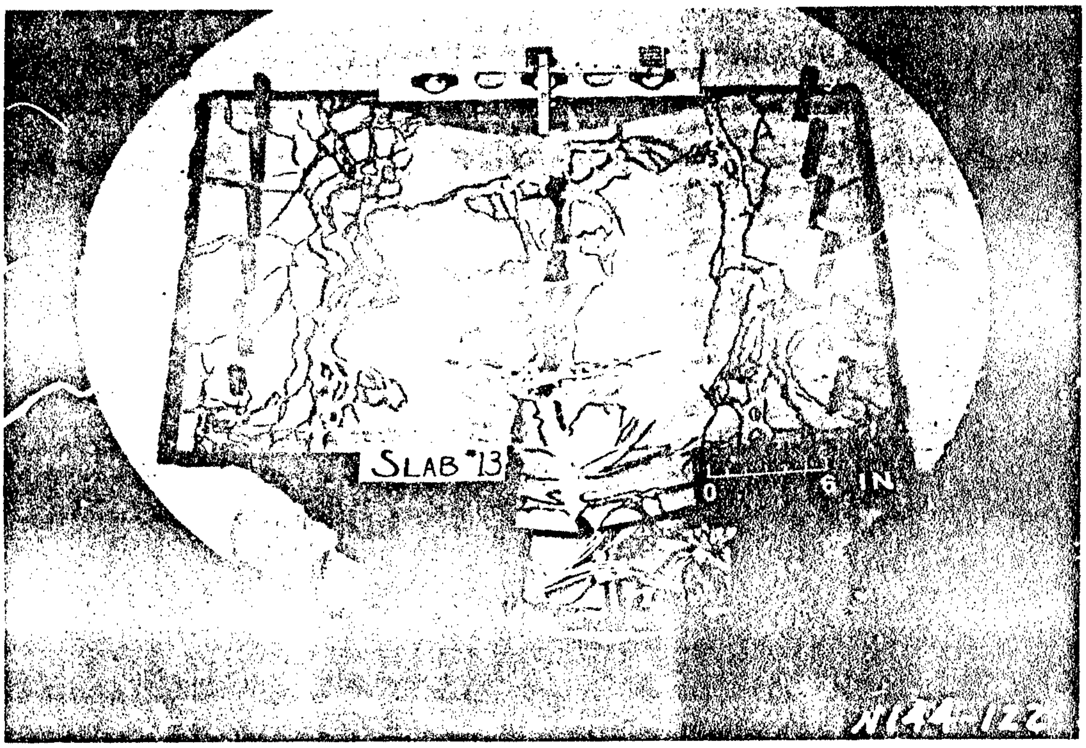

Figure 4.28. Slab 13, posttest.

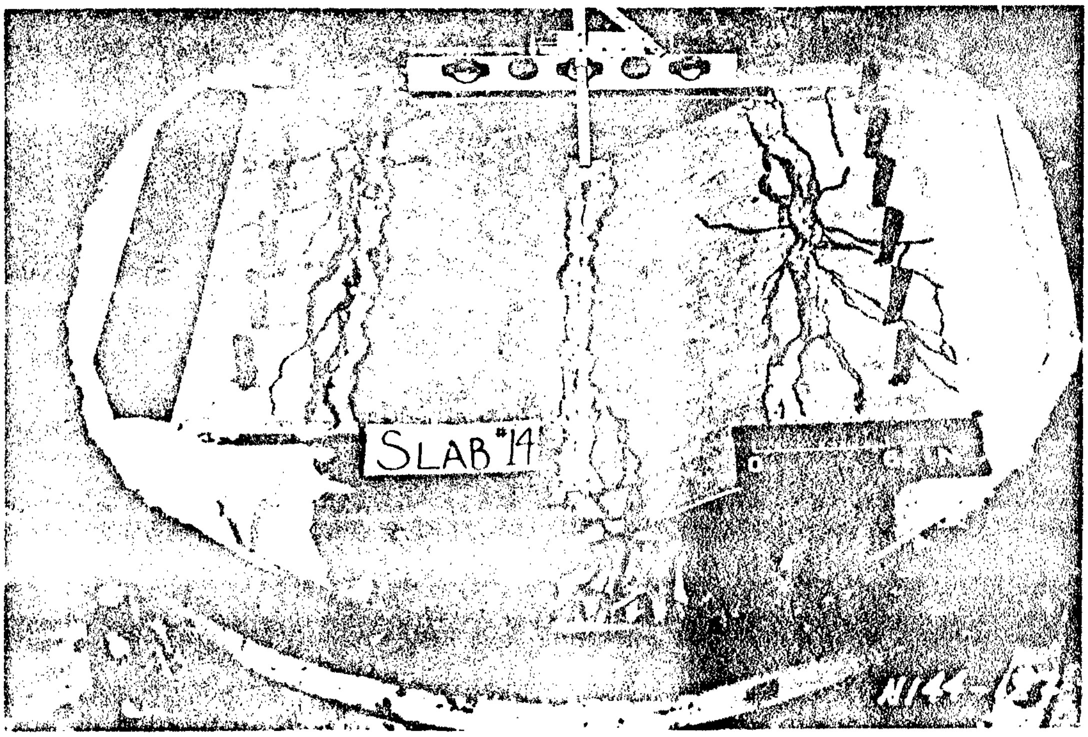

Figure 4.29. Slab 14, posttest.

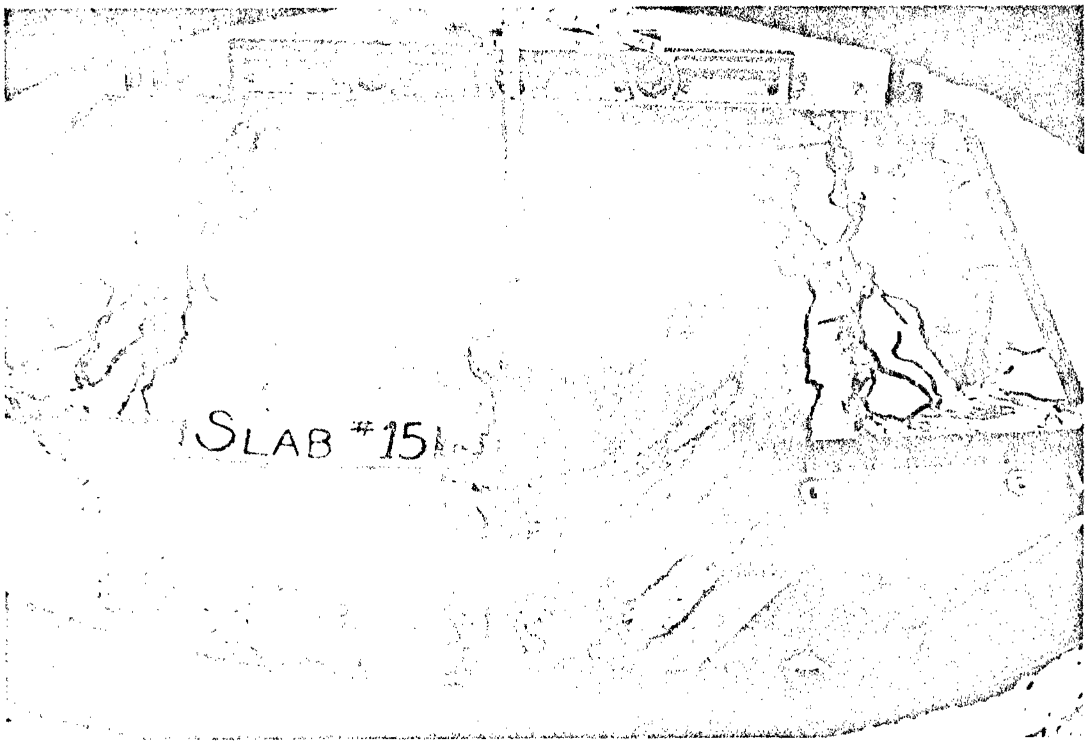

Figure 4.30. Slab 15, posttest.

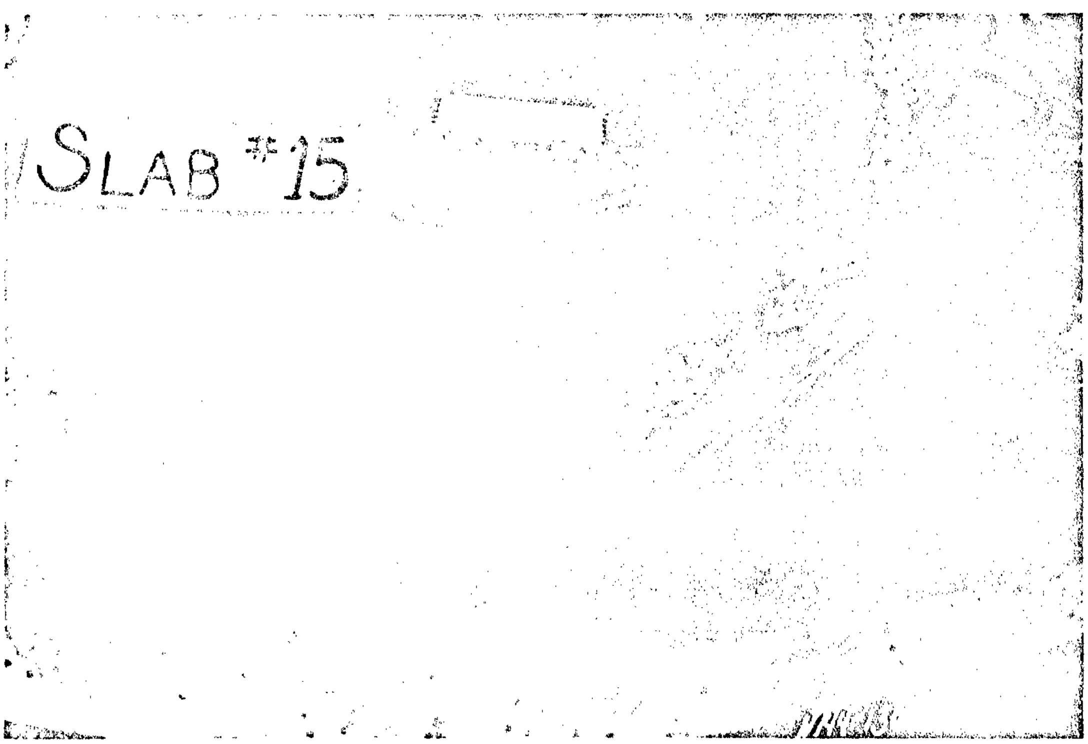

Figure 4.31. Closeup view of Slab 15, posttest.

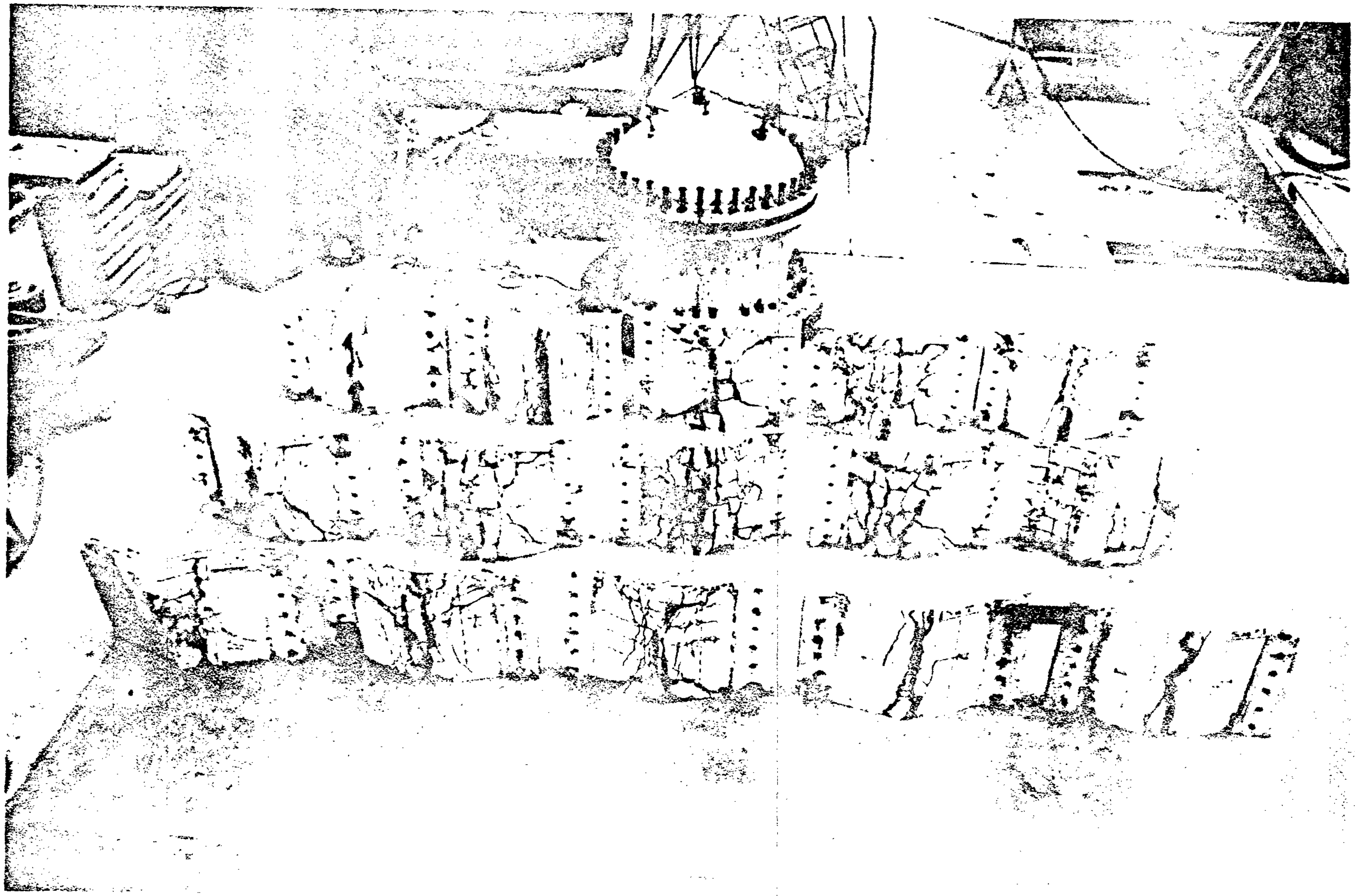

Figure 4.32. Slabs 1-15, posttest.

CHAPTER 5

DATA EVALUATION

5.1 YIELD-LINE CAPACITY

For a one-way slab with no thrust, yield-line capacity increases with the percentage of reinforcement in the tensile region. Predicted yield-line capacity was greatest for Slab 6 ($\rho = 0.0158$) and for Slabs 7 through 13 ($\rho = 0.0113$).

The experimental capacity for Slab 6 was much lower than expected due to the four-hinge failure mechanisms induced by the reinforcing pattern (Figure 5.1). Interior hinges formed near the center of the diagonal section of rebar between bends, resulting in a reduced depth of section and reduced capacity

Yield-line capacities for all slabs are listed in Table 5.1. The capacity for Slab 6 has been revised to reflect test hinge locations.

5.2 COMPRESSIVE MEMBRANE BEHAVIOR

Due to compressive membrane forces, ultimate capacity in laterally restrained slabs can be several times greater than yield-line capacity. The greatest increase occurs for thick unreinforced slabs fully restrained against edge displacement (Reference 9). The ratio of ultimate capacity to yield-line capacity, q_{ult}/q_{yl} , decreases as the percentage of tensile reinforcement increases and increases as the span-to-thickness ratio becomes smaller

Previous tests have been conducted on one-way slabs with larger L/h ratios (≥ 19) by Christiansen and by Roberts as summarized by Iqbal and Derecho (Reference 10). The reinforcement ratio, ρ , was 0.0062 in Christiansen's tests and varied from 0.0023 to 0.0093 in Roberts' tests. Ratios of q_{ult}/q_{yl} for Christiansen's test varied from 1.42 to 3.83 for $L/h = 20$ and $\rho = 0.0062$. Roberts reported values of q_{ult}/q_{yl} as high as 17 for $L/h = 19$ and $\rho = 0.0023$.

For the 15 slabs tested, ρ varied from 0.0074 to 0.0114 and q_{ult}/q_{yl} varied from 1.05 to 1.55. The lowest ratios of q_{ult}/q_{yl} were for Slabs 7 through 9 and Slab 13. Most of the reinforcement in these slabs was in the tensile zone, and relatively little thrust was developed. Ratios of q_{ult}/q_{yl} for slabs with ρ' equal to ρ (Slabs 1, 2, and 14) ranged from

1.38 to 1.42. This agrees with Keenan's conclusion (Reference 11) that for ρ greater than some critical value (0.6 to 0.8 percent for two-way slabs) ultimate capacity increases with ρ'/ρ

Values of q_{ult}/q_{yl} for Slabs 10 through 12 were slightly greater than those for Slabs 7 through 9 and Slab 13. Although principal reinforcing was similar for Slabs 7 through 13, closely spaced stirrups in Slabs 9 through 12 provided concrete confinement. The ultimate capacity was further enhanced in Slab 12 by the placement of temperature steel on the outside of principal steel, which resulted in a larger core of confined concrete. The small increase in capacity is probably the result of increased ultimate concrete strain and a slight increase in concrete compressive strength due to confinement. Results for Slab 9, in which 26 strain gages were embedded, may have been affected by the gages and their wiring. The large number of wires may have affected the crack pattern.

Slabs 3 and 4 behaved similarly up to ultimate capacity. Slab 4 test pressure was lost near ultimate capacity, and the Slab was reloaded. The ratio, q_{ult}/q_{yl}, for Slabs 3 and 4 was 1.55. This ratio is the highest for all slabs tested. The large enhancement in capacity is not explained by Park's equations, which give q_{ult}/q_{yl} of 1.04 and 1.14, respectively, at the experimental ultimate deflections.

For Slab 5, with ρ' approximately equal to ρ at supports, q_{ult}/q_{yl} was 1.27. Due to the four-hinge failure mechanism of Slab 6, very little deflection was required to develop ultimate capacity, resulting in a relatively large q_{ult}/q_{yl} of 1.32.

In spite of high enhancement factors for Slabs 1 and 2, the more efficient placement of reinforcement in Slab 5 and Slabs 7 through 12 resulted in higher ultimate capacities. Average q_{ult} for Slabs 1 and 2 was 65 psi. Average q_{ult} for Slab 5 and Slabs 7 through 12 was 70.9 psi. Slab 13, with cutoff bars rather than bent continuous bars, had a q_{ult} of 664 psi.

Park's formulas (Reference 3) were used to predict ultimate capacity and for reference are given in Appendix B. Park recommends using a ratio of deflection at ultimate capacity (Δ_{ult}) to slab thickness (h) of 0.5. Experimental values ranged from 0.11 for Slab 6 to 0.52 for Slab 3. Excluding Slab 6, average Δ_{ult}/h was 0.4.

After completion of the test, ultimate capacity was recalculated using experimental values for Δ_{ult}/h and hinge location. Recalculated ultimate capacities were within 5 to 6 percent of the experimental values in most cases. The exceptions were Slabs 1, 3 through 5,10, and 11. The difference for Slab 1 probably resulted from a poor choice of Δ_{ult}. For a deflection of 1 inch, calculated ultimate capacity is 56.5 psi. For a deflection of 3/4 inch, q_{ult} is 65.5 psi. The pressure-deflection curve for Slab 1 (see Appendix A) changes slope sharply near maximum pressure, indicating that the peak may have been "pushed over" by slip at the supports and that a lower Δ_{ult} should be used. The large ultimate capacities of Slabs 3 and 4 have not been explained. Ultimate capacities for Slabs 10 and 11 may have exceeded predicted values due to the confinement provided by close stirrup spacing.

Experimental values for ultimate capacity are compared with calculated values in Table 5.1.

The resistance curves predicted by Park's equations for the region from B to C were conservative for all slabs except Slab 6. For Slab 6, resistance in the compressive membrane region was limited by concrete crushing and an apparent sudden loss of compressive strength.

Results of the Park equations for Slabs 1, 3, 6, and 8 are plotted in Figures 5.2 through 5.5.

5.3 SECONDARY RESISTANCE

In the theoretical resistance curve of Figure 4.1, secondary resistance is equal to the yield-line capacity and is represented by Point C.

In general, slabs with little enhancement due to compressive membrane forces should have little decrease in capacity after q_{ult} Those whose ultimate capacity is dependent on large compressive forces should experience a large decrease, often to less than yield-line capacity, as concrete crushes and compressive reinforcing goes into tension.

Theoretical deflection at Point C, Δ_c, can be calculated using Park's equation for tensile membrane capacity (Reference 4) with W equal to yield-line capacity. If the ratio of tensile forces in the y and x directions, T_y/T_x, is equal to infinity for a one-way slab, Park's equation becomes

$$\frac{wL_y^2}{\Delta T_y} = 8 \tag{5.1}$$

T_y is assumed to be equal to the total area of reinforcing multiplied by yield stress. In the slabs tested, however, tensile reinforcement began to rupture shortly after ultimate capacity was reached. Because of the reduced T_y, slab resistance did not follow the theoretical curve (Figure 4.1) beyond Point B. Slip at the supports may have also contributed to the variation from the theoretical curve.

The behavior of the test slabs is better represented by Figure 5.6 with C_1 approximately the point at which compressive membrane behavior ends and C_2 the point at which capacity begins to increase due to tensile membrane behavior.

Pressure and deflection at Points C_1 and C_2 are given in Table 5.2. Deflections calculated at yield-line capacity are given for comparison.

5.4 TENSILE MEMBRANE BEHAVIOR

Capacity in the tensile membrane region is proportional to deflection. Capacity for various deflections was predicted using Equation 5.1. All reinforcement was assumed to rupture at or near Point D.

After testing was completed, the tensile membrane slope was recalculated using the area of reinforcing remaining intact at the end of each test. The recalculated slope closely followed the slope of the end of the resistance curve for most slabs.

Slab 6 was the only slab that exhibited predictable tensile membrane behavior. Because of the reinforcement arrangement and the four-hinge failure mechanism, Slab 6 was able to carry large loads with relatively little deflection, and no reinforcing was ruptured. Predicted tensile membrane capacity was conservative, probably due to the neglect of reinforcement strain hardening. Predicted and actual resistance curves for Slabs 1, 3, 6, and 8 are shown in Figures 5.2 through 5.5.

For all slabs except 5, 11, 13, and 15, maximum capacity in the tensile membrane region was greater than q_{yl}. The percentage of reinforcing in Slab 15 was lower than for the other slabs. Cutoff bars and dowels in Slabs 5 and 13 may not have been effective in tension because of bond as concrete began to spall off.

Experimental values for Point D are given in Table 5.2. These values represent maximum attained load resistance rather than incipient collapse. Although significantly damaged (e.g., crushed concrete and ruptured reinforcing at hinges), the slabs were still capable of supporting substantial load.

Ratios of midspan deflection to clear span length (Δ/L) for Point D varied from 0.17 to 0.23. In Reference 5, Keenan and others state that two-way laterally restrained slabs should be able to support substantial load at rotations exceeding 12 degrees. For the test slabs and a three-hinge mechanism, a 12-degree rotation at the supports implies a Δ/L of 0.106. Black (Reference 12) recommended using a deflection at maximum tensile membrane capacity of 0.15 L for two-way slabs rather than the 0.1 considered "safe" by Park. Based on the results of this study, the keyworker blast shelter roof would appear to be able to support substantial load at deflections exceeding 0.15 L. However, since the shelter walls are not as rigid as the test slab supports, roof deflection predictions should not be based solely on the slab tests. The original design of the shelter was based on a roof deflection of 0.05 L (Reference 13).

5.5 FAILURE PATH

Except for Slab 3 and possibly Slab 4, tensile reinforcement at interior hinges yielded before support tensile reinforcement, indicating a first hinge at midspan. Gurfinkel (Reference 9) noted that for a beam with infinitely stiff restraints and $\rho \leq 0.006$, the first hinge will form at supports, while for a more heavily reinforced beam, the first hinge will form at midspan for $L/h > 20$. Test results at $L/h < 20$ may be due to restraints that are not perfectly rigid. The small percentage of tensile reinforcing at supports in Slabs 3 and 4 resulted in early yield of support reinforcing.

For Slabs 5 and 7 through 9, reinforcing at the supports yielded near ultimate capacity, possibly indicating a brittle failure at the supports. Strain gage data at the supports for Slabs 10 and 11 were not available.

5.6 COMPARISON OF SLAB 14 AND DYNAMIC TEST RESULTS

Slab 14 failed in a three-hinged mechanism rather than in the tensile membrane mode suspected in the roof slab of the buried box structure tested by Getchell and Kiger (Reference 7). Differences in behavior may be due to differences in loading conditions and support restraints. Slab 14 was restrained more rigidly at the supports than the roof slab of the box structure. Also, Slab 14 was tested under surface-flush conditions, whereas sand covered the roof slab of the buried box. Initial static test load was uniform, but after a slab deflected, the load distribution across the width of the slab became nonuniform. Because of the tendency of the rubber membrane to span the drop between the reaction structure sides and the slab, the load at slab edges was relieved and more load was distributed across the center of the slab. In dynamic tests, midspan loads are reduced by deflection and soil arching and load distribution across the width of a one-way slab should be uniform.

Table 5.1. Comparison of tneoretical and test values for ultimate resistance.

Slab No.	Yield Line Resistance psi	Initial Design Values[a]					Test Results						Posttest Analysis[b]	
		Δ/h	β	f'_c ksi	f_y ksi	Ultimate Resistance q_{ult}, psi	Δ/h	β	f'_c ksi	f_y ksi	Ultimate Resistance q_{ult}, psi	$\frac{q_{ult}}{q_{yl}}$	Ultimate Resistance q_{ult}, psi	$\frac{q_{ult}}{q_{yl}}$
1	46.7	0.5	0.5	4.0	60	46.3	0.43	0.5	4.47	66.0	66	1.41	56.5	1.21
2	46.3	0.5	0.5	4.0	60	45.7	0.35	0.5	4.47	66.0	64	1.38	62.9	1.36
3	43.9	0.5	0.5	4.0	60	43.6	0.52	0.5	4.47	63.0-63.5	68	1.55	45.8	1.04
4	43.9	0.5	0.5	4.0	60	59.3	0.48	0.5	4.49	63.0-63.5	68	1.55	50.0	1.14
5	60.9	0.5	0.5	4.0	60	59.3	0.43	0.5	4.49	63.0-63.5	77	1.26	68.0	1.12
6	51.6	0.5	0.5	4.0	60	59.3	0.11	0.21	4.49	66.0	68	1.32	71.6	1.39
7	61.2	0.5	0.5	4.0	60	57.7	0.43	0.5	4.27	66.0	67	1.09	66.6	1.09
8	61.2	0.5	0.5	4.0	60	57.7	0.35	0.5	4.27	66.0	68	1.11	71.3	1.17
9	61.2	0.5	0.5	4.0	60	57.7	0.35	0.5	4.03	66.0	67	1.09	67.4	1.10
10	61.2	0.5	0.5	4.0	60	57.7	0.39	0.5	4.03	66.0	73	1.19	67.4	1.10
11	61.2	0.5	0.5	4.0	60	57.7	0.41	0.5	4.16	66.0	73	1.19	67.1	1.10
12	61.2	0.5	0.5	4.0	60	57.7	0.35	0.5	4.16	66.0	71	1.15	70.5	1.15
13	61.2	0.5	0.5	4.0	60	57.7	0.32	0.5	4.16	66.0	64	1.05	--	--
14	88.5	0.5	0.5	4.0	60	100.7	0.28	0.5	3.56	60.3	126	1.42	123.71	1.40
15	44.2	0.5	0.5	4.0	60	45.1	0.43	0.5	3.56	66.0	52	1.20	49.9	1.13

[a] Using Park's equations.
[b] Using Park's equations and test values for Δ/h, β, f'_c, f_y.

Table 5.2. Experimental pressure-deflection curves.

Slab No.	Point B: q psi	Point B: Δ in	Point B: q/q_{y1}	Point B: Δ/h	Point C_1: q psi	Point C_1: Δ in	Point C_1: q/q_{y1}	Point C_1: Δ/h	Point C_2: q psi	Point C_2: Δ in	Point C_2: q/q_{y1}	Point C_2: Δ/h	Point D: q psi	Point D: Δ in	Point D: q/q_{ult}	Point D: q/q_{y1}	Point D: q Δ/L	Theoretical Point C: q psi	Theoretical Point C: in	Theoretical Point C: Δ/h
	Experimental Values																			
1	66	1.0	1.41	0.43	39	1.8	0.84	0.78	37	3.3	0.79	1.12	48	4.1	0.73	1.03	0.17	46.7	2.14	0.925
2	64	0.8	1.38	0.35	37	2.4	0.80	1.04	37	2.7	0.80	1.17	55	4.3	0.86	1.19	0.18	46.3	2.12	0.917
3	68	1.2	1.55	0.52	45	2.5	1.03	1.08	37	3.0	0.84	1.30	58	4.6	0.85	1.32	0.19	43.9	2.06	0.891
4	68	1.1	1.55	0.48	--	--	--	--	53	2.2	1.21	0.95	60	4.5	0.88	1.37	0.19	43.9	2.06	0.891
5	77	1.0	1.16	0.43	42	2.7	0.71	1.17	43	3.2	0.71	1.38	55	4.4	0.71	0.90	0.18	60.9	2.86	1.237
6A	68	0.25	1.32	0.11	41	0.4	0.79	0.17	41	0.7	0.79	0.30	100	3.05	1.47	1.94	0.13	51.6	2.36	1.237
6B													122	5.0	1.79	2.36	0.21			
7	67	1.0	1.09	0.43	60	1.9	0.98	0.82	50	3.7	0.82	1.60	63	5.7	0.94	1.03		61.2	2.80	1.211
8	63	0.8	1.11	0.35	60	2.0	0.98	1.64	57	3.5	0.93	1.51	70	5.0	1.03	1.14	0.21	61.2	2.80	1.211
9	67	0.8	1.09	0.35	60	1.8	0.98	0.78	56	4.0	0.92	1.73	71	5.3	1.06	1.16	0.22	61.2	2.80	1.211
10	73	0.9	1.19	0.39	52	1.9	0.85	0.82	41	3.2	0.67	1.38	62	5.2	0.85	1.01	0.22	61.2	2.80	1.211
11	73	0.95	1.19	0.41	--	--	--	--	33	2.5	0.54	1.08	54	4.2	0.74	0.68	0.18	61.2	2.80	1.211
12	71	0.8	1.16	0.35	--	--	--	--	54	2.3	0.88	0.99	77	4.2	1.08	1.27	0.18	61.2	2.80	1.211
13	64	0.75	1.05	0.32	37	1.8	0.60	0.78	33	2.6	0.54	1.12	46	5.4	0.72	0.75	0.23	61.2	2.80	1.211
14	126	0.8	1.42	0.28	32	2.3	0.36	0.99	26	3.5	0.29	1.51	96	5.0	0.76	1.08	[illegible]	88.5	2.16	0.745
15	52	1.0	1.18	0.43	27	2.6	0.61	1.12	24	3.4	0.54	1.47	36	5.2	0.69	0.81	0.22	44.2	7.58	1.116

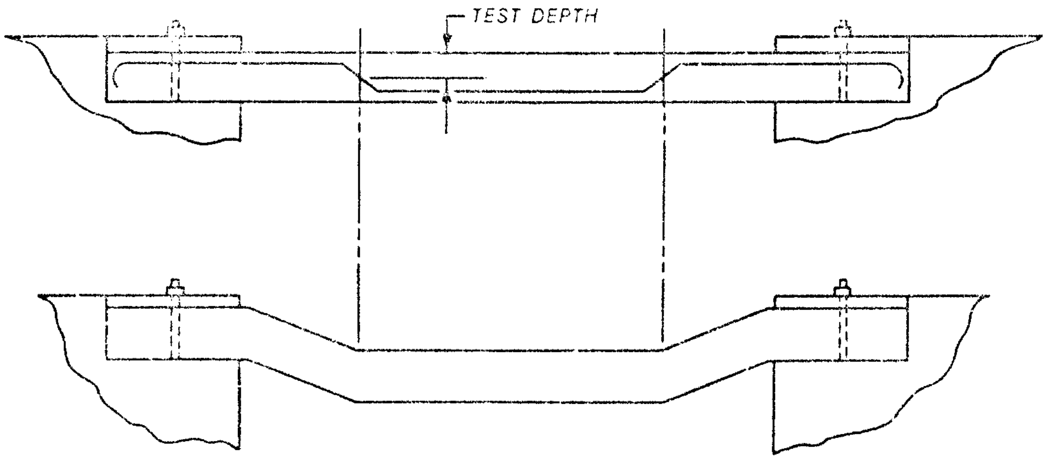

Figure 5.1. Four-hinge failure mechanisms induced by reinforcing pattern.

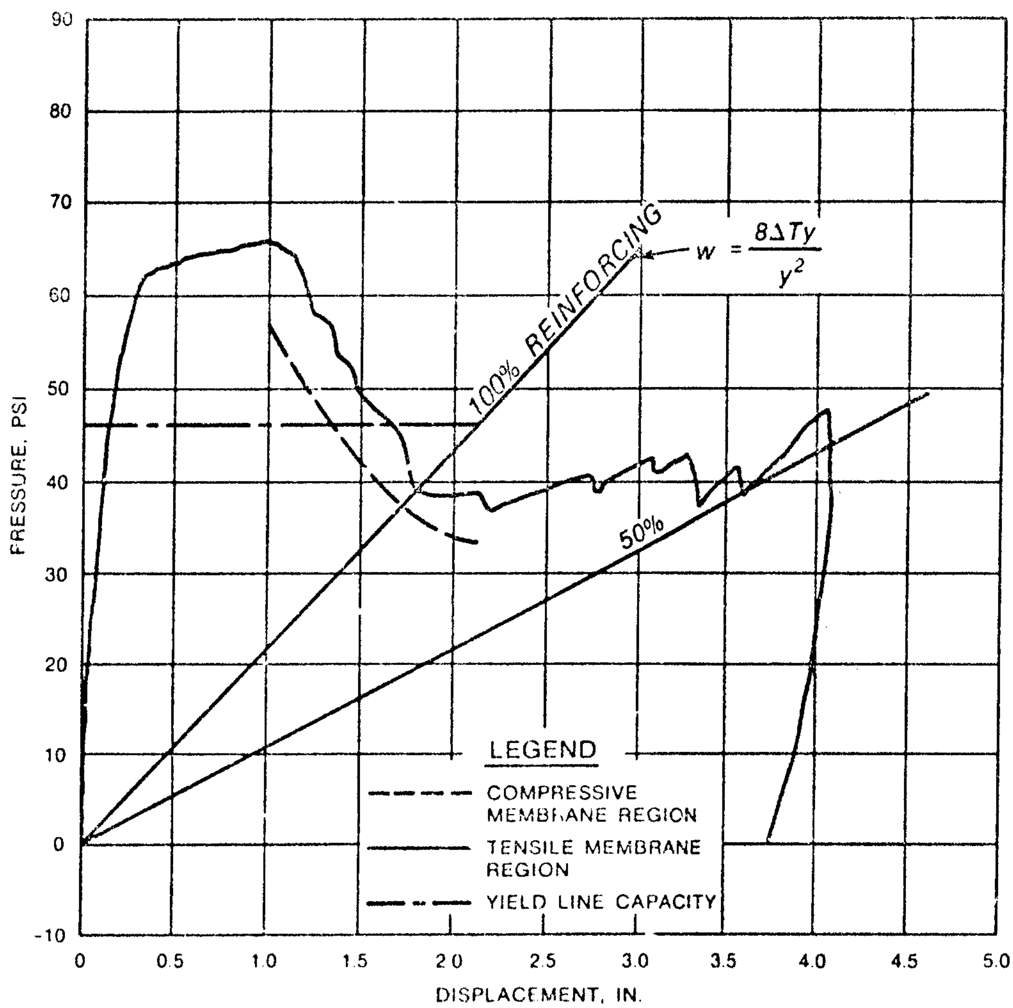

Figure 5.2. Predicted and actual resistance curves, Slab 1.

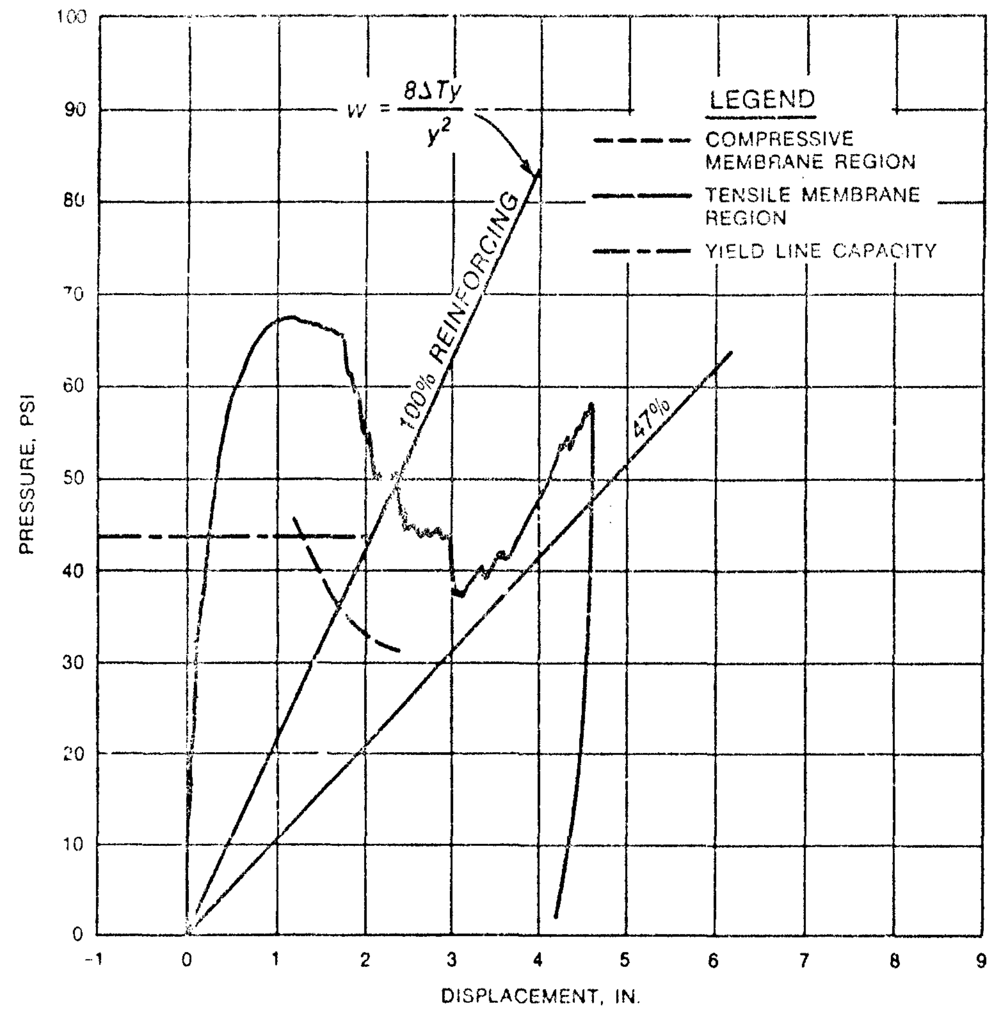

Figure 5.3. Predicted and actual resistance curves, Slab 3.

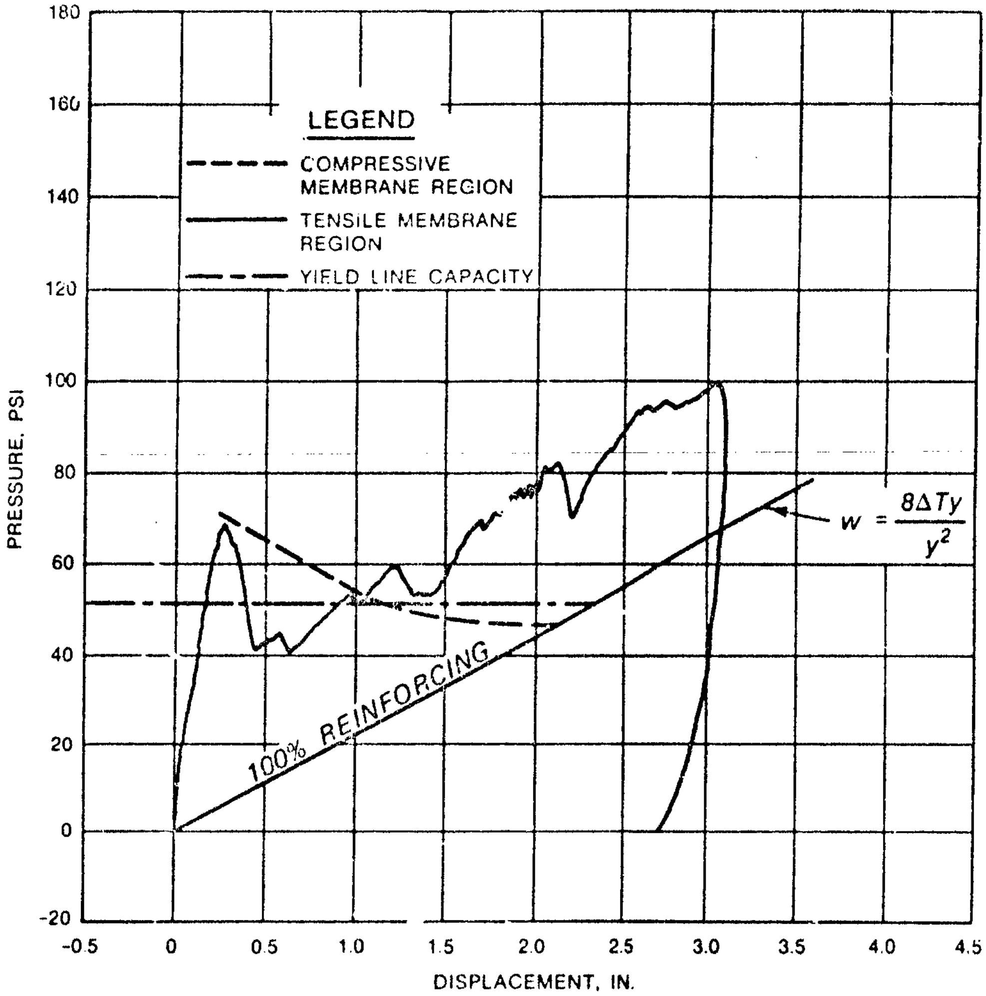

Figure 5.4. Predicted and actual resistance curves, Slab 6.

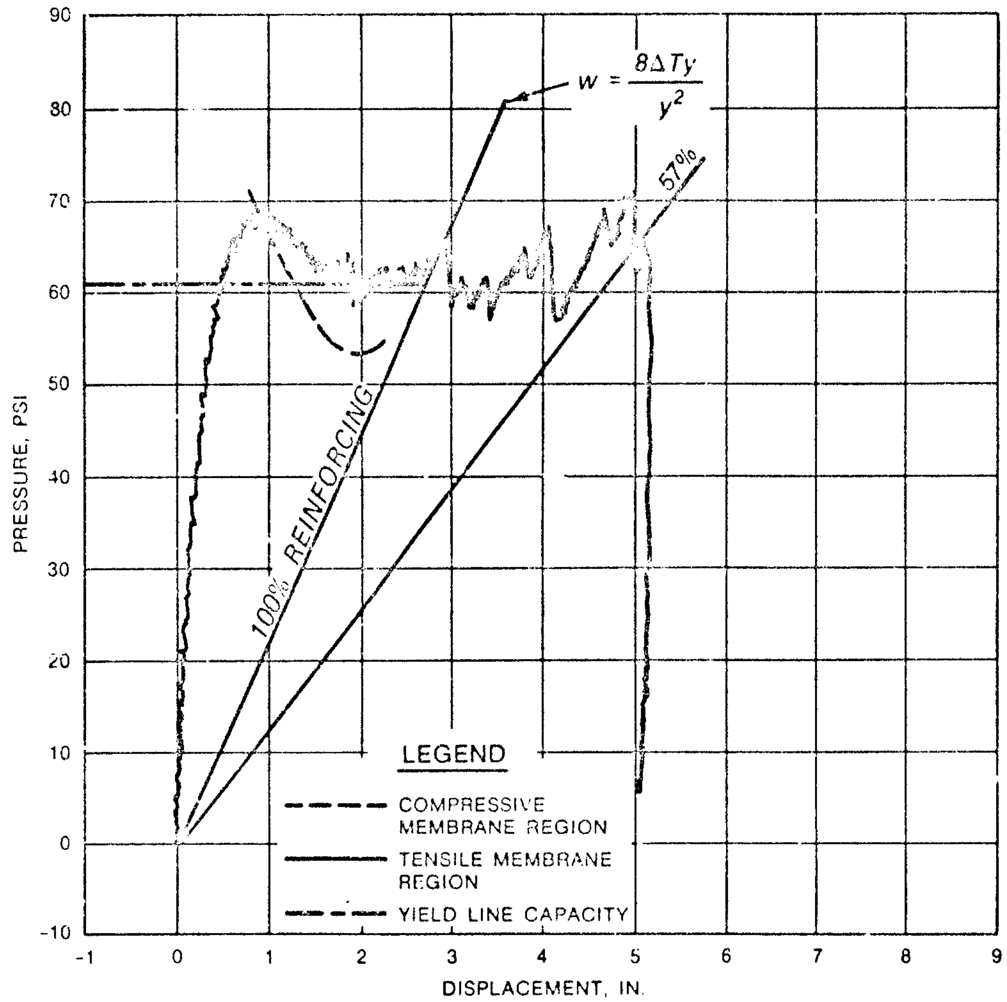

Figure 5.5. Predicted and actual resistance curves, Slab 8.

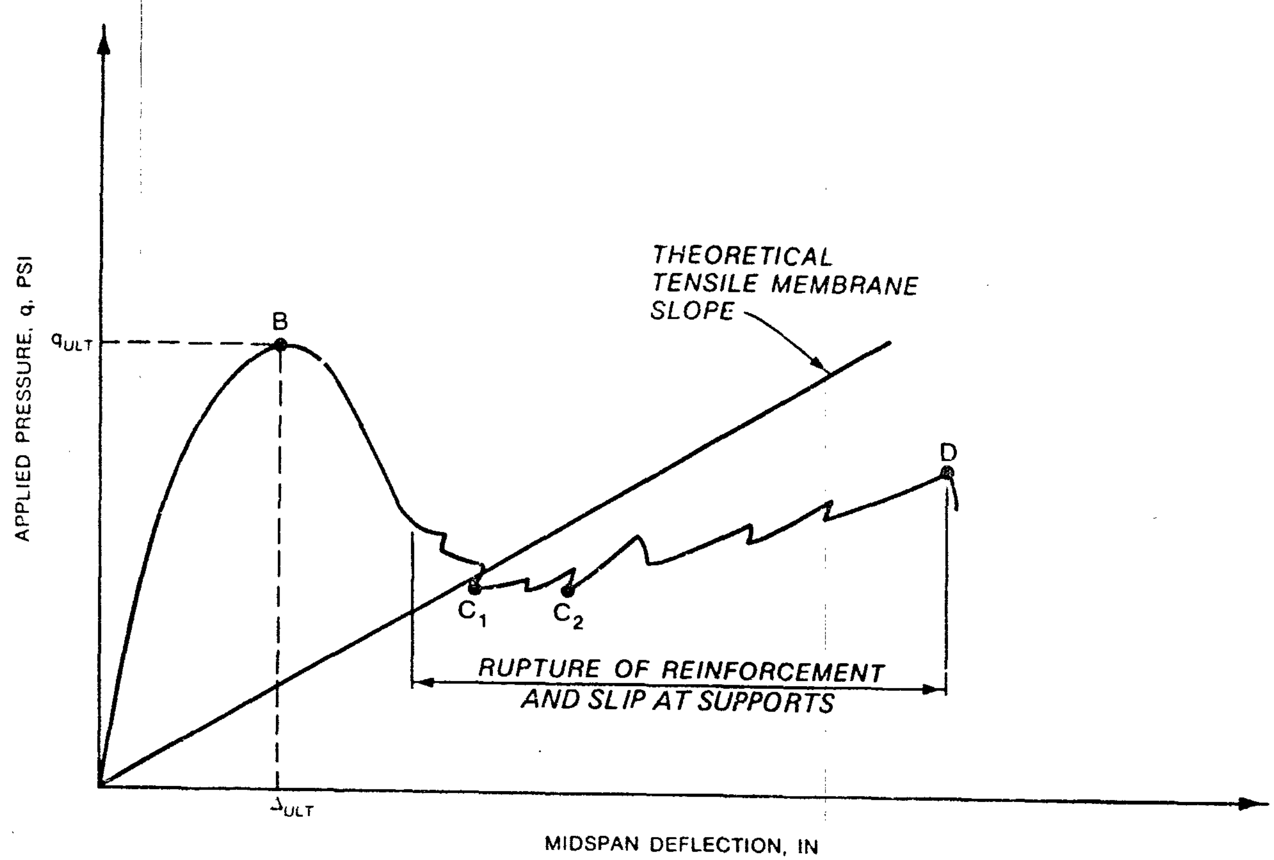

Figure 5.6. Revised load-deflection relationship.

CHAPTER 6

CONCLUSIONS AND RECOMMENDATIONS

6.1 CONCLUSIONS

The primary objective of this project was to determine the reinforcing pattern that would provide the greatest tensile membrane capacity for given depth and total area of steel in the FEMA keyworker shelter roof slab. Secondary objectives were (1) to determine the effect of reinforcing patterns on ultimate and secondary capacity, (2) to determine the effect of stirrups and placement of temperature reinforcement on slab capacity, and (3) to relate the behavior of the clamped slabs to that of a dynamically tested buried box. The following conclusions relating to those objectives are based on the data for the 15 slabs tested.

Slabs with reinforcement configurations that produce the greatest yield-line capacity exhibit the best tensile membrane behavior for a given total area of steel. Bending all principal reinforcement such that only initial tension zones are reinforced and compression zones are not (e.g., Slab 6) provides good tensile membrane behavior, but significant concrete spalling occurs due to the lack of confinement. Tensile membrane action is considerably less in slabs having 50 percent of the reinforcement bent into tension zones with the remaining 50 percent divided equally among the top and bottom faces (e.g., Slab 7). The reinforcement configuration used in Slab 7 results in ductile behavior with the load resistance remaining near the ultimate resistance up to midspan deflections exceeding 24 percent of clear span.

Placement of stirrups on 50 percent of the reinforcement in the Slab 7 configuration (e.g., Slabs 8 and 9) aids in the development of tension between top bars broken at the supports and bottom bars broken at midspan. This improves tensile membrane behavior slightly. The enhancement is not significant because the stirrups are placed on only 50 percent of the reinforcement (not on the bent bars). For the same reason, stirrup spacing only slightly affects the load-response behavior of slabs with this principal reinforcement configuration. The combination of closely spaced stirrups with temperature steel placed exterior to the principal steel affects the load response of similarly reinforced slabs (e.g., Slab 12) to a greater degree. The load resistance of

Slab 12 was equivalent to or above the ultimate resistance at midspan deflections around 23 percent of clear span.

For the slabs with a total percentage of reinforcing of about 1.6 percent, ultimate capacity varied little with the reinforcement arrangement. Slabs with the most reinforcement in tension zones had a high yield-line capacity but almost no enhancement due to compressive membrane action. Slabs with $\rho = \rho'$ had a lower yield-line capacity, but compressive membrane action resulted in an ultimate resistance approximately 40 percent greater than the yield-line capacity. Using a Δ_{ult}/h value of 0.4 in compressive membrane theory calculations predicted the ultimate capacity more closely than the 0.5 value recommended by Park (Reference 3).

Due to differences in loading conditions and support restraints the three-hinge failure mode of a surface-flush clamped slab (Slab 14) differed from the general cracking pattern across much of the slab span observed in the buried box's roof slab (Reference 7).

6.2 RECOMMENDATIONS

The most predictable tensile membrane behavior was observed in the slab reinforced only in tension zones (Slab 6). However, because of concrete spalling, Slab 6 is not a recommended roof design.

The recommended roof slab design for the keyworker shelter consists of bending 50 percent of the principal reinforcement into the tension zones and dividing the remaining 50 percent equally between the top and bottom faces of the slab. This design resulted in an average static ultimate capacity of 68.5 psi and an end-of-test capacity approximately equal to or greater than the ultimate capacity in Slabs 7, 8, 9, and 12 of this test series. The omission of stirrups is recommended for this reinforcement configuration, since the benefits of stirrups are not great enough to justify their expense.

Recommendation for temperature steel placement given in Reference 6 is supported by this test series. The temperature steel should be placed "exterior" to the principal steel when stirrups are used, and probably should have the same bar diameter as the stirrups in order to maintain concrete cover. In the absence of stirrups, benefits from exterior placement may not occur since there would be a reduction in the effective depth of principal reinforcement for a given slab thickness and concrete cover.

All slabs tested had rigid supports. Tests of similar slabs with varying rotational restraint are presently being conducted at WES. These tests should be reviewed to evaluate the accuracy of modeling the prototype keyworker blast shelter roof, in which some rotation will occur at supports.

Further tests also should be conducted to determine the effect of dynamic loading and soil cover on the response of the shelter roof.

REFERENCES

1. S. A. Kiger, T. R. Slawson, and D. W. Hyde; "A Procedure for Computing the Vulnerability of Shallow-Buried Flat-Roof Structures (U)"; Technical Report SL-84-5, April 1984; US Army Engineer Waterways Experiment Station, Vicksburg, Miss.

2. T. R. Slawson and others; "Structural Element Tests in Support of the Keyworker Blast Shelter Program" (in preparation); US Army Engineer Waterways Experiment Station, Vicksburg, Miss.

3. R. Park and W. L. Gamble; "Reinforced Concrete Slabs"; 1980; John Wiley and Sons, New York, N. Y.

4. R. Park; "Tensile Membrane Behaviour of Uniformly Loaded Rectangular Reinforced Concrete Slabs with Fully Restrained Edges"; Magazine of Concrete Research, Vol. 16, No. 46, March 1964.

5. W. Keenan and others; "Structures to Resist the Effects of Accidental Explosions" (revision in preparation); Department of the Army Technical Manual TM 5-1300, Department of the Navy Publication NAVFAC P-397, Department of the Air Force Manual AFM 88-22, Department of the Army, the Navy, and the Air Force; Washington, DC.

6. S. C. Woodson; "Effects of Shear Stirrup Details on Ultimate Capacity and Tensile Membrane Behavior in Reinforced Concrete Slabs" (in preparation); US Army Engineer Waterways Experiment Station, Vicksburg, Miss.

7. J. V. Getchell and S. A. Kiger; "Vulnerability of Shallow-Buried Flat-Roof Structures; Report 2, Foam HEST 1"; Technical Report SL-80-7, October 1980; US Army Engineer Waterways Experiment Station, Vicksburg, Miss.

8. W. L. Huff; "Test Devices, Blast Load Generator Facility"; Miscellaneous Paper N-69-1, April 1969; US Army Engineer Waterways Experiment Station, Vicksburg, Miss.

9. G. R. Gurfinkel; "Analysis of Behavior of Reinforced Concrete Beams Restrained at the Ends Against Longitudinal Displacement"; M.S. Thesis, 1966; University of Illinois, Urbana, Ill.

10. M. Iqbal and A. T. Derecho; "Design Criteria for Deflection Capacity of Conventionally Reinforced Concrete Slabs, Phase I--State of the Art Report"; Report No. CR 80.026, October 1980; Construction Technology Laboratories, Portland Cement Association, Skokie, Ill.

11. W. A. Keenan; "Strength and Behavior of Restrained Reinforced Concrete Slabs Under Static and Dynamic Loads"; Technical Report R621, April 1969; US Naval Engineering Laboratory, Port Hueneme, Calif.

12. M S. Black; "Ultimate Strength Study of Two-Way Concrete Slabs"; Journal, Structural Division, American Society of Civil Engineers, Vol. 101, No. S71, January 1975, Pagès 311-324.

13. US Army Engineer Division, Huntsville; "Structural Cost Optimization for Keyworker Blast Shelters"; March 1985; Huntsville, Ala.

14. American Concrete Institute; "Building Code Requirements for Reinforced Concrete", ACI 318-83, November 1983; Detroit, Mich.

APPENDIX A

STATIC TEST DATA

PREVIOUS PAGE IS BLANK

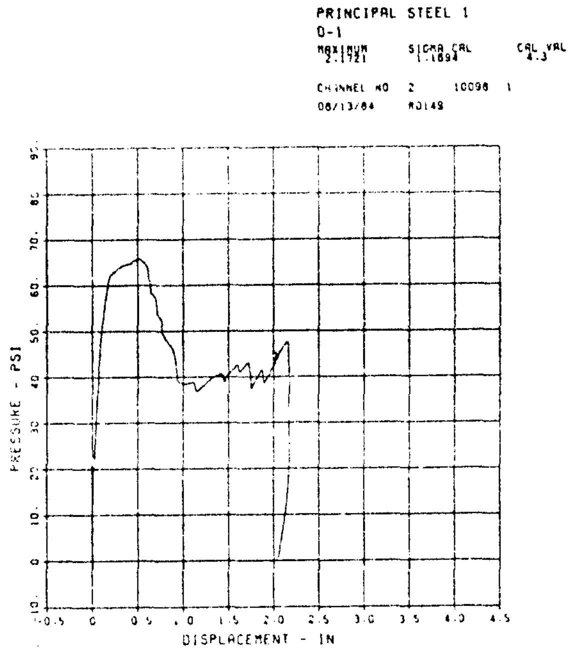
PRINCIPAL STEEL 1
D-1
MAXIMUM 2.1721
SIGMA CAL 1.1694
CAL VAL 4.3
CHANNEL NO 2 10098 1
08/13/84 R0149
PRESSURE - PSI
DISPLACEMENT - IN

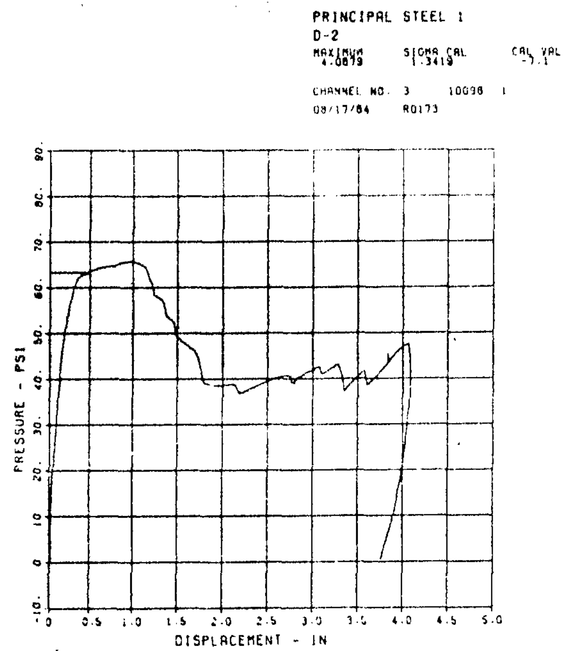
PRINCIPAL STEEL 1
D-2
MAXIMUM 4.0879
SIGMA CAL 1.3419
CAL VAL -7.1
CHANNEL NO. 3 10098 1
08/17/84 R0173
PRESSURE - PSI
DISPLACEMENT - IN

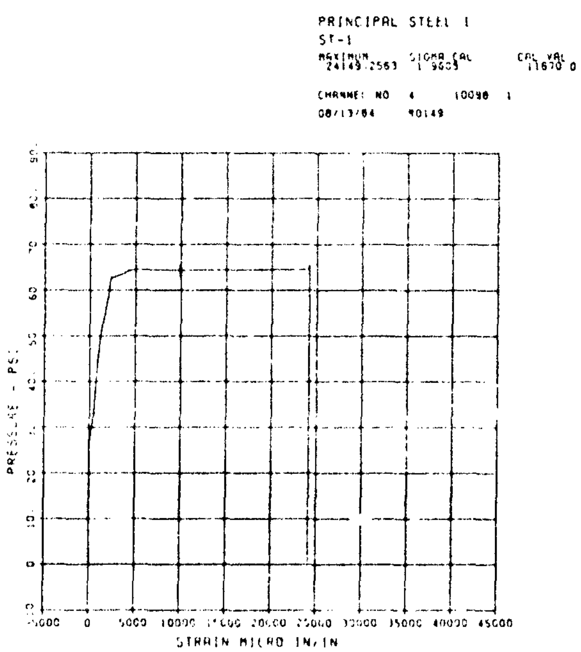
PRINCIPAL STEEL 1
ST-1
MAXIMUM 24149.2563
SIGMA CAL 1.9605
CAL VAL 11670.0
CHANNEL NO 4 10098 1
08/13/84 R0149
PRESSURE - PSI
STRAIN MICRO IN/IN

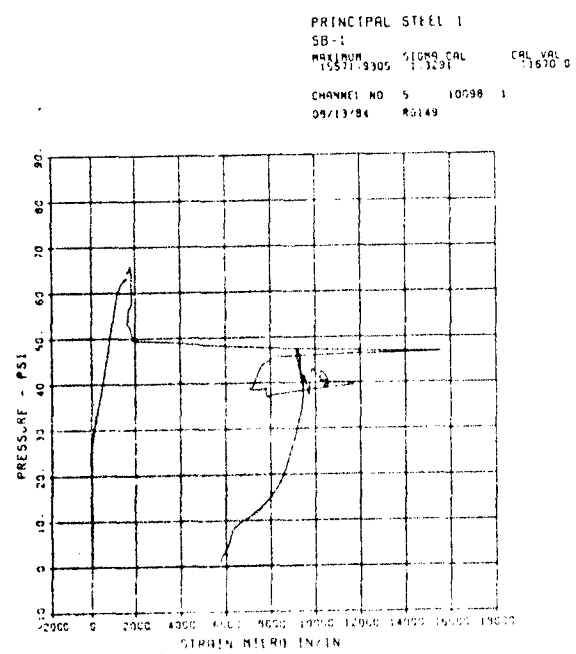
PRINCIPAL STEEL 1
SB-1
MAXIMUM 15571.9305
SIGMA CAL 1.3291
CAL VAL 11670.0
CHANNEL NO 5 10098 1
09/13/84 R0149
PRESSURE - PSI
STRAIN MICRO IN/IN

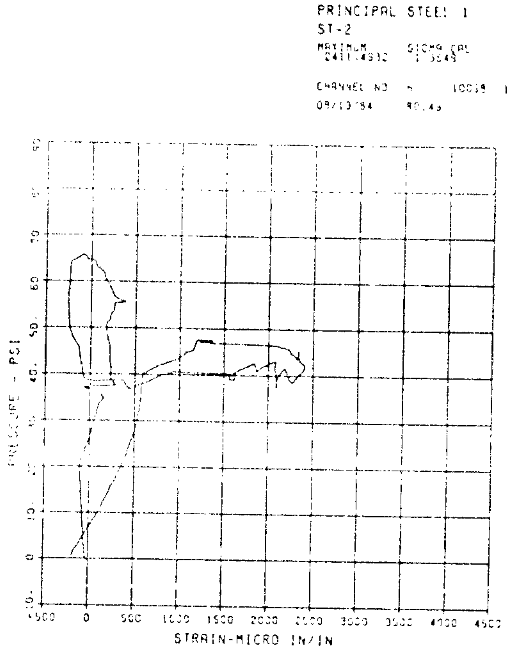
PRINCIPAL STEEL 1
ST-2
PRESSURE - PSI
STRAIN-MICRO IN/IN

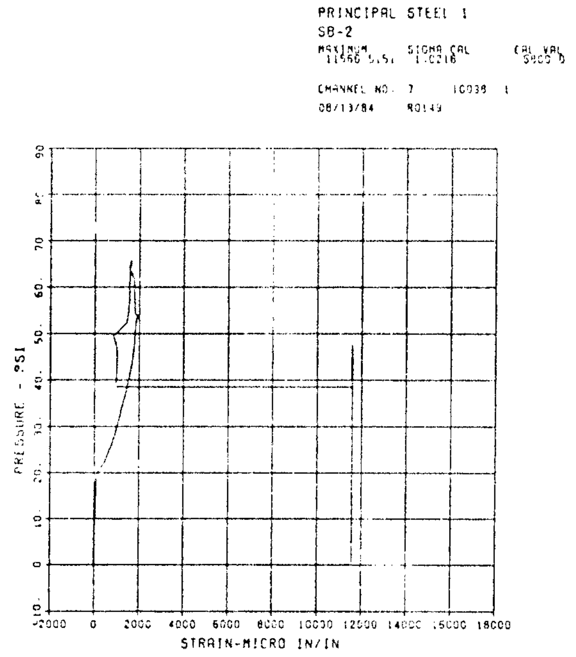
PRINCIPAL STEEL 1
SB-2
CHANNEL NO. 7
08/13/84
PRESSURE - PSI
STRAIN-MICRO IN/IN

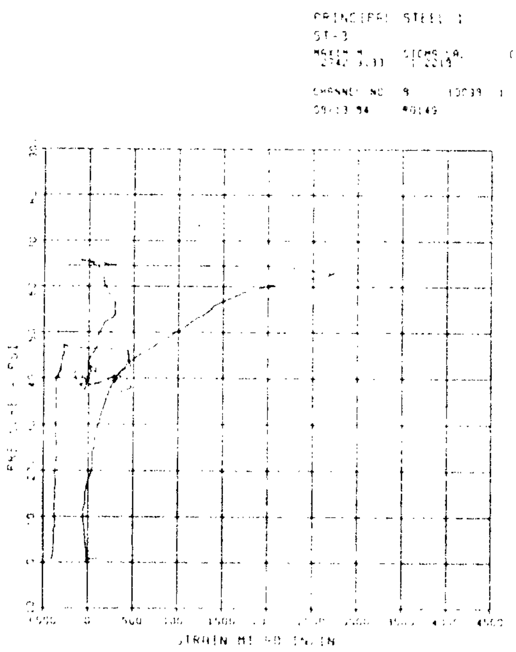

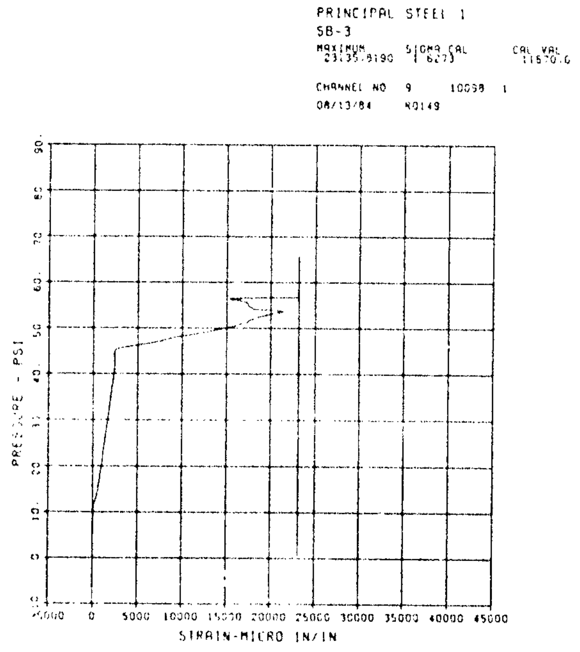
PRINCIPAL STEEL 1
SB-3
CHANNEL NO 9
08/13/84
PRESSURE - PSI
STRAIN-MICRO IN/IN

PRINCIPAL STEEL 2
D-1
MAXIMUM 2.0823 SIGMA CAL 1.1259 CAL VAL 4.3
CHANNEL NO. 2 10099 2
08/13/84 R0143

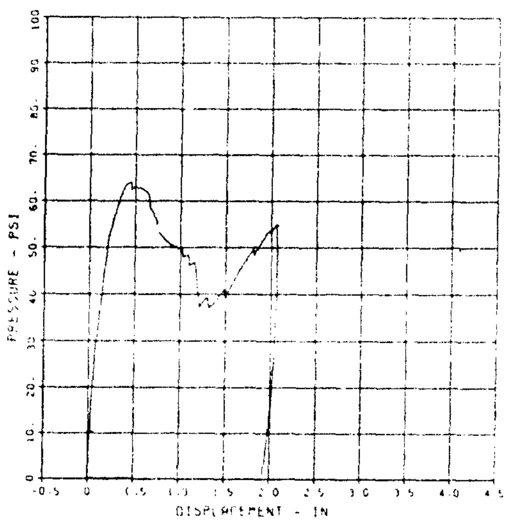

PRINCIPAL STEEL 2
D-2
MAXIMUM 4.2674 SIGMA CAL 1.2936 CAL VAL 7.1
CHANNEL NO. 3 10098 2
08/13/84 R0149

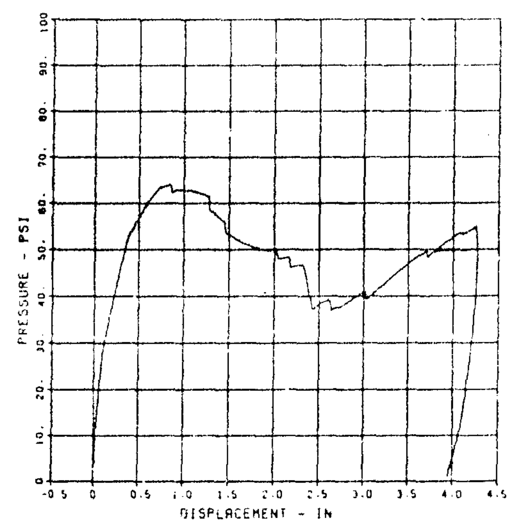

PRINCIPAL STEEL 2
ST-1
MAXIMUM 24060.6921 SIGMA CAL 2.0852 CAL VAL 11570.0
CHANNEL NO. 4 10098 2
08/13/84 R0149

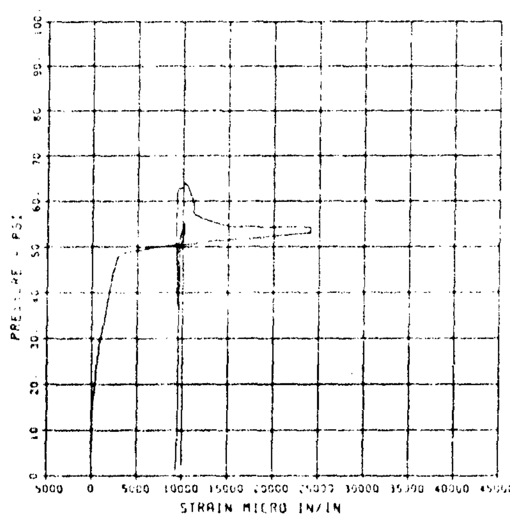

PRINCIPAL STEEL 2
SB-1
10099 2
09/26/84 R0740

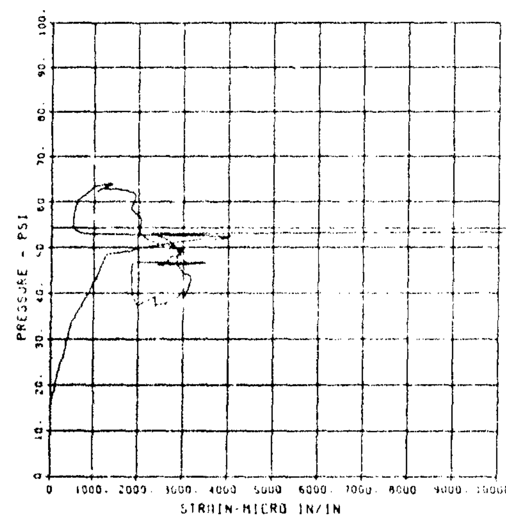

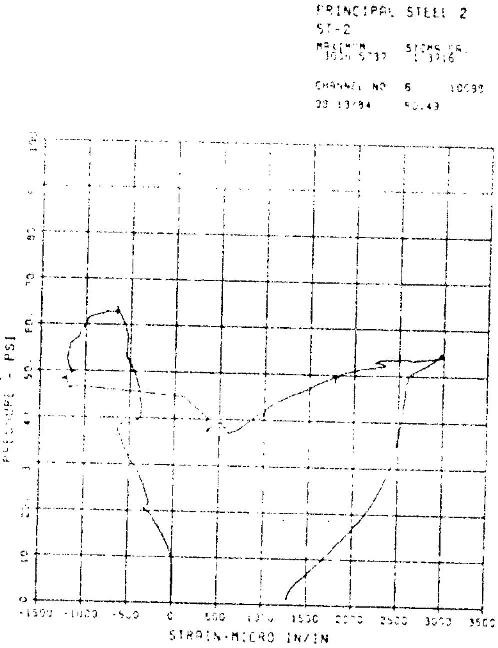
PRINCIPAL STEEL 2
ST-2
PRESSURE - PSI
STRAIN-MICRO IN/IN

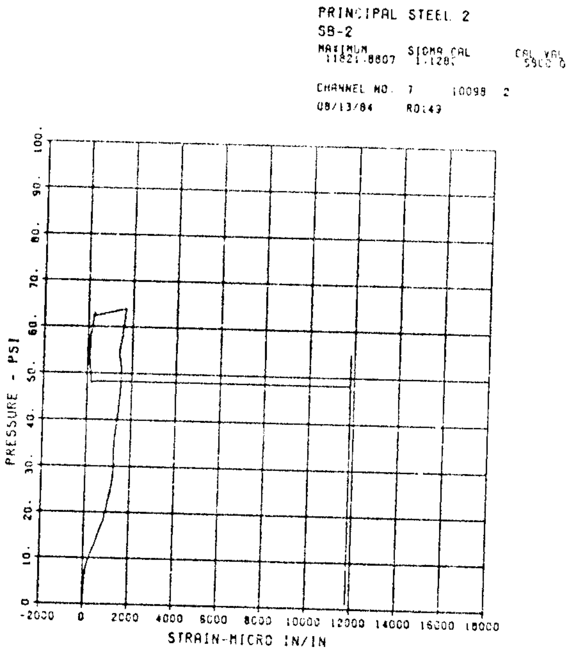
PRINCIPAL STEEL 2
SB-2
MAXIMUM
11821.8807
SIGMA CAL
CAL VAL
CHANNEL NO. 7
10098 2
08/13/84
R0:49
PRESSURE - PSI
STRAIN-MICRO IN/IN
-2000 0 2000 4000 6000 8000 10000 12000 14000 16000 18000

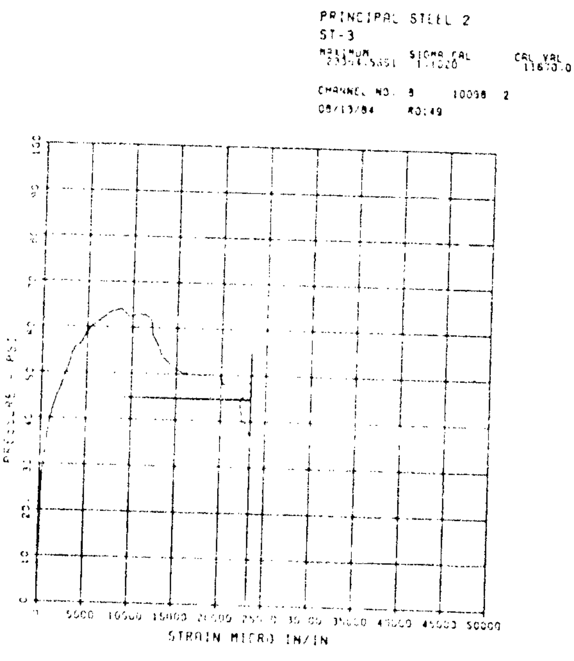
PRINCIPAL STEEL 2
ST-3
MAXIMUM
SIGMA CAL
CAL VAL
11670.0
CHANNEL NO. 8
10098 2
08/13/84
R0:49
STRAIN MICRO IN/IN

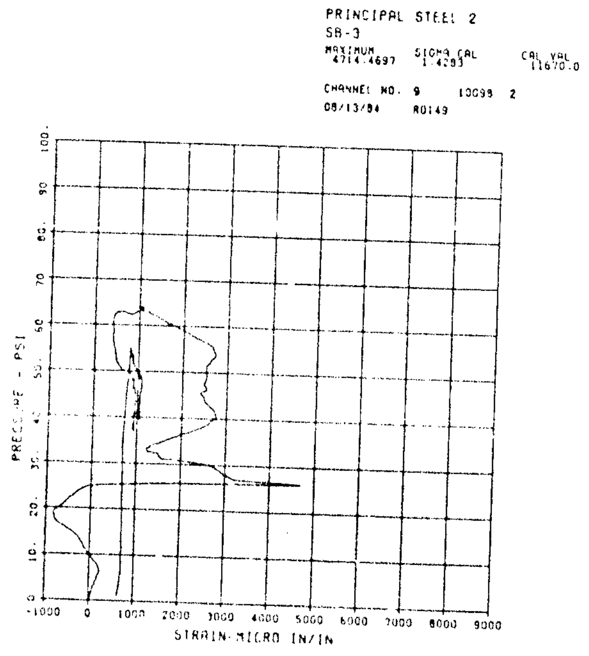
PRINCIPAL STEEL 2
SB-3
MAXIMUM
4714.4697
SIGMA CAL
1.4293
CAL VAL
11670.0
CHANNEL NO. 9
10098 2
08/13/84
R0:49
STRAIN-MICRO IN/IN
-1000 0 1000 2000 3000 4000 5000 6000 7000 8000 9000

PRINCIPAL STEEL 3
D-1
MAXIMUM 2.4806 SIGMA CAL 1.1697 CAL VAL 4.3
CHANNEL NO. 2 10288 1
08/24/84 R0173

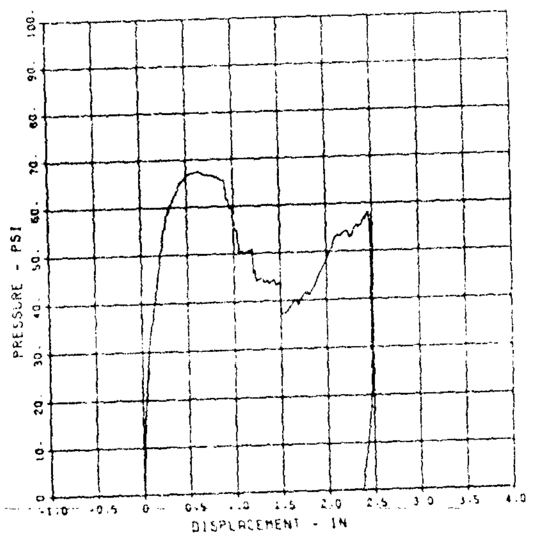

PRINCIPAL STEEL 3
D-2
MAXIMUM 4.5972 SIGMA CAL 1.4144 CAL VAL 7.1
CHANNEL NO. 3 10288 1
08/24/84 R0173

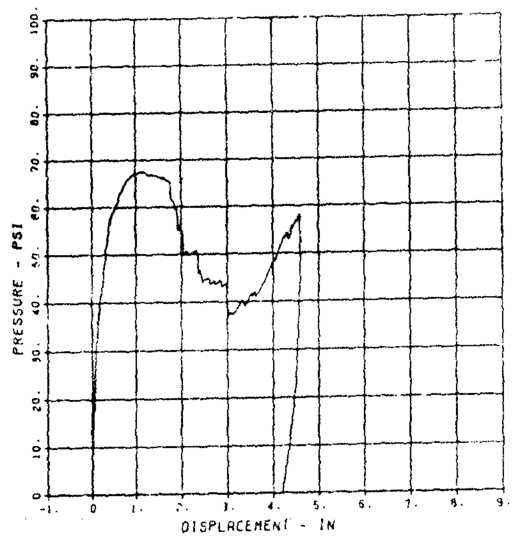

PRINCIPAL STEEL 3
ST-1
MAXIMUM 9265.2192 SIGMA CAL 1.9910 CAL VAL 11450.0
CHANNEL NO. 4 10289 1
10/19/84 R0534

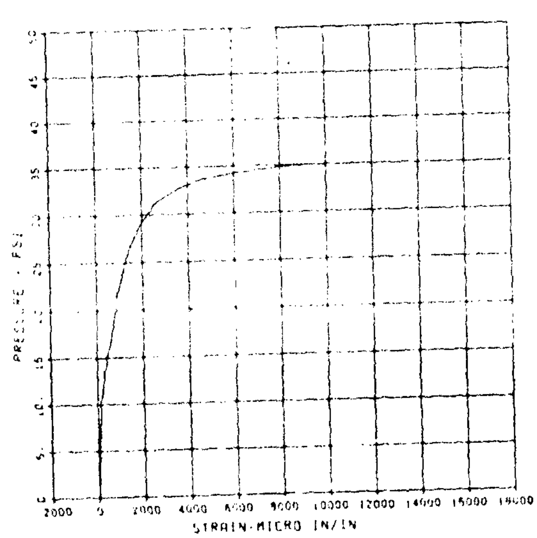

PRINCIPAL STEEL 3
SB-1
MAXIMUM 8044.7313 SIGMA CAL 1.3147 CAL VAL 11480.0
CHANNEL NO. 5 10288 1
08/24/84 R0173

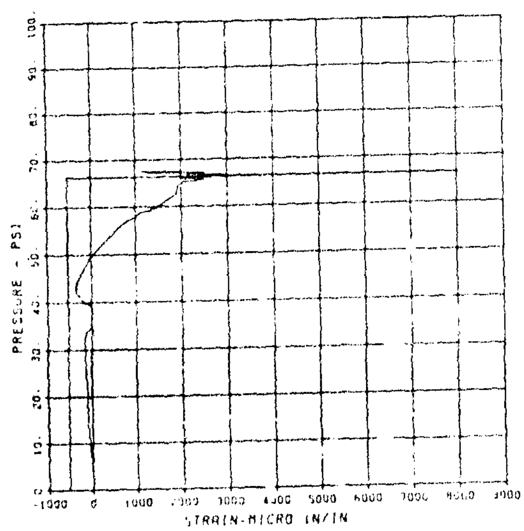

PRINCIPAL STEEL 3
ST-2
MAXIMUM 11740.5046 SIGMA CAL 1.2014 CAL VAL 5700.0
CHANNEL NO. 6 10288 1
08/24/84 R0173

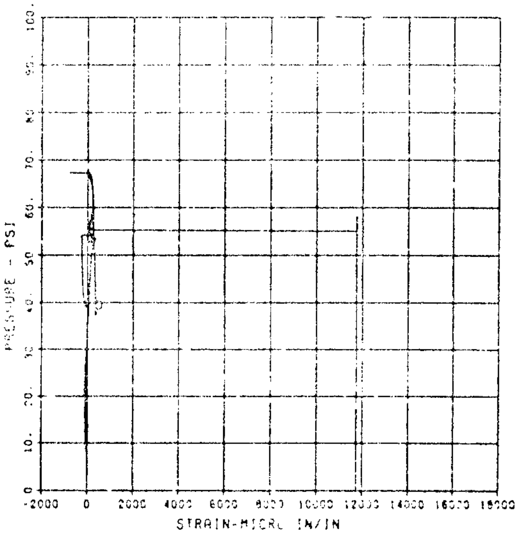

PRINCIPAL STEEL 3
SB-2
MAXIMUM 11598.2335 SIGMA CAL 1.1130 CAL VAL 5700.0
CHANNEL NO. 7 10289 1
08/24/84 R0173

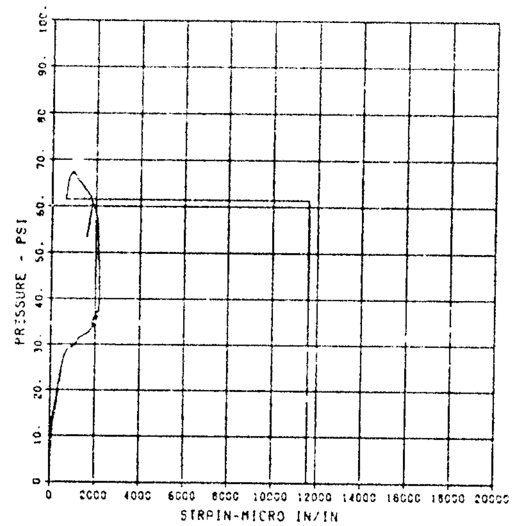

PRINCIPAL STEEL 3
ST-3
MAXIMUM -9855.2557 SIGMA CAL 1.1364 CAL VAL 11450.0
CHANNEL NO 8 10288 1
10/18/84 R0524

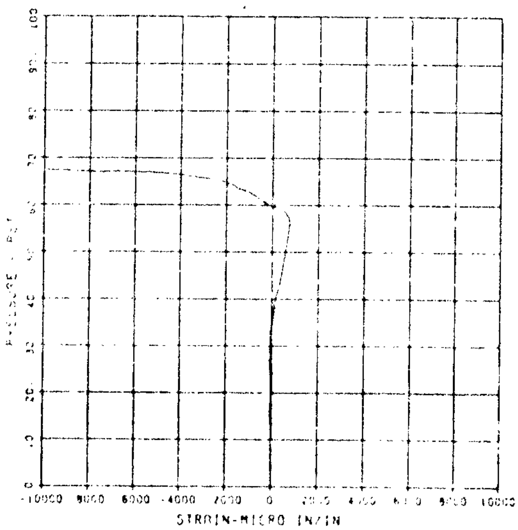

PRINCIPAL STEEL 3
SB-3
MAXIMUM 22564.0024 SIGMA CAL 1.6027 CAL VAL 11480.0
CHANNEL NO. 9 10289 1
08/24/84 R0173

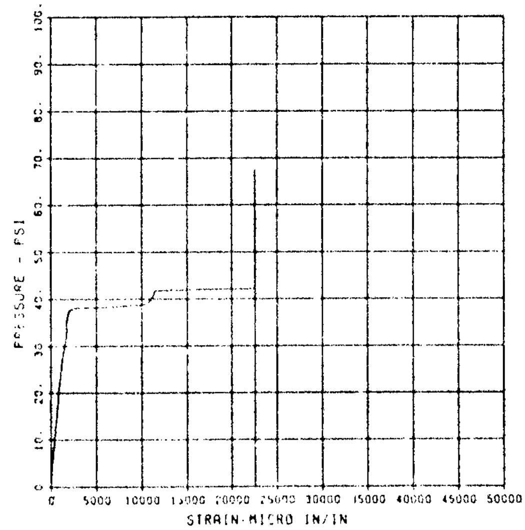

PRINCIPAL STEEL 4
D-1
MAXIMUM 2.2317 SIGMA CAL 0.7259 CAL VAL 4.2

CHANNEL NO. 2 1468 2
08/20/84 K0217

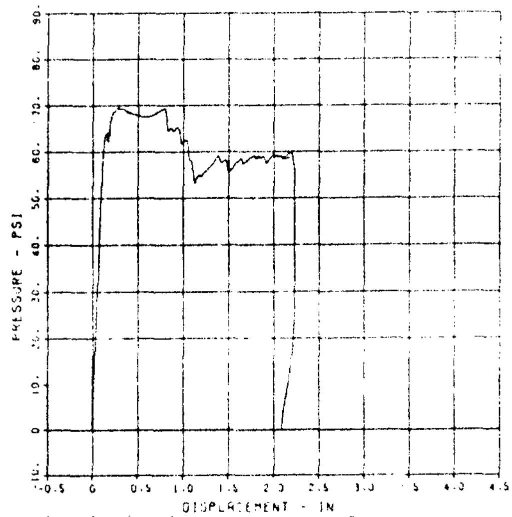

PRINCIPAL STEEL 4
D-2
MAXIMUM 4.5902 SIGMA CAL 0.7389 CAL VAL 7.1

CHANNEL NO. 3 1468 2
08/20/84 K0217

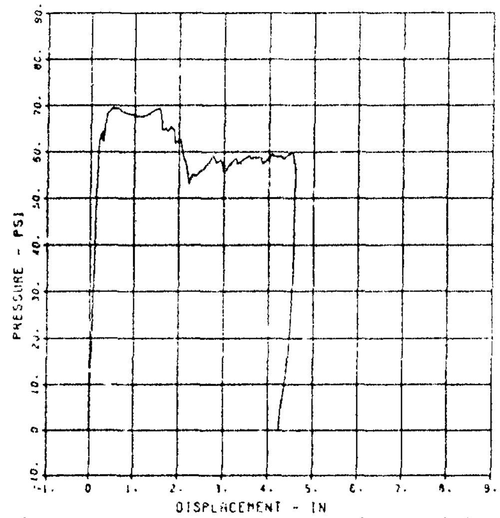

PRINCIPAL STEEL 4
ST-1
MAXIMUM 2309.0114 SIGMA CAL 1.9439 CAL VAL 11480.0

CHANNEL NO 4 1468 2
08/20/84 K0217

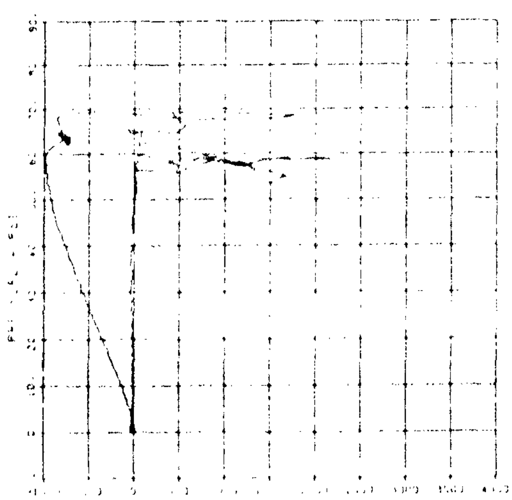

PRINCIPAL STEEL 4
ST-2
MAXIMUM 11545.5625 SIGMA CAL 0.9200 CAL VAL 5790.0

CHANNEL NO. 6 1468 2
08/20/84 K0217

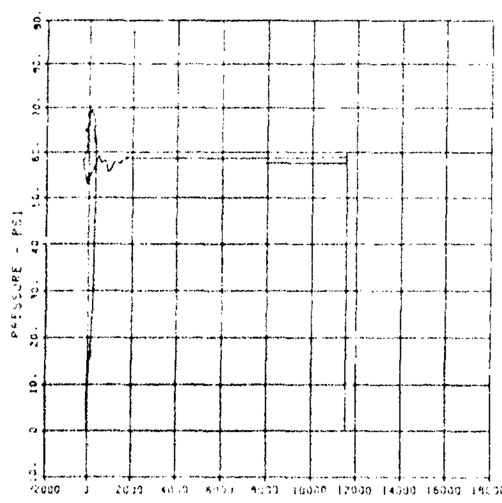

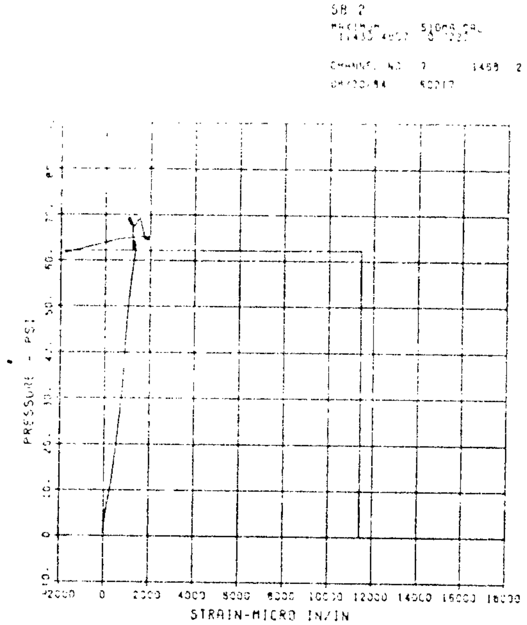
PRINCIPAL STEEL 4
SB 2
CHANNEL NO. 7 1459 2
PRESSURE - PSI
STRAIN-MICRO IN/IN

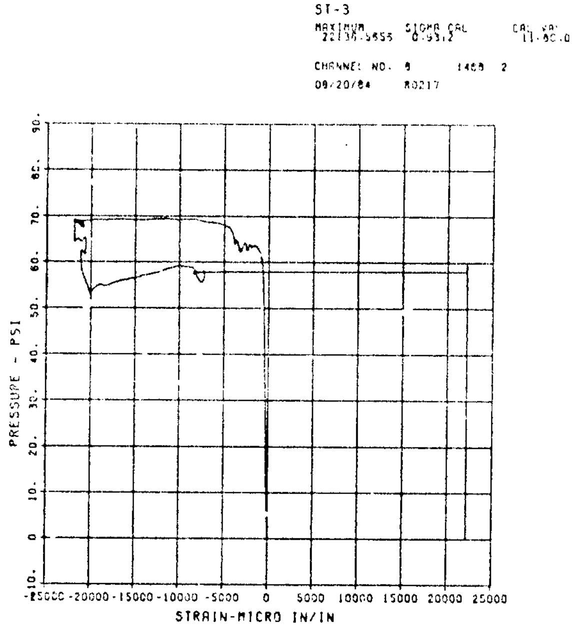
PRINCIPAL STEEL 4
ST-3
MAXIMUM 22130.5855 SIGMA CAL 0.9512
CHANNEL NO. 8 1469 2
09/20/84 R0217
PRESSURE - PSI
STRAIN-MICRO IN/IN

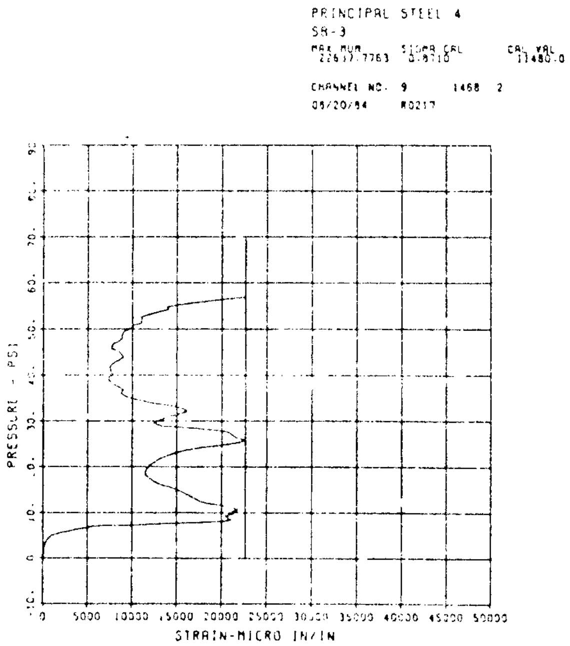
PRINCIPAL STEEL 4
SB-3
MAX MUM 22637.7763 SIGMA CAL 0.8710 CAL VAL 11480.0
CHANNEL NO. 9 1468 2
09/20/84 R0217
PRESSURE - PSI
STRAIN-MICRO IN/IN

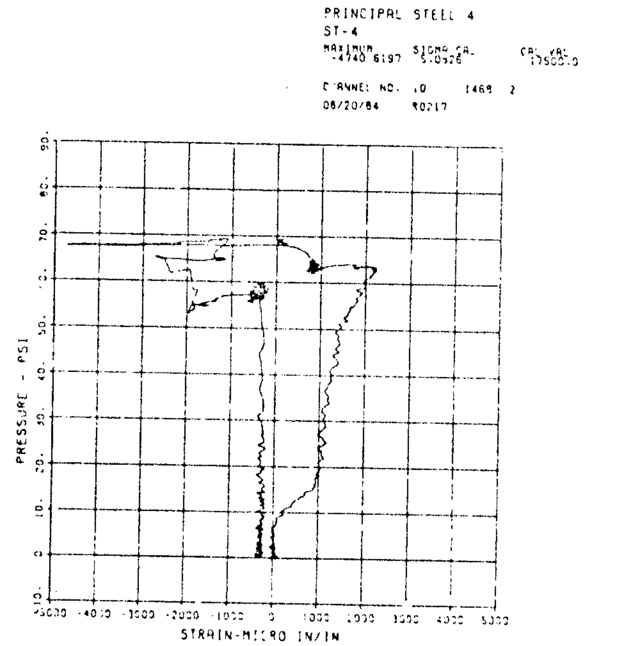
PRINCIPAL STEEL 4
ST-4
MAXIMUM -4740.6197 SIGMA CAL 5.0526 CAL VAL 17500.0
08/20/84 R0217
PRESSURE - PSI
STRAIN-MICRO IN/IN

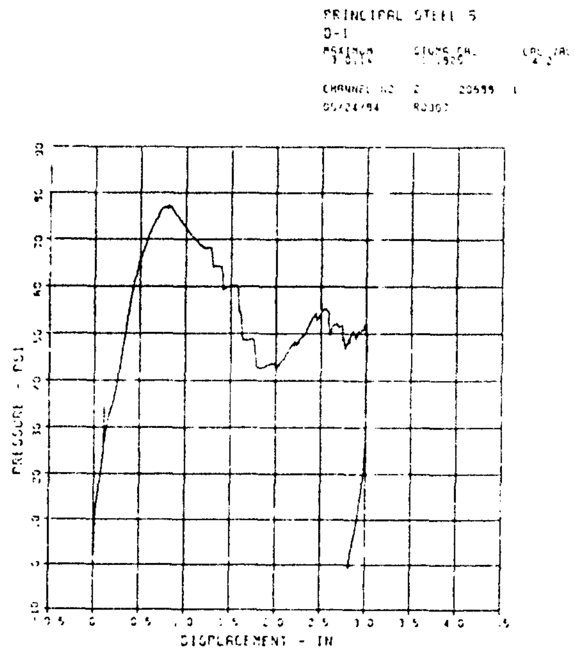
PRINCIPAL STEEL 5
D-1
CHANNEL NO 2 20599 1
05/24/94
PRESSURE - PSI
DISPLACEMENT - IN

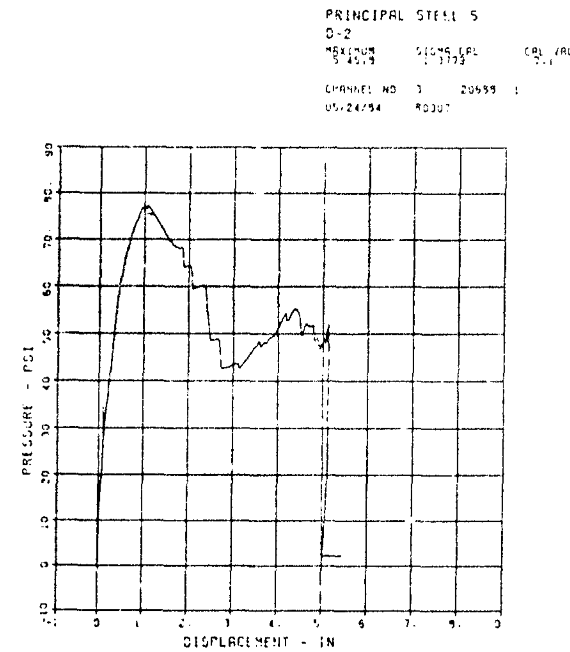
PRINCIPAL STEEL 5
D-2
CHANNEL NO 3 20599 1
05/24/94
PRESSURE - PSI
DISPLACEMENT - IN

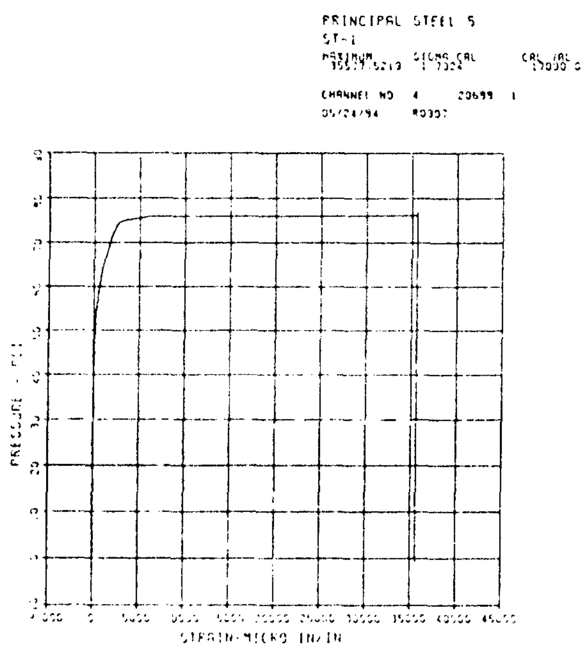
PRINCIPAL STEEL 5
ST-1
CHANNEL NO 4 20599 1
05/24/94
PRESSURE - PSI
STRAIN-MICRO IN/IN

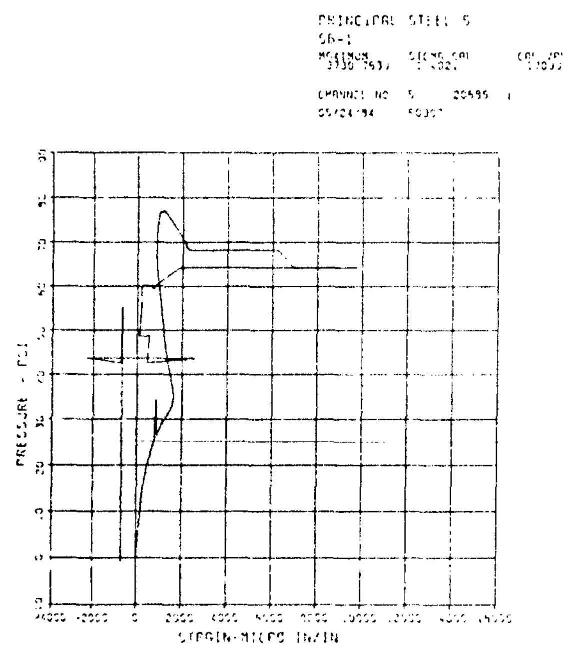
PRINCIPAL STEEL 5
SG-1
PRESSURE - PSI
STRAIN-MICRO IN/IN

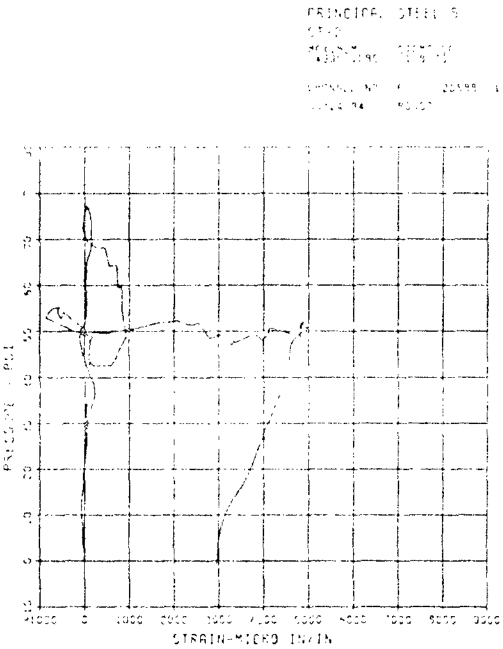
PRINCIPAL STEEL 5
STRAIN-MICRO IN/IN

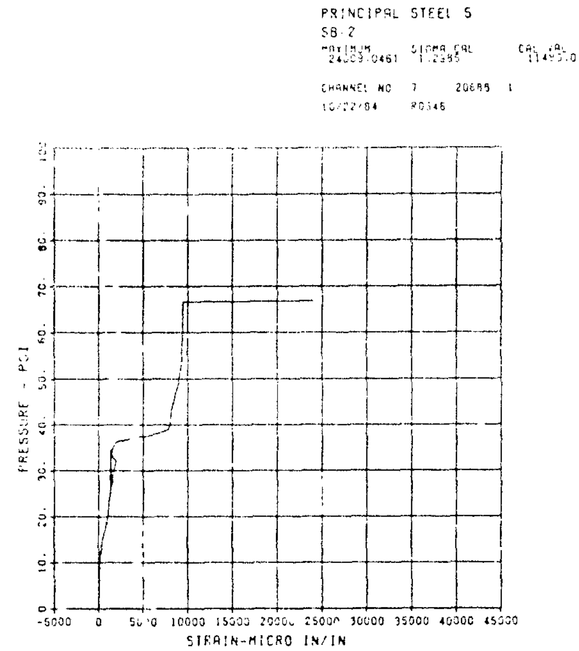
PRINCIPAL STEEL 5
SB-2
MAXIMUM 24003.0461
SIGMA CAL 1.2385
CAL VAL 11493.0
CHANNEL NO 7 20685 1
10/22/84 P0346
PRESSURE - PSI
0.
10.
20.
30.
40.
50.
60.
70.
80.
90.
100
-5000
0
5000
10000
15000
20000
25000
30000
35000
40000
45000
STRAIN-MICRO IN/IN

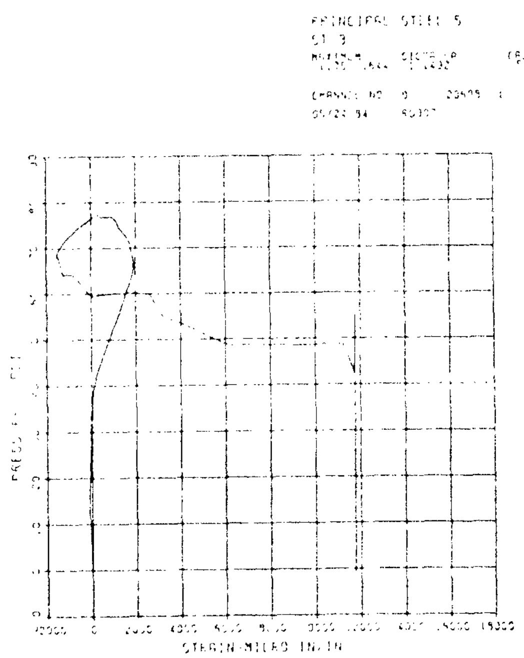
PRINCIPAL STEEL 5
ST-3
STRAIN-MICRO IN/IN

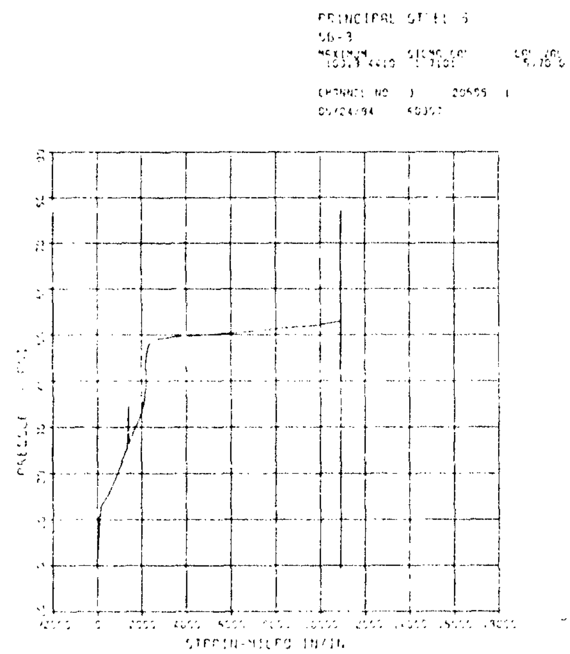
PRINCIPAL STEEL 5
SB-3

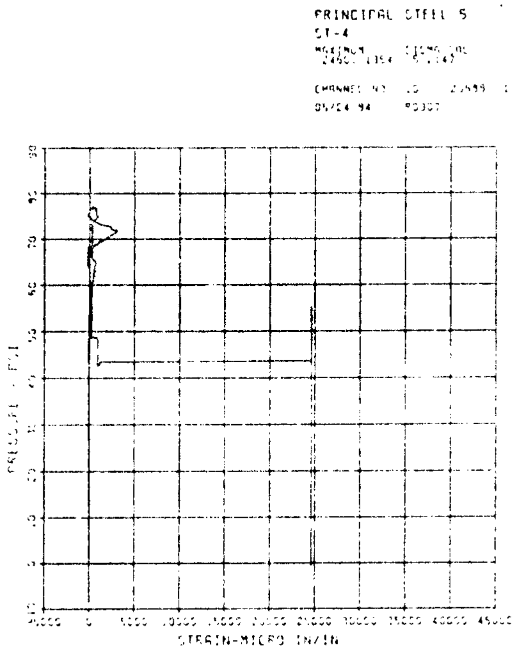
PRINCIPAL STEEL 5
ST-4
PRESSURE - PSI
STRAIN-MICRO IN/IN

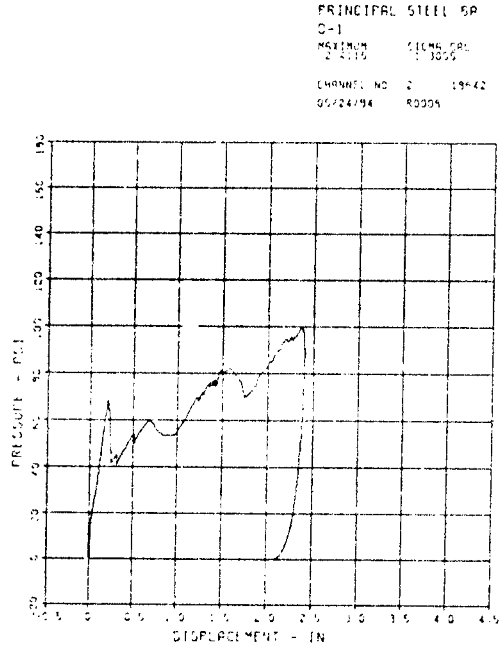
PRINCIPAL STEEL 5A
D-1
PRESSURE - PSI
DISPLACEMENT - IN

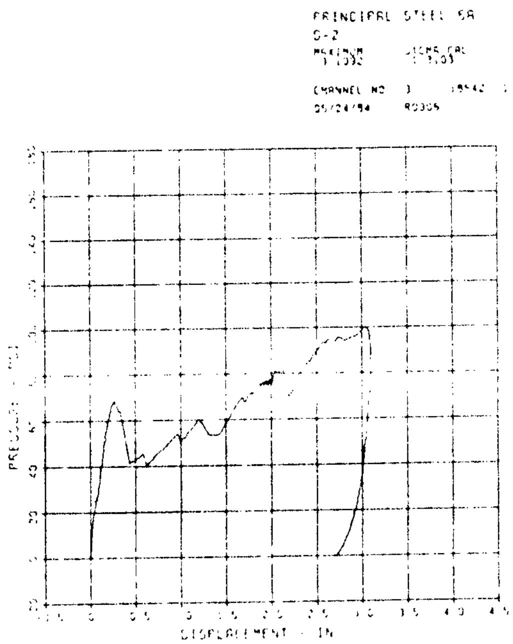
PRINCIPAL STEEL 5A
D-2
PRESSURE - PSI
DISPLACEMENT - IN

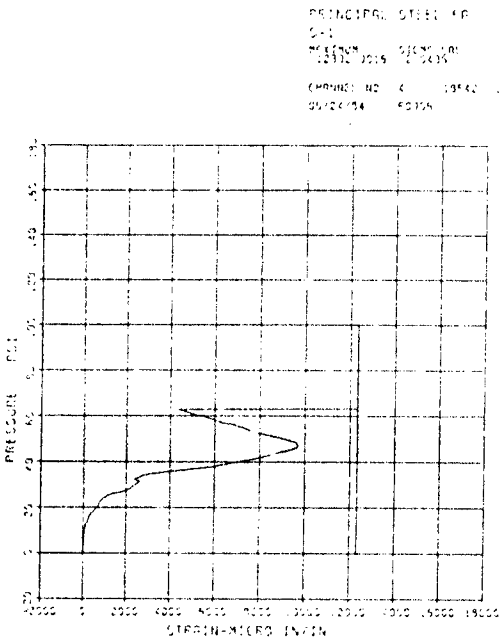
PRINCIPAL STEEL 5A
PRESSURE - PSI
STRAIN-MICRO IN/IN

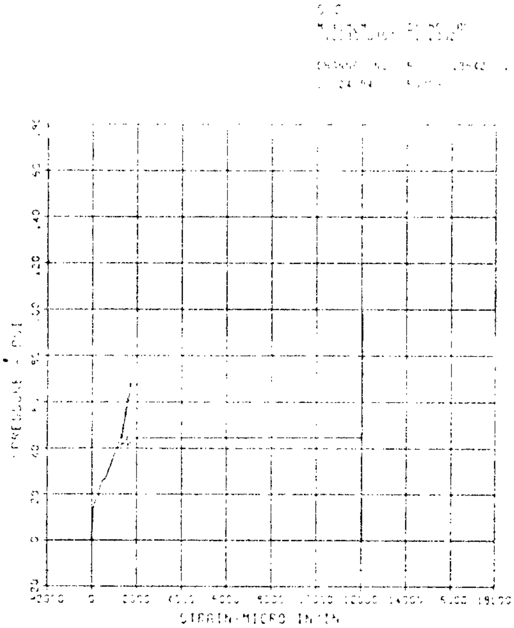
PRINCIPAL STEEL 5A
STRAIN-MICRO IN/IN

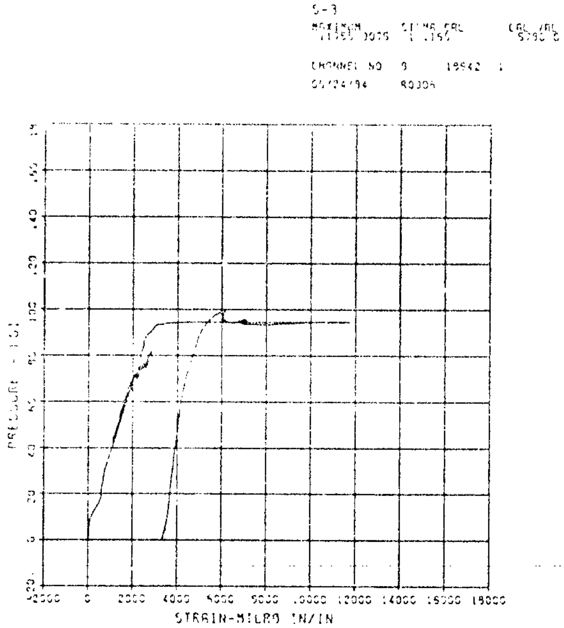
PRINCIPAL STEEL 5A
S-3
CHANNEL NO 9
PRESSURE - PSI
STRAIN-MICRO IN/IN

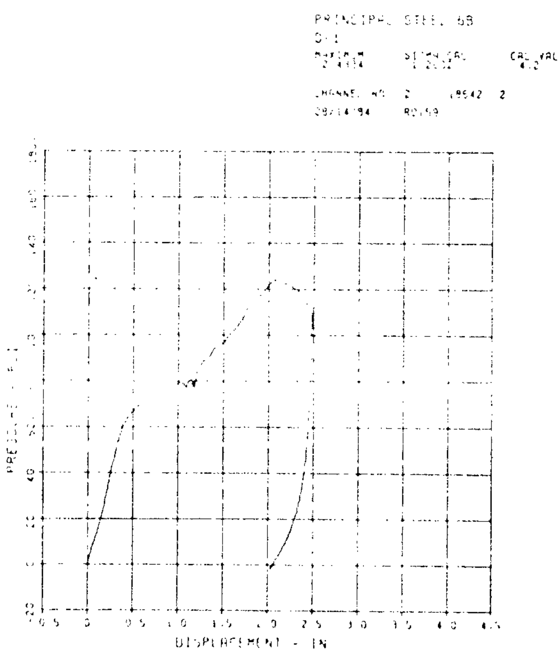
PRINCIPAL STEEL 6B
D-1
MAXIMUM
CAL VAL
CHANNEL NO 2 18542 2
09/14/94 R0159
DISPLACEMENT - IN

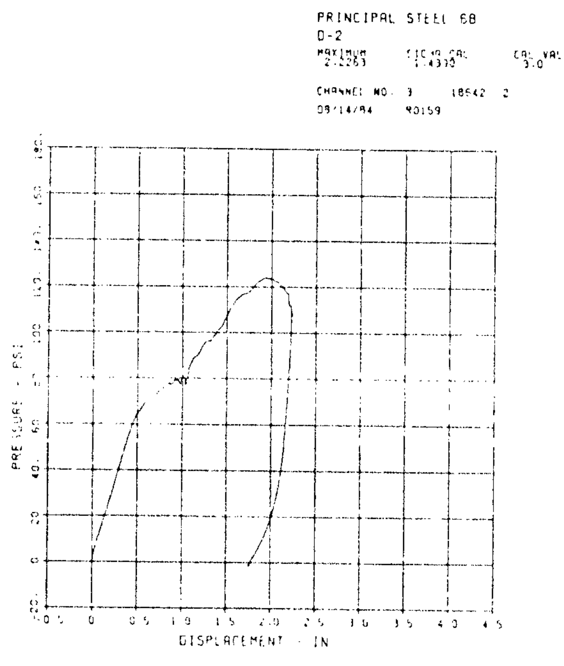
PRINCIPAL STEEL 6B
D-2
MAXIMUM
2.2263
CAL VAL
3.0
CHANNEL NO. 3 18542 2
09/14/94 R0159
PRESSURE - PSI
DISPLACEMENT - IN

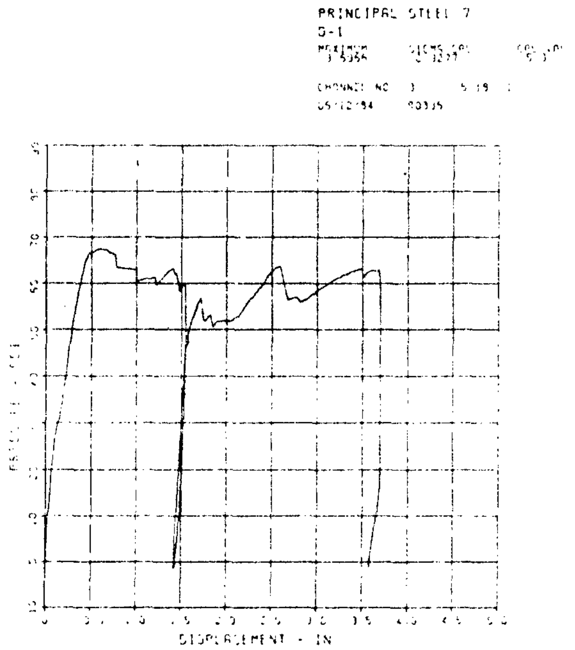
PRINCIPAL STEEL 7
D-1
DISPLACEMENT - IN

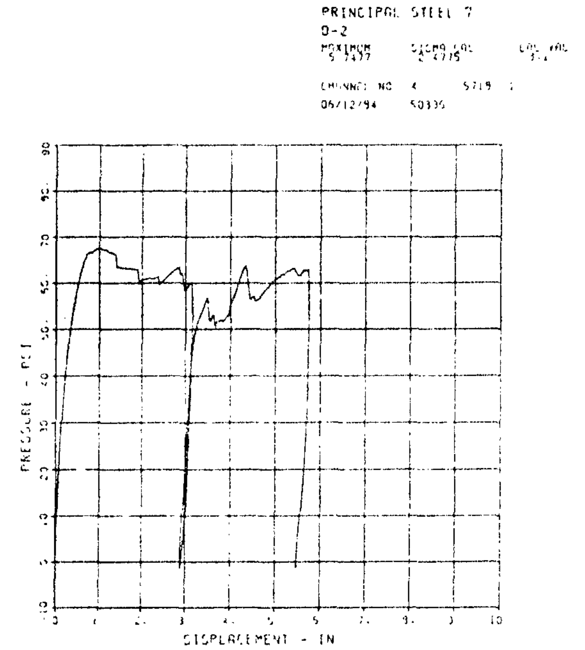
PRINCIPAL STEEL 7
D-2
06/12/94
PRESSURE - PSI
DISPLACEMENT - IN

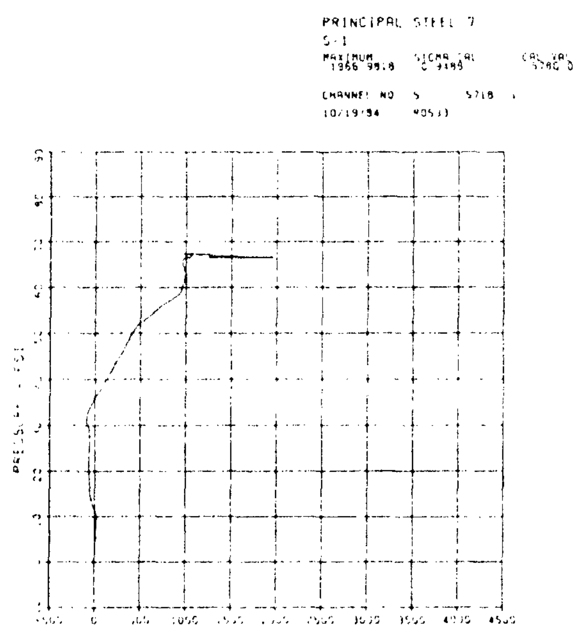
PRINCIPAL STEEL 7
S-1
MAXIMUM
CHANNEL NO
10/19/94
STRAIN MICRO IN/IN

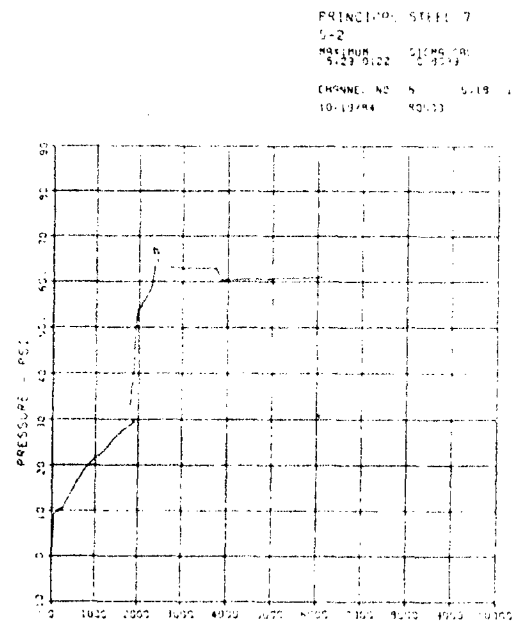
PRINCIPAL STEEL 7
S-2
PRESSURE - PSI
STRAIN MICRO IN/IN

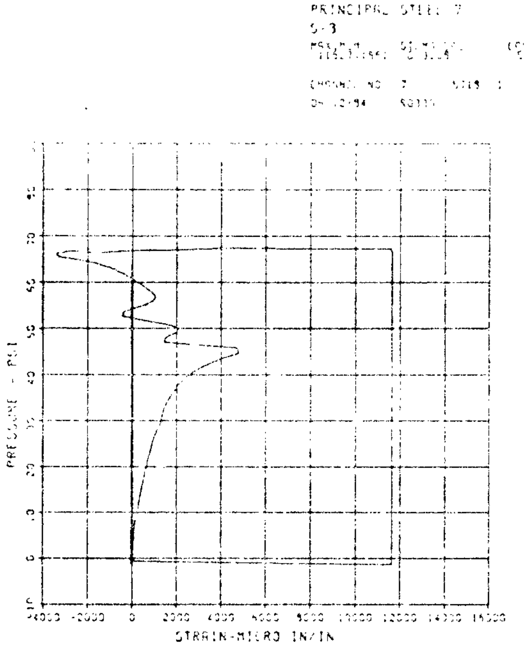
PRINCIPAL STEEL 7
PRESSURE - PSI
STRAIN-MICRO IN/IN

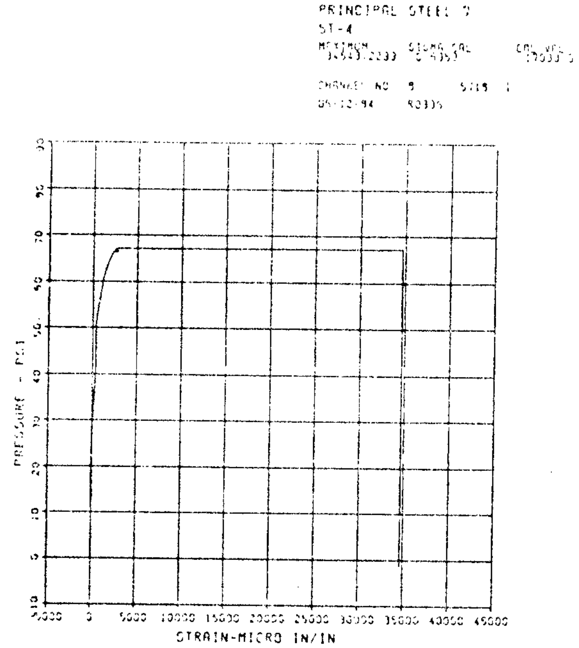
PRINCIPAL STEEL 7
ST-4
PRESSURE - PSI
STRAIN-MICRO IN/IN

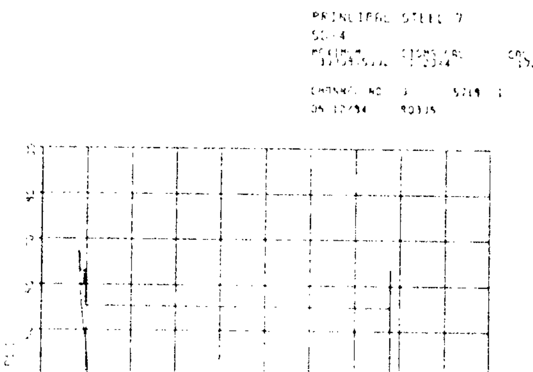
PRINCIPAL STEEL 7
STRAIN MICRO IN/IN

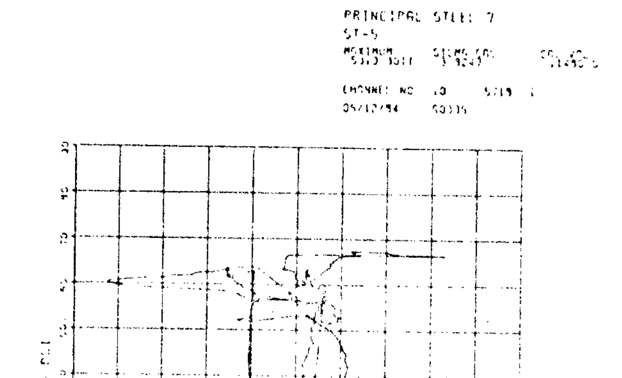
PRINCIPAL STEEL 7
ST-5
PRESSURE - PSI

PRINCIPAL STEEL 7
SB-5
MAXIMUM 9569.2595 SIGMA CAL 1.2153 CAL VAL 11480.0
CHANNEL NO. 11 5719 1
10/19/94 R0533

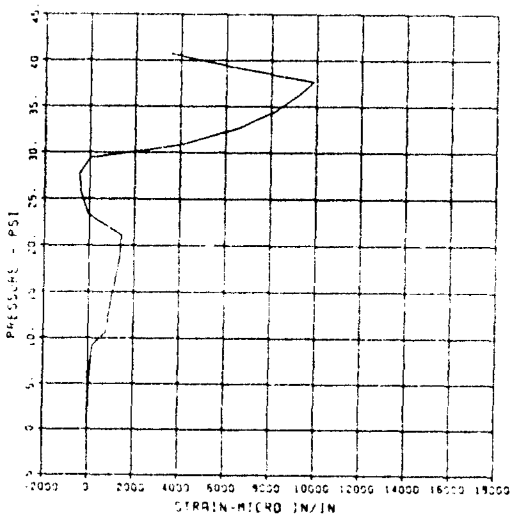

PRINCIPAL STEEL 7
T-6
MAXIMUM 9783.7989 SIGMA CAL 34.0355 CAL VAL 17093.0
CHANNEL NO 12 5719 1
10/19/94 R0533

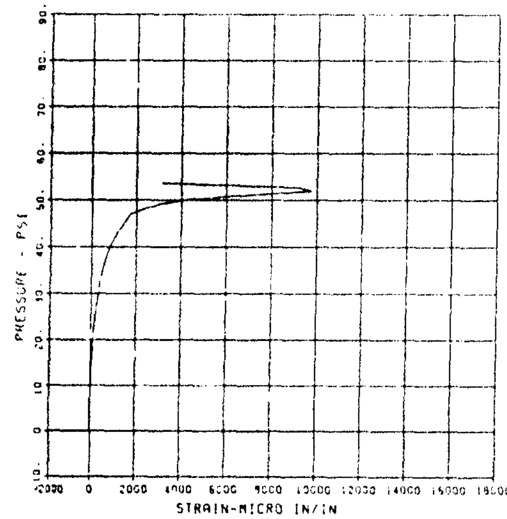

PRINCIPAL STEEL 7
SB-5
MAXIMUM 15355 10.1 SIGMA CAL 1.0213 CAL VAL 17093.0
CHANNEL NO 13 5719 1
05/12/94 R0335

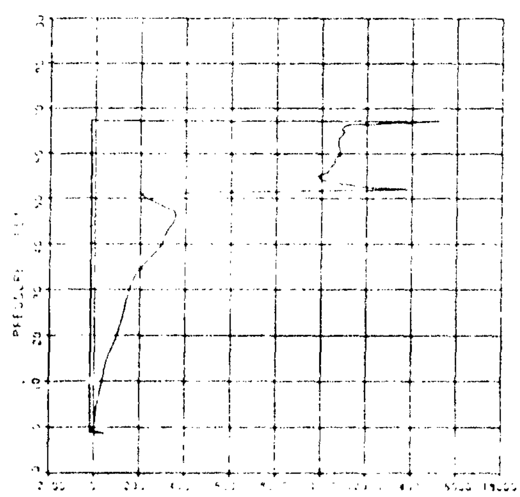

PRINCIPAL STEEL 8
D-1
MAXIMUM 3.2959 SIGMA CAL 2.5749 CAL VAL 4.2
CHANNEL NO. 3 12535 2
06/06/94 R0279

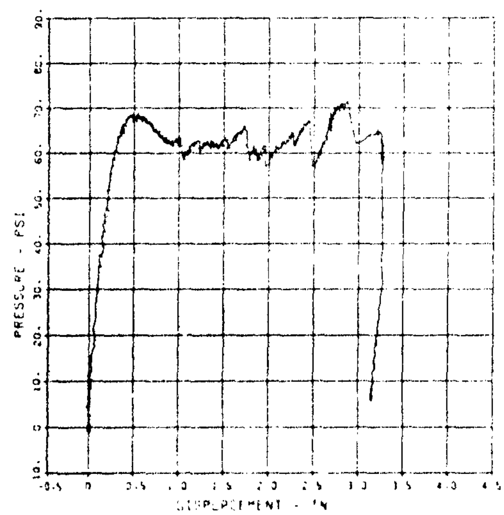

PRINCIPAL STEEL B
D-2
MAXIMUM [illegible] SIGMA CAL [illegible] CAL VAL 7.1
CHANNEL NO. 4 12535 2
06/05/84 R0279

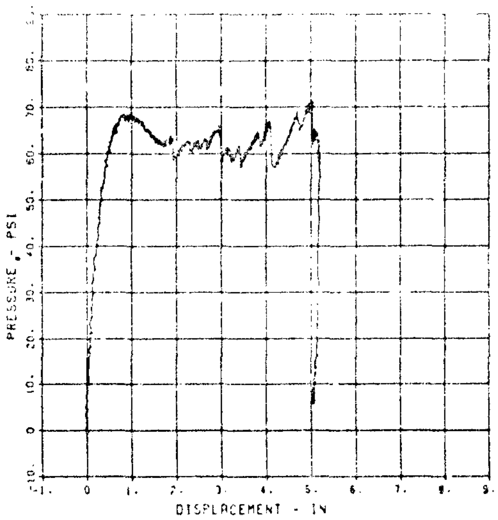

PRINCIPAL STEEL B
S-1
MAXIMUM 11370.6992 SIGMA CAL 2.5395 CAL VAL 5760.0
CHANNEL NO. 5 12535 2
06/06/84 R0275

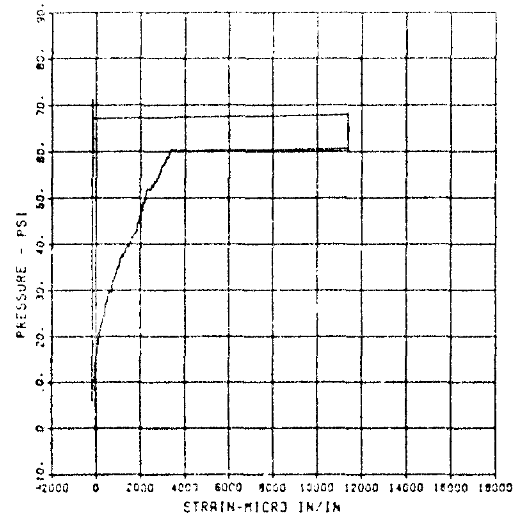

PRINCIPAL STEEL B
S-2
MAXIMUM [illegible] SIGMA CAL [illegible] CAL VAL 5760.0
CHANNEL NO. 6 12535 2
06/06/84 R0273

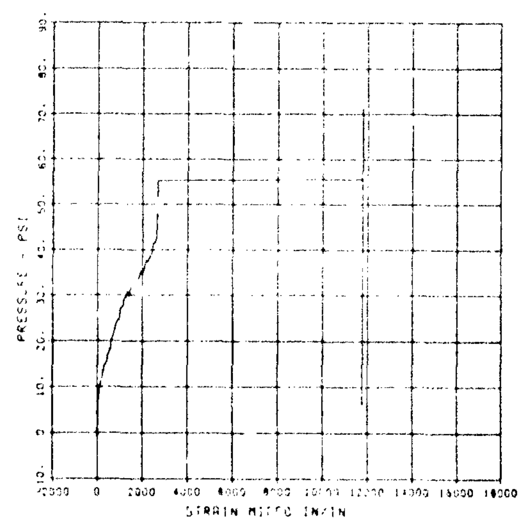

PRINCIPAL STEEL B
ST-4
MAXIMUM 35171.1074 SIGMA CAL 2.9390 CAL VAL 17090.0
CHANNEL NO. 8 12538 2
06/06/84 R0279

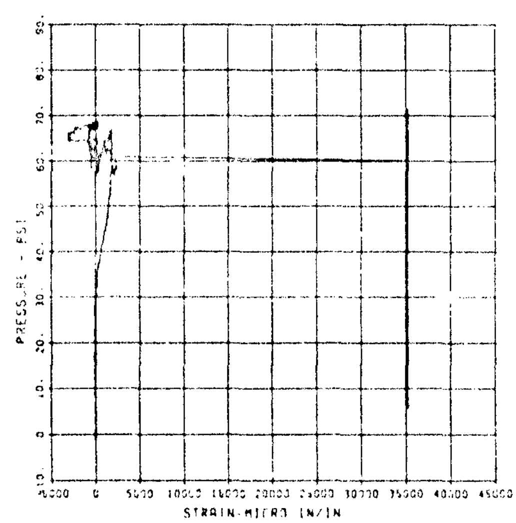

PRINCIPAL STEEL B
SB-4
MAXIMUM 32267.1425 SIGMA CAL 3.0237 CAL VAL 17090.0

CHANNEL NO. 9 12536 2
06/06/84 R0279

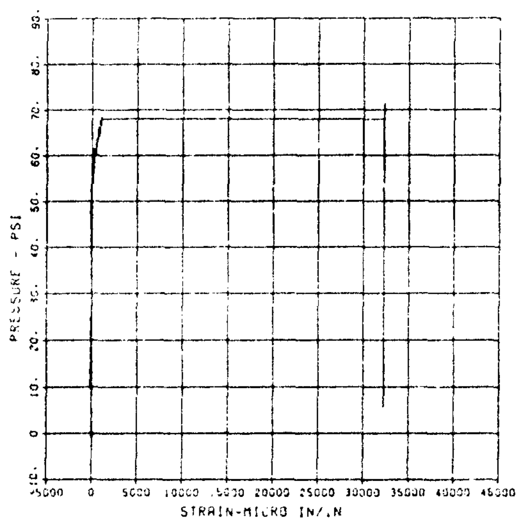

PRINCIPAL STEEL B
ST-5
MAXIMUM 24197.4982 SIGMA CAL 2.7811 CAL VAL 11480.0

CHANNEL NO. 10 12536 2
06/06/84 R0279

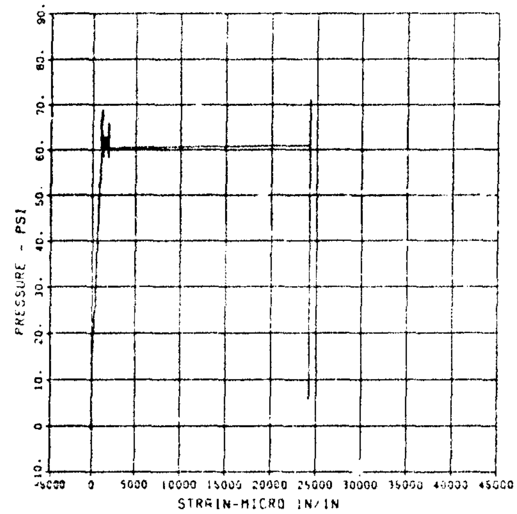

PRINCIPAL STEEL B
SB-5
MAXIMUM -21172.6867 SIGMA CAL 8.3221 CAL VAL 11480.0

CHANNEL NO 11 12535 2
10/19/84 R0520

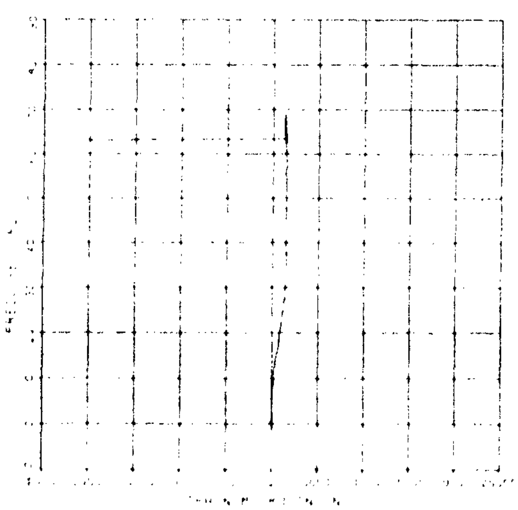

PRINCIPAL STEEL S
ST-6
MAXIMUM 32303.1557 SIGMA CAL 2.6459 CAL VAL 17090.0

CHANNEL NO. 12 12535 2
06/06/84 R0279

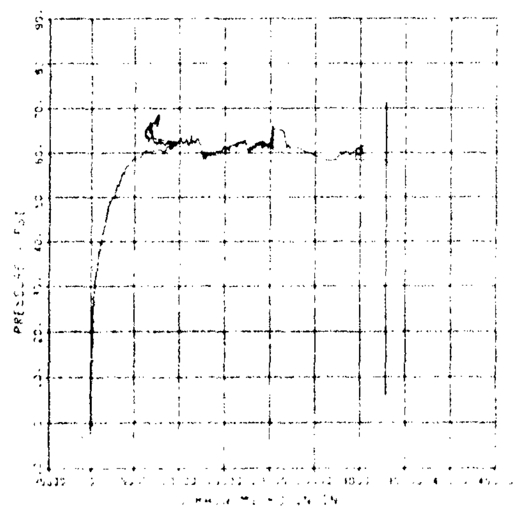

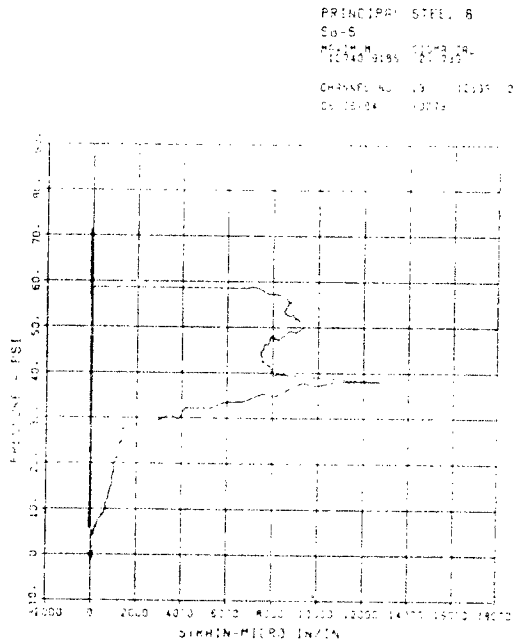
Sо-S
STRAIN-MICRO IN/IN

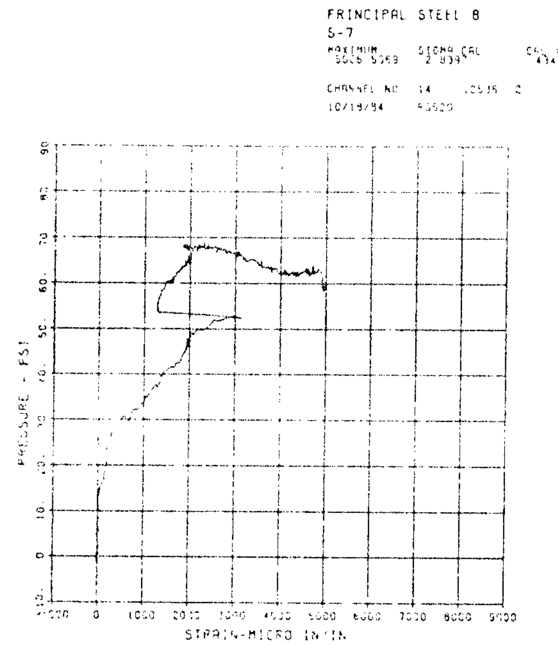
FRINCIPAL STEEL 8
S-7
MAXIMUM
5006 5969
SIGMA CAL
2 939
CHANNEL NO 14
10/19/94
PRESSURE - PSI
STRAIN-MICRO IN/IN

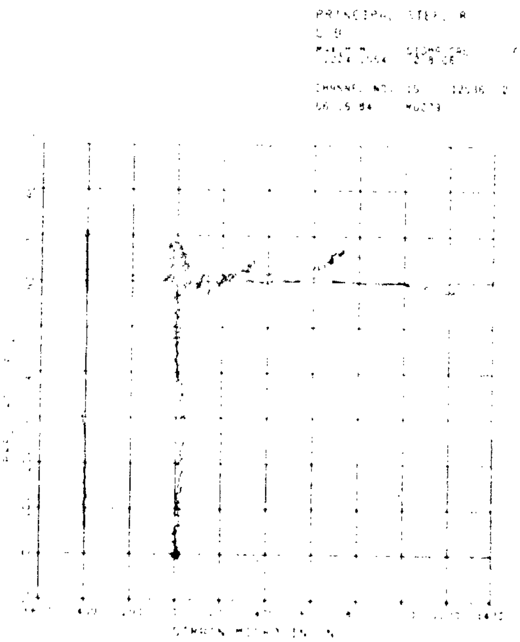

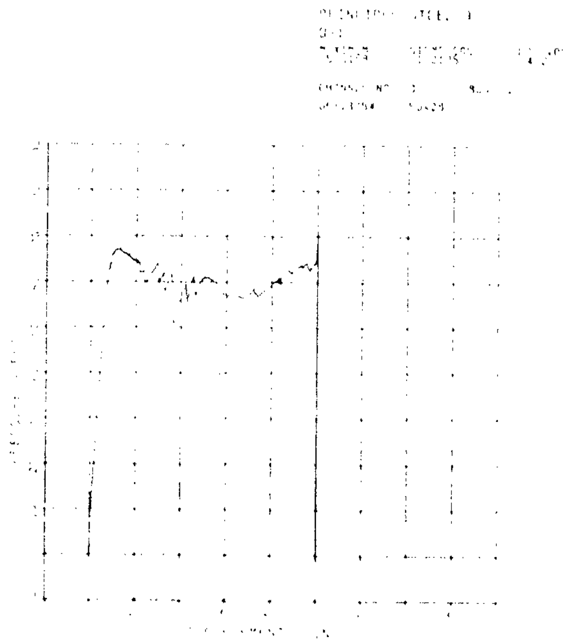

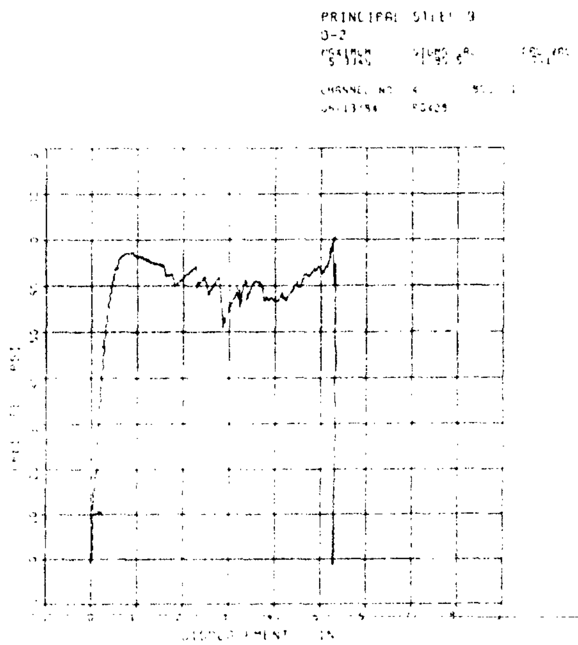
PRINCIPAL STEEL 9
D-2

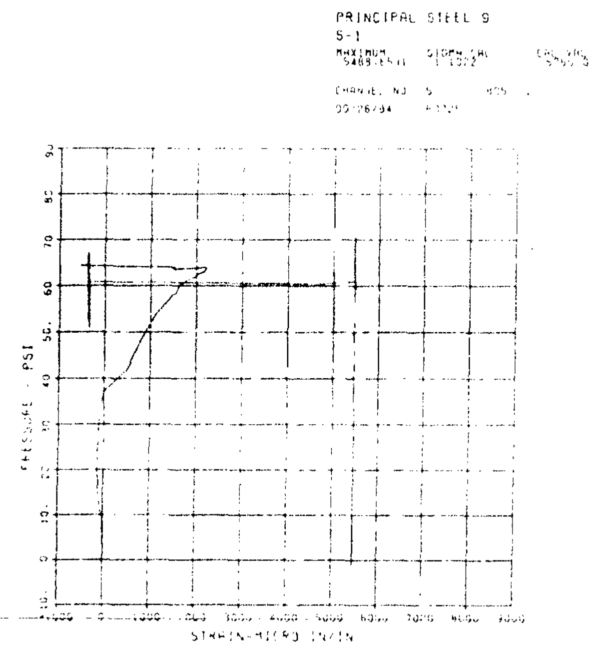
PRINCIPAL STEEL 9
S-1
PRESSURE - PSI
STRAIN-MICRO IN/IN

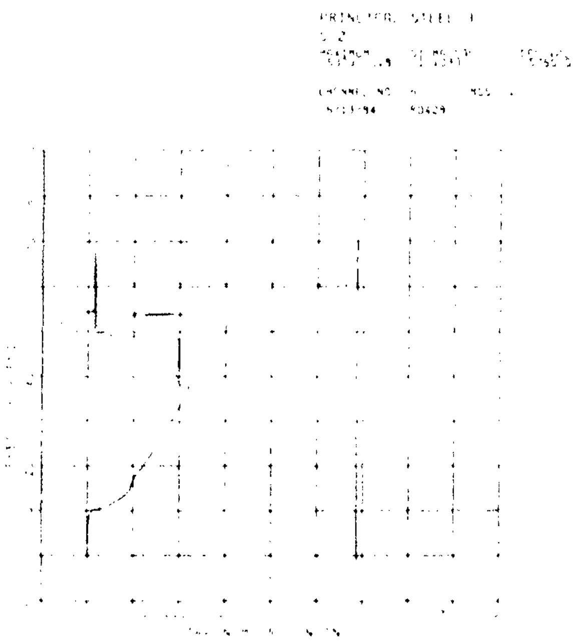

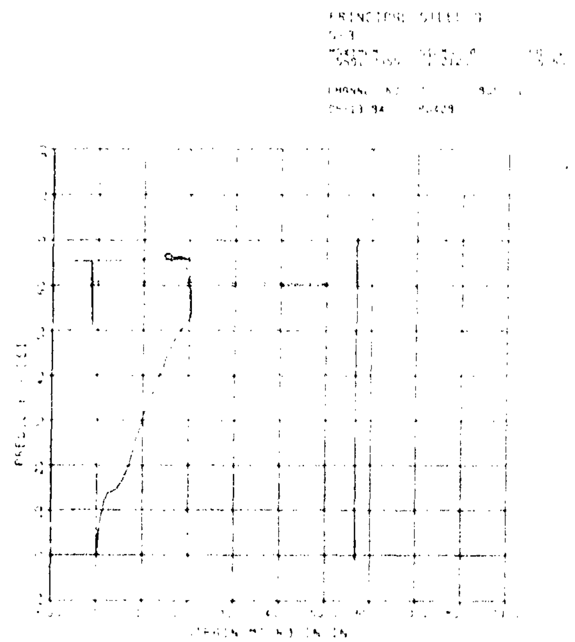
PRINCIPAL STEEL 9

PRINCIPAL STEEL 3
ST-4
MAXIMUM SIGMA CAL CAL VAL

CHANNEL NO. 9
05/13/94 80429

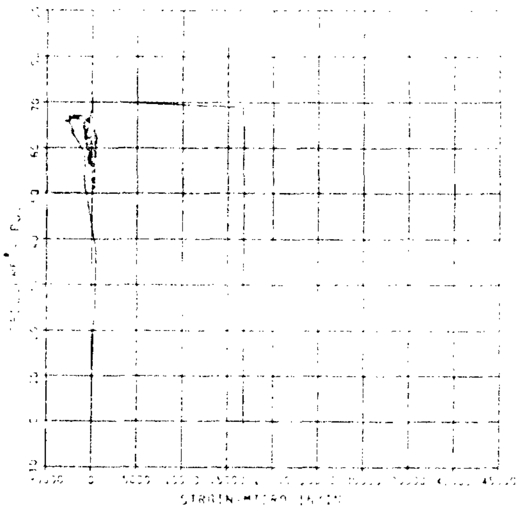

PRINCIPAL STEEL 3
SB 4
MAXIMUM 15755.0337 SIGMA CAL CAL VAL

CHANNEL NO. 3
05/13/94 80429

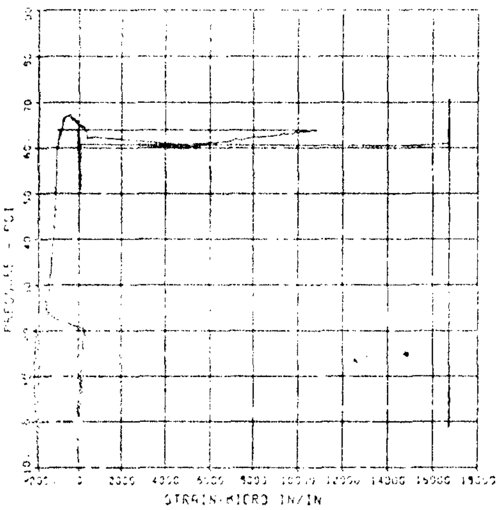

PRINCIPAL STEEL 9
ST-5
MAXIMUM SIGMA CAL CAL VAL

CHANNEL NO 10
80429

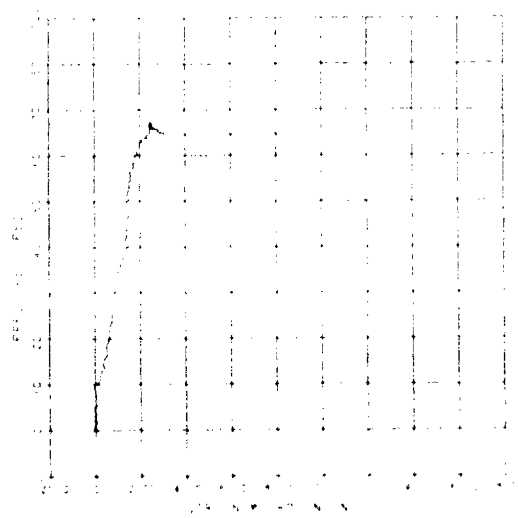

PRINCIPAL STEEL 3
SB-5
MAXIMUM SIGMA CAL CAL VAL

CHANNEL NO
05/13/94 80429

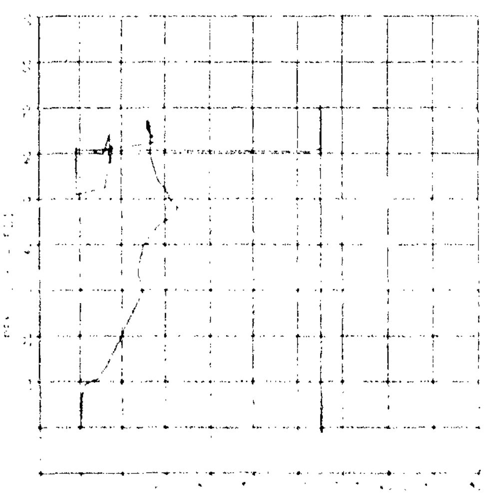

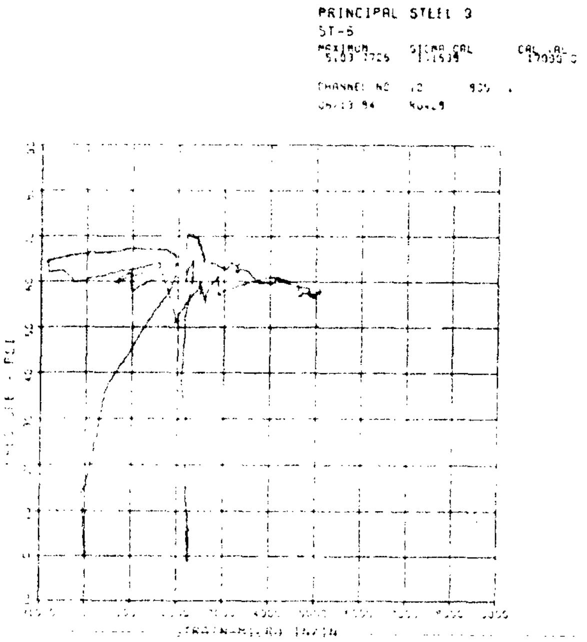
PRINCIPAL STEEL 3
ST-5
MAXIMUM
SIGMA CAL
CHANNEL NO
STRAIN-MICRO IN/IN

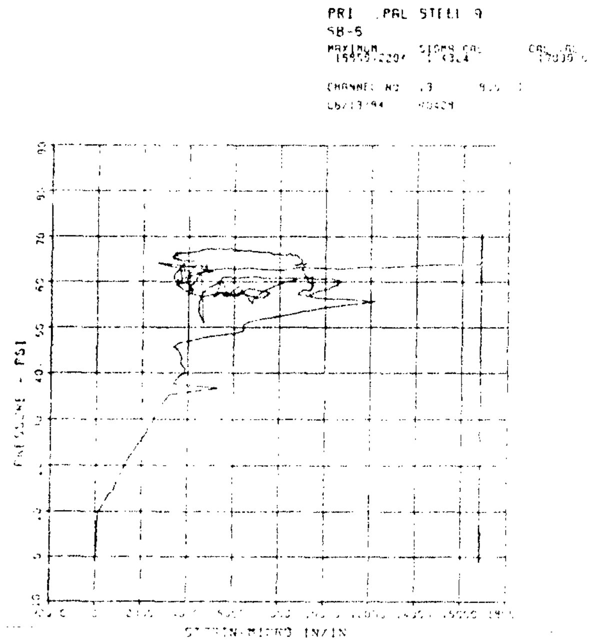
SB-5
MAXIMUM
CHANNEL NO
PRESSURE - PSI
STRAIN-MICRO IN/IN

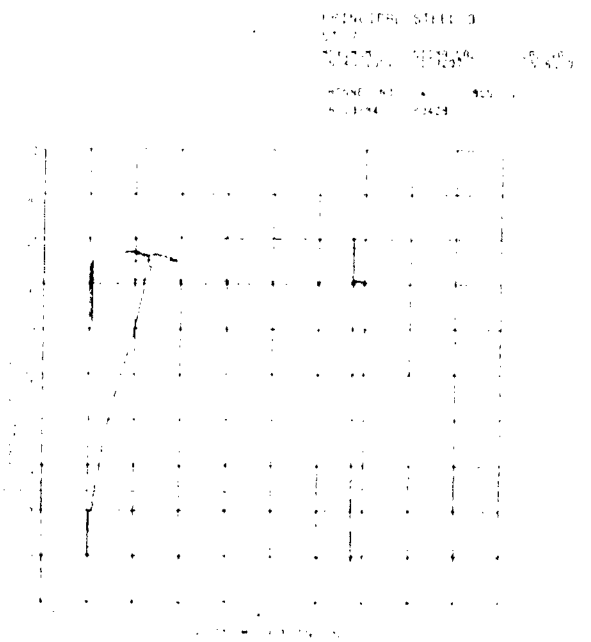
PRINCIPAL STEEL 3

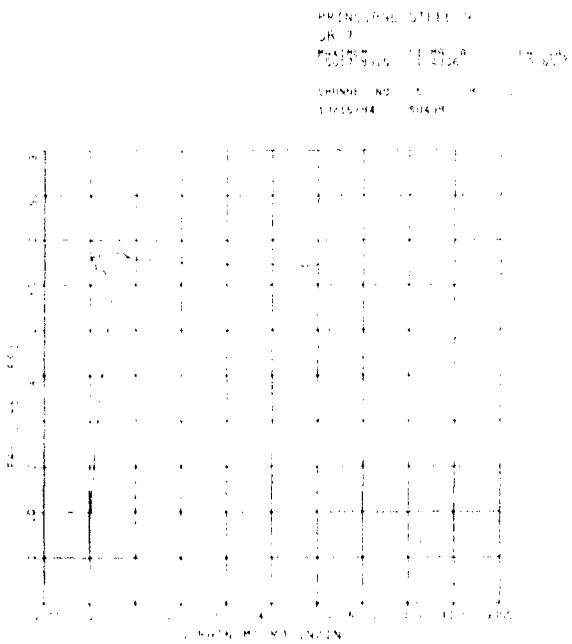

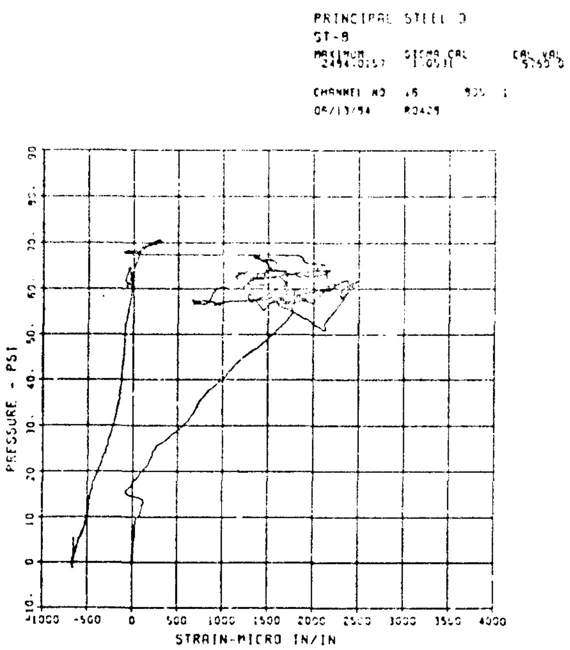
PRINCIPAL STEEL
ST-9
MAXIMUM
SIGMA CAL
CAL VAL
CHANNEL NO
PRESSURE - PSI
STRAIN-MICRO IN/IN

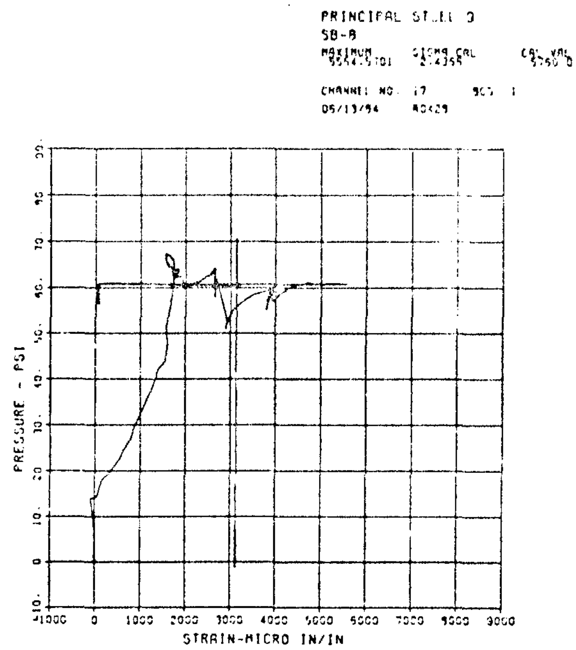
PRINCIPAL
SB-8
MAXIMUM
SIGMA CAL
CAL VAL
CHANNEL NO.
05/13/94
PRESSURE - PSI
STRAIN-MICRO IN/IN

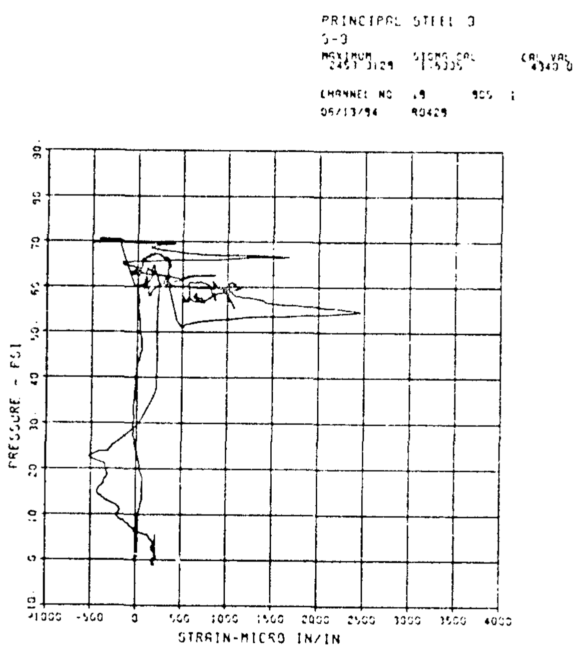
PRINCIPAL STEEL
MAXIMUM
SIGMA CAL
CAL VAL
CHANNEL NO
STRAIN-MICRO IN/IN

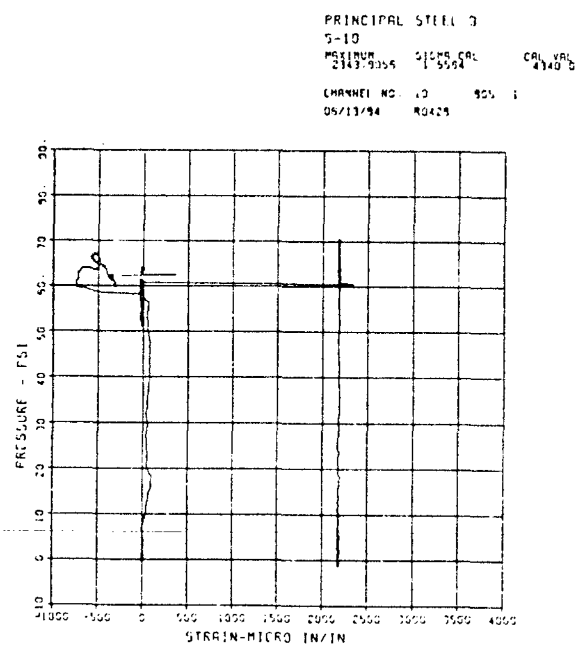
PRINCIPAL STEEL
S-10
MAXIMUM
SIGMA CAL
CAL VAL
CHANNEL NO.
05/13/94
STRAIN-MICRO IN/IN

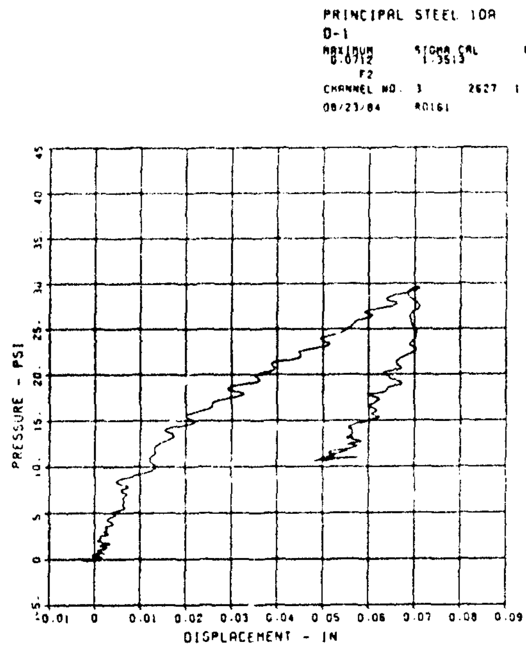
PRINCIPAL STEEL 10A
D-1
MAXIMUM 0.0712
SIGMA CAL 1.3513
CAL VAL 4.2
F2
CHANNEL NO. 3 2627 1
08/23/84 R0161
PRESSURE - PSI
-5 0 5 10 15 20 25 30 35 40 45
-0.01 0 0.01 0.02 0.03 0.04 0.05 0.06 0.07 0.08 0.09
DISPLACEMENT - IN

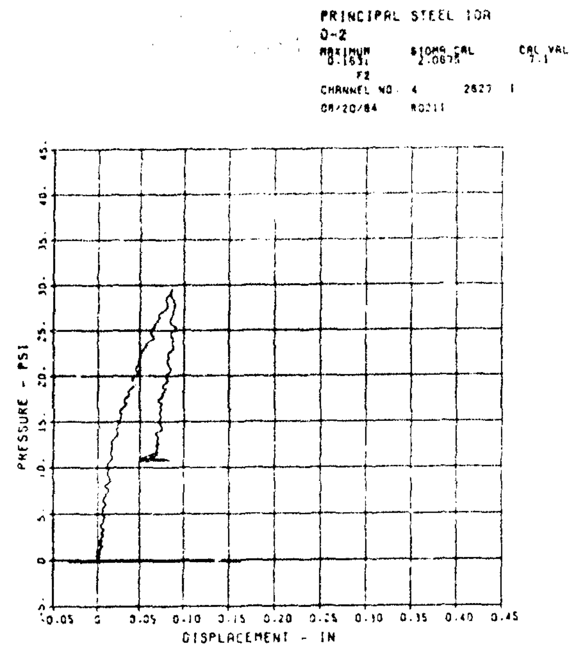
PRINCIPAL STEEL 10A
D-2
MAXIMUM 0.1631
SIGMA CAL 2.0875
CAL VAL 7.1
F2
CHANNEL NO. 4 2627 1
08/20/84 R0211
PRESSURE - PSI
-5 0 5 10 15 20 25 30 35 40 45
-0.05 0 0.05 0.10 0.15 0.20 0.25 0.30 0.35 0.40 0.45
DISPLACEMENT - IN

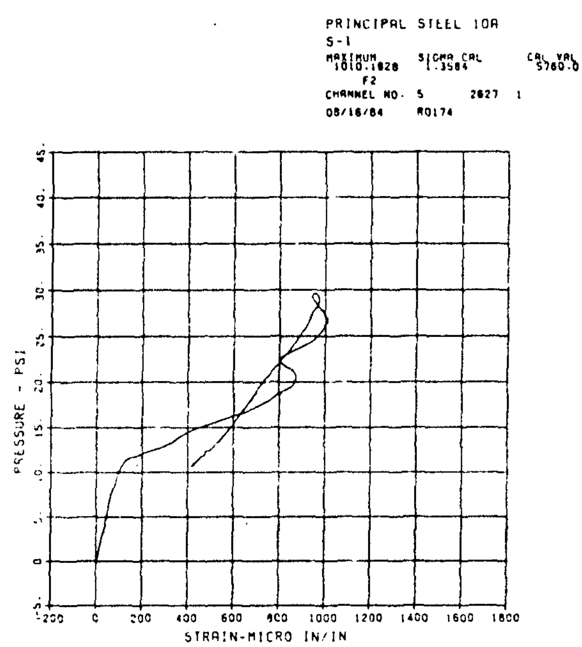
PRINCIPAL STEEL 10A
S-1
MAXIMUM 1010.1828
SIGMA CAL 1.3584
CAL VAL 5760.0
F2
CHANNEL NO. 5 2627 1
08/16/84 R0174
PRESSURE - PSI
-5 0 5 10 15 20 25 30 35 40 45
-200 0 200 400 600 800 1000 1200 1400 1600 1800
STRAIN-MICRO IN/IN

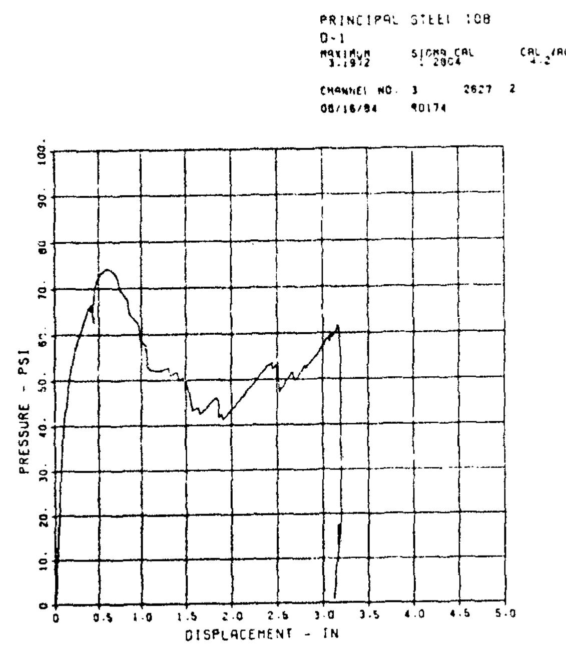
PRINCIPAL STEEL 10B
D-1
MAXIMUM 3.1972
SIGMA CAL 1.2804
CAL VAL 4.2
CHANNEL NO. 3 2627 2
08/16/84 R0174
PRESSURE - PSI
0 10 20 30 40 50 60 70 80 90 100
0 0.5 1.0 1.5 2.0 2.5 3.0 3.5 4.0 4.5 5.0
DISPLACEMENT - IN

PRINCIPAL STEEL 10B
D-2
MAXIMUM 6.2196 SIGMA CAL 2.1203 CAL VAL 7.1
CHANNEL NO 4 2627 2
08/16/84 R0174

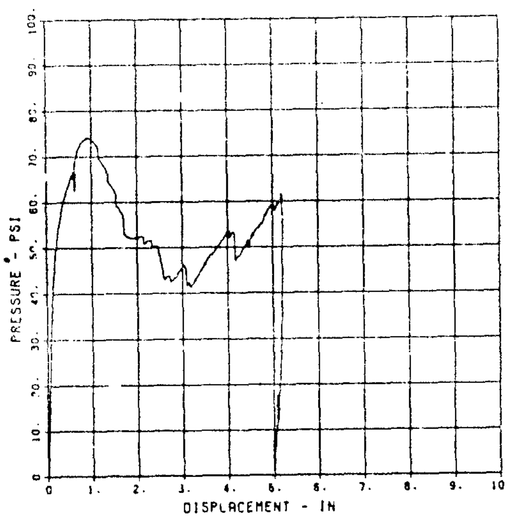

PRINCIPAL STEEL 10B
S-1
MAXIMUM 11087.2445 SIGMA CAL 1.2751 CAL VAL 5760.0
CHANNEL NO. 5 2627 2
08/16/84 R0174

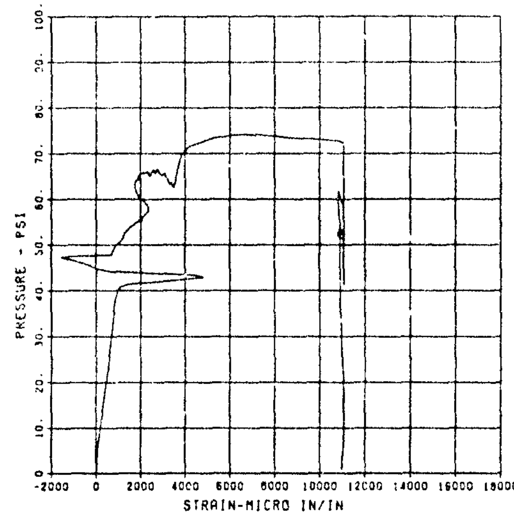

PRINCIPAL STEEL 11
D-1
MAXIMUM 2.3253 SIGMA CAL 1.2136 CAL VAL 4.2
CHANNEL NO 3 0571 1
05/13/84 R0423

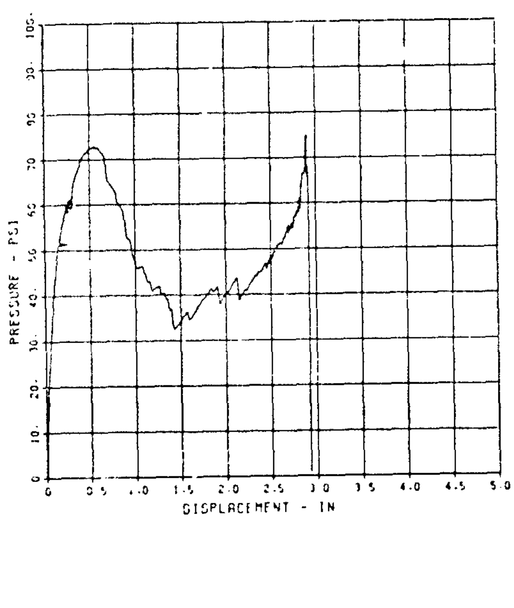

PRINCIPAL STEEL 11
D-2
MAXIMUM 4.2244 SIGMA CAL 13.5377 CAL VAL 7.1
CHANNEL NO. 4 0571 1
05/13/84 R0423

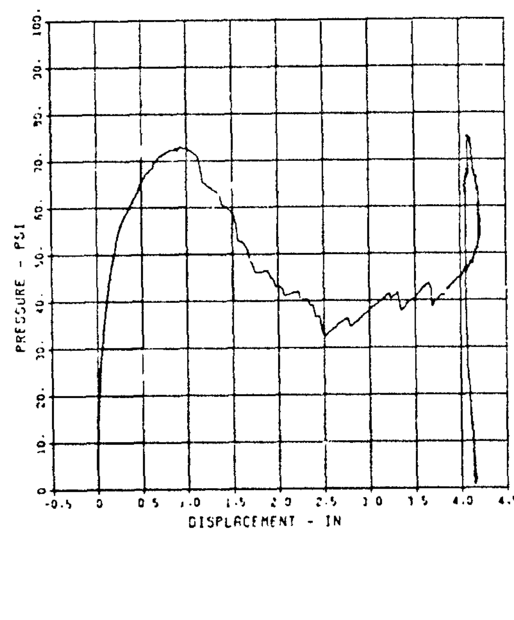

PRINCIPAL STEEL 11
S-1
MAXIMUM 7447.3286 SIGMA CAL 1.2949 CAL VAL 5760.0
CHANNEL NO 5 9571 1
10/01/94 90295

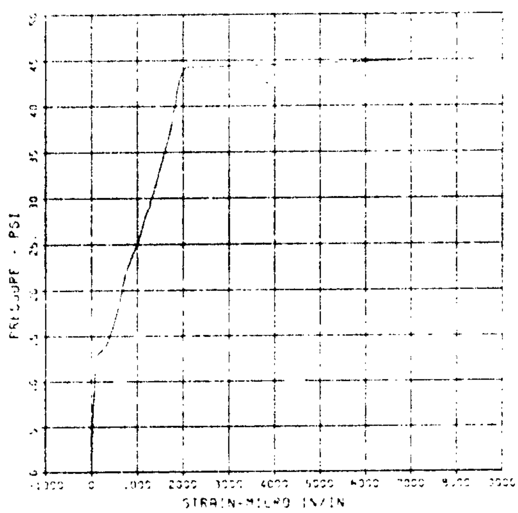

PRINCIPAL STEEL 12
D-1
MAXIMUM 3.3373 SIGMA CAL 1.0294 CAL VAL 4.2
CHANNEL NO 2 9375 1
09/10/94 90110

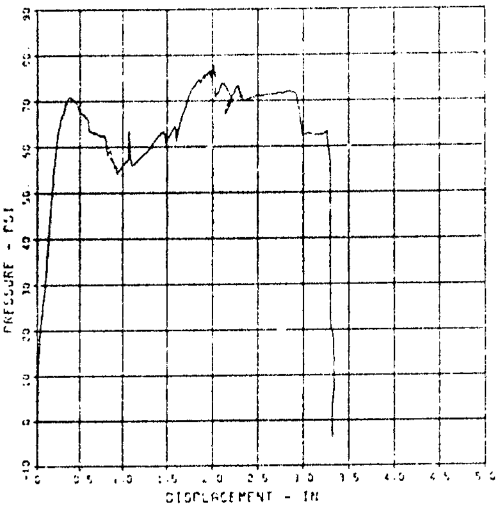

PRINCIPAL STEEL 12
D-2
MAXIMUM 5.7474 SIGMA CAL 1.4930 CAL VAL 7.1
CHANNEL NO 3 9375 1
09/10/94 90110

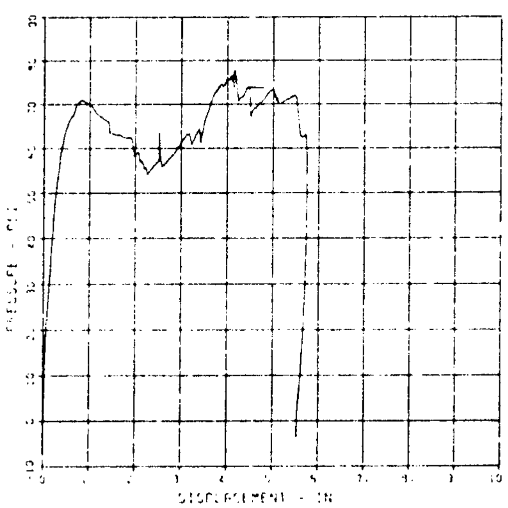

PRINCIPAL STEEL 12
S-1
MAXIMUM 11519.2399 SIGMA CAL 2.1423 CAL VAL 5760.0
CHANNEL NO 4 9375 1
09/10/94 90110

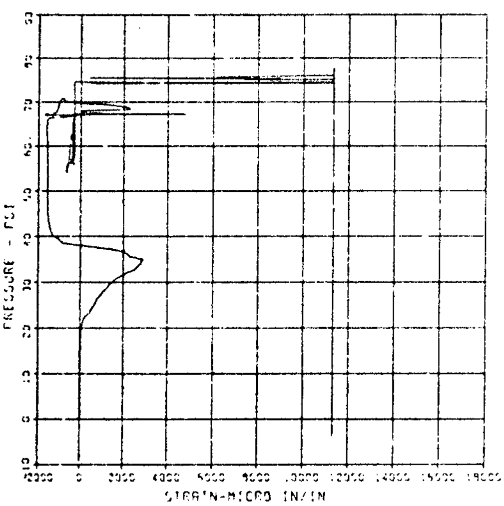

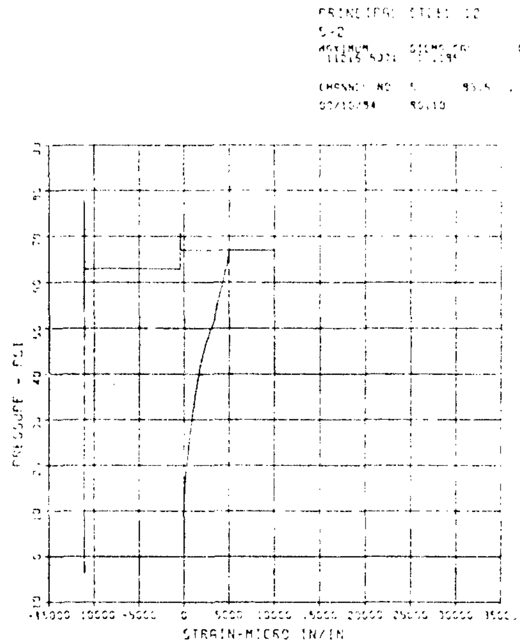
STRAIN-MICRO IN/IN

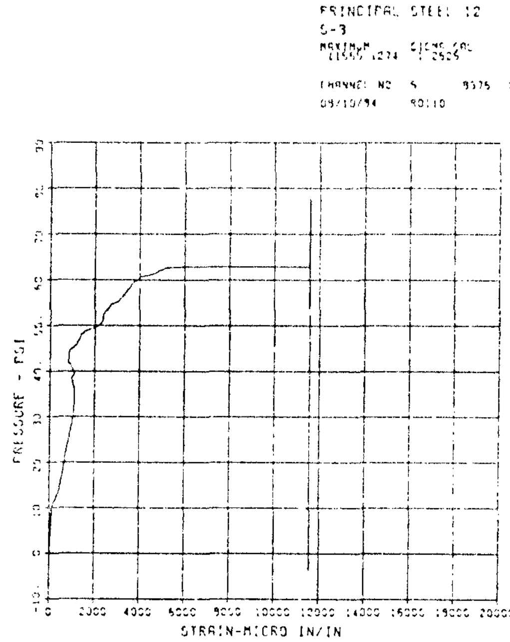
PRINCIPAL STEEL 12
S-3
STRAIN-MICRO IN/IN

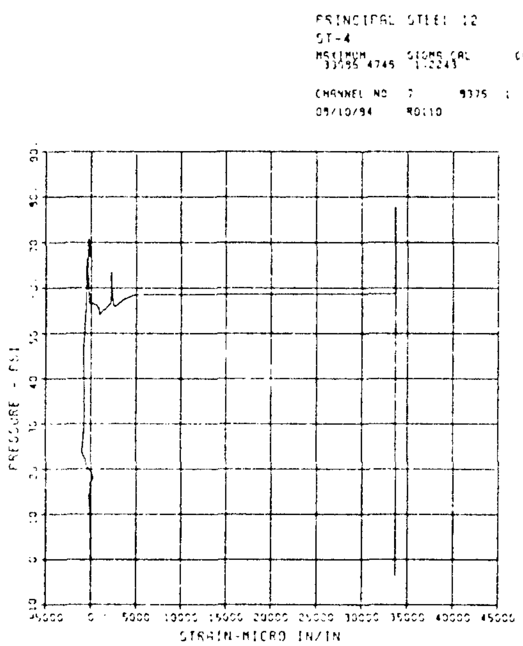
PRINCIPAL STEEL 12
ST-4
CHANNEL NO 7
STRAIN-MICRO IN/IN

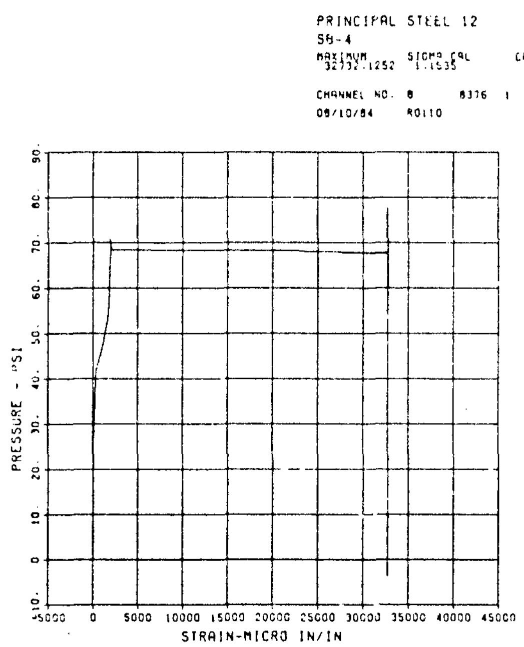
PRINCIPAL STEEL 12
SB-4
MAXIMUM
SIGMA CAL
CAL VAL
CHANNEL NO. 8
08/10/84
PRESSURE - PSI
STRAIN-MICRO IN/IN

PRINCIPAL STEEL 12
ST-5
MAXIMUM -2403.2101 SIGMA CAL 1.5929 CAL VAL 11490.0

CHANNEL NO. 9 8376 1
10/16/84 R04

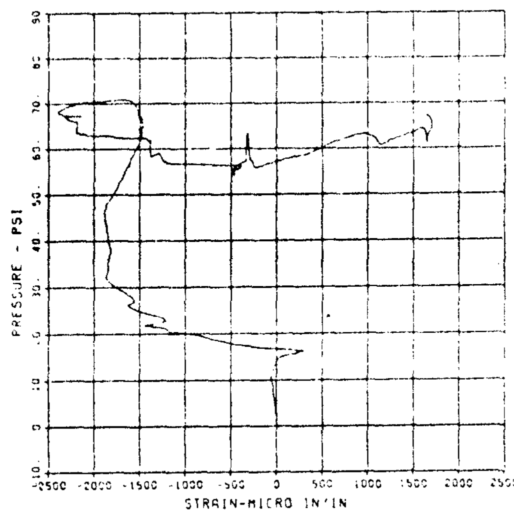

PRINCIPAL STEEL 12
SB-5
MAXIMUM 2035.3494 SIGMA CAL 7.0398 CAL VAL 11480.0

CHANNEL NO. 10 8376 1
10/16/84 R049

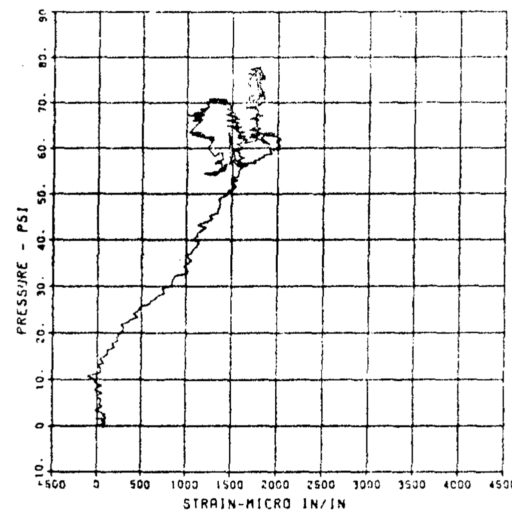

PRINCIPAL STEEL 12
ST-6
MAXIMUM -33174.3408 SIGMA CAL 1.4394 CAL VAL 17090.0

CHANNEL NO. 11 8376 1
08/10/84 R0110

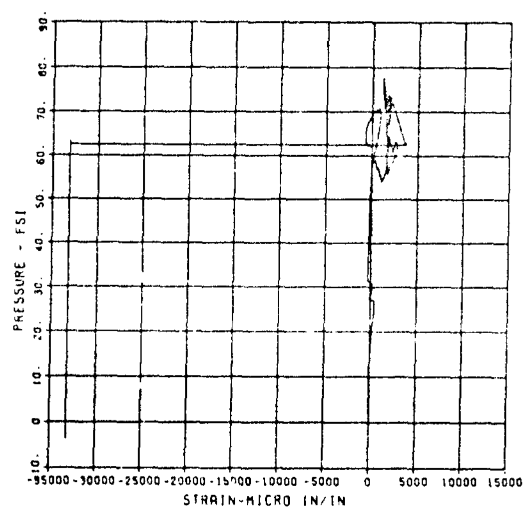

PRINCIPAL STEEL 12
SB-6
MAXIMUM 8737.8182 SIGMA CAL 1.5762 CAL VAL 17090.0

CHANNEL NO. 12 8376 1
08/10/84 R0110

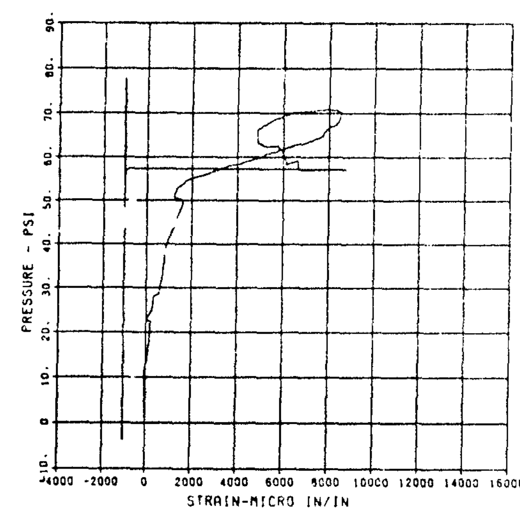

PRINCIPAL STEEL 12
ST-7
MAXIMUM 5421.7911 SIGMA CAL 1.7047 CAL VAL 5760.0
CHANNEL NO. 13 8376 1
10/16/84 [illegible]

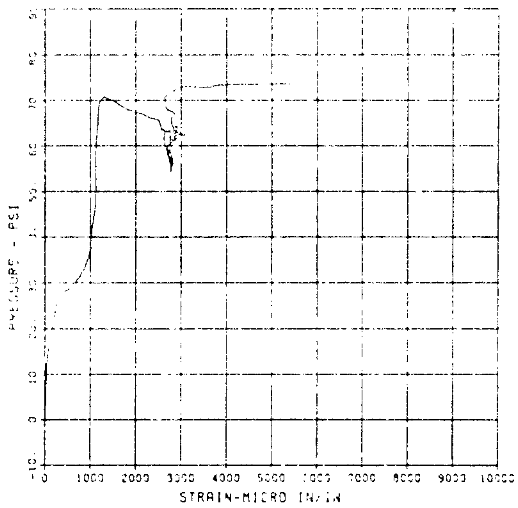

PRINCIPAL STEEL 12
SB-7
MAXIMUM 5667.8422 SIGMA CAL 2.0237 CAL VAL 5760.0
CHANNEL NO. 14 8376 1
10/16/84 R0497

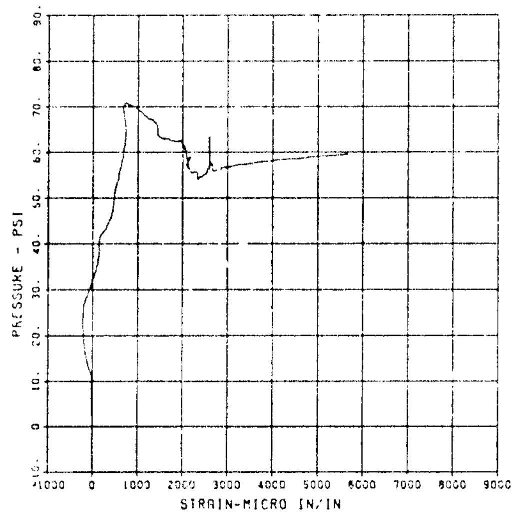

PRINCIPAL STEEL 12
ST-8
MAXIMUM 9173.1997 SIGMA CAL 1.7837 CAL VAL 5760.0
CHANNEL NO. 15 8376 1
08/10/84 R0110

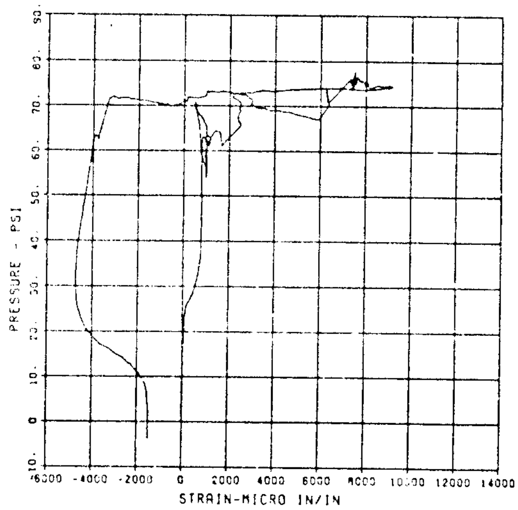

PRINCIPAL STEEL 12
SB-8
8376 2
08/20/84 R0210

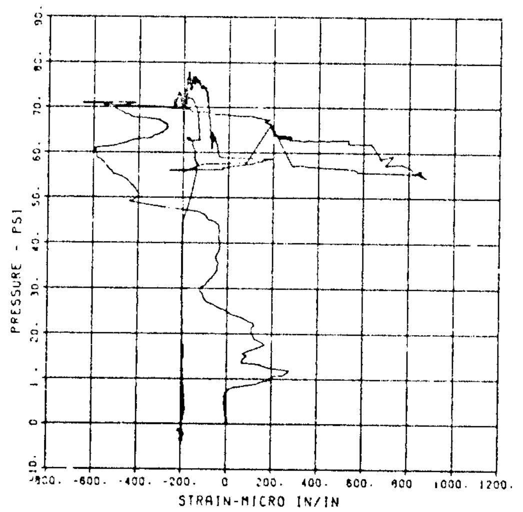

PRINCIPAL STEEL 12
S-9

08/20/94

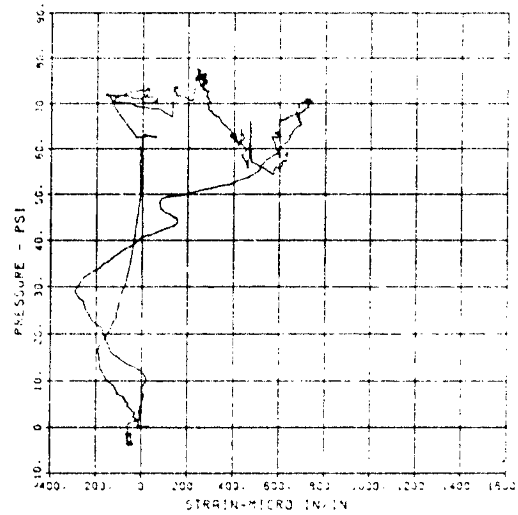

PRINCIPAL STEEL 13
D-1
MAXIMUM SIGMA CAL CAL VAL

CHANNEL NO. 2
06/13/94

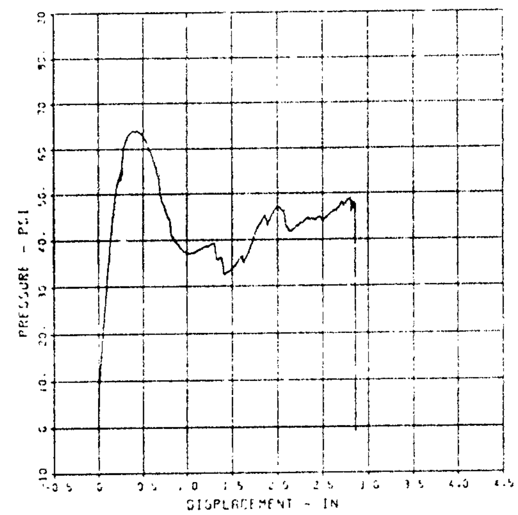

PRINCIPAL STEEL 13
D-2
MAXIMUM SIGMA CAL CAL VAL

CHANNEL NO. 3
06/13/94

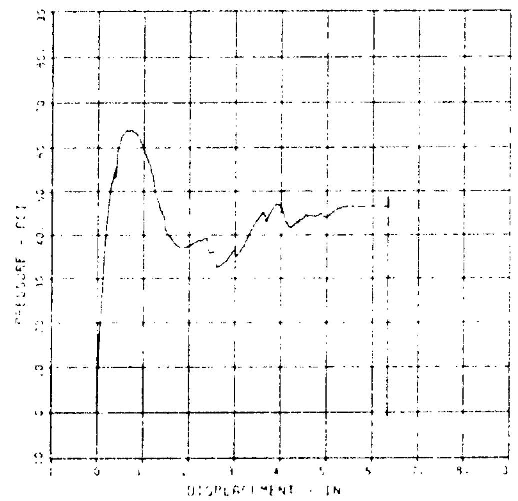

PRINCIPAL STEEL 13
ST-1
MAXIMUM SIGMA CAL CAL VAL

CHANNEL NO. 4
06/13/94

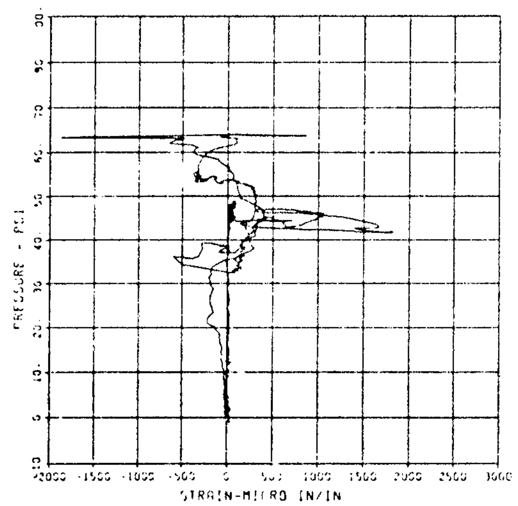

PRINCIPAL STEEL 13
SB-1
MAXIMUM 1934.0457 SIGMA CAL 1.4104 CAL VAL 7090.0
CHANNEL NO 5 5755 1
10/15/84 R0435

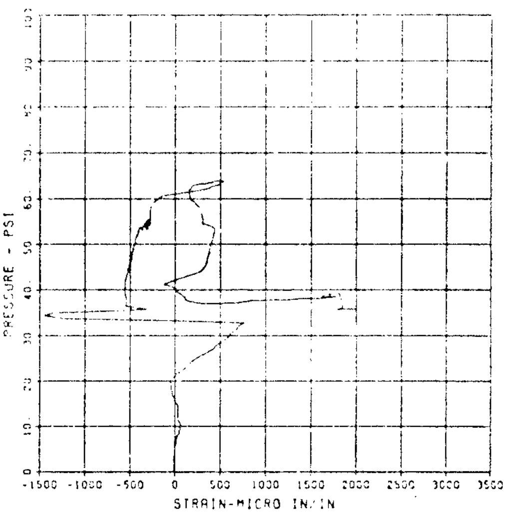

PRINCIPAL STEEL 13
ST-2
MAXIMUM -19257.7990 SIGMA CAL 1.2373 CAL VAL 11490.0
CHANNEL NO 8 5755 1
05/13/94 R0424

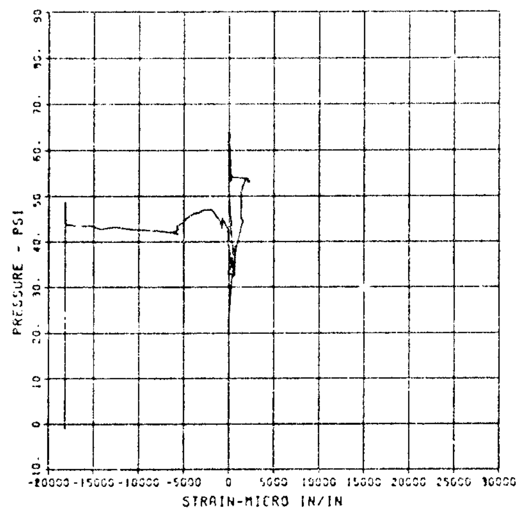

PRINCIPAL STEEL 13
SB-2
MAXIMUM -1113.5432 SIGMA CAL 1.3275 CAL VAL 11490.0
CHANNEL NO 7 5755 1
05/13/94 R0424

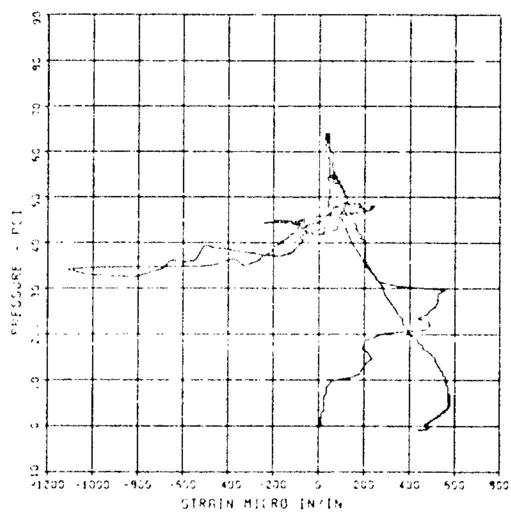

PRINCIPAL STEEL 13
ST-3
MAXIMUM 32549.4157 SIGMA CAL 1.2714 CAL VAL 17030.0
CHANNEL NO. 9 5754 1
05/13/94 R0424

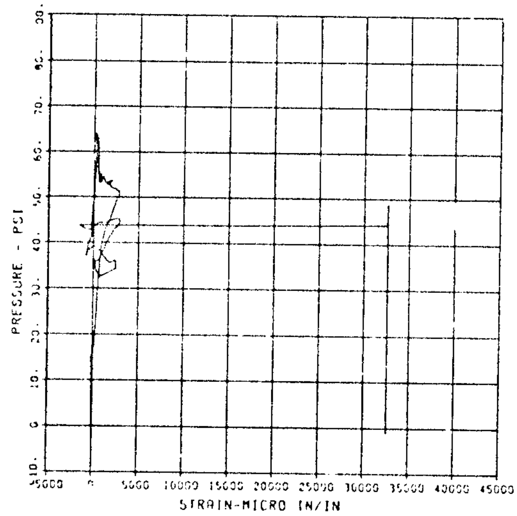

PRINCIPAL STEEL 13
SB-3
MAXIMUM 1500.3252 SIGMA CAL 1.7572 CAL VAL 17030.0
CHANNEL NO 3 5755 1
05/13/94 R0424

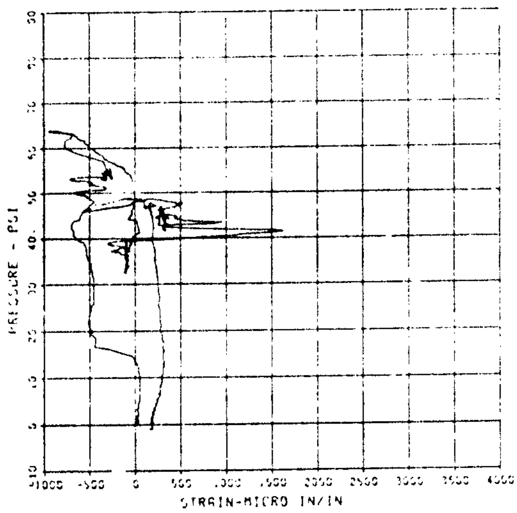

PRINCIPAL STEEL 13
ST-4
MAXIMUM 24553.3933 SIGMA CAL 5.0271 CAL VAL 11450.0
CHANNEL NO 10 5755 1
05/13/94 R0424

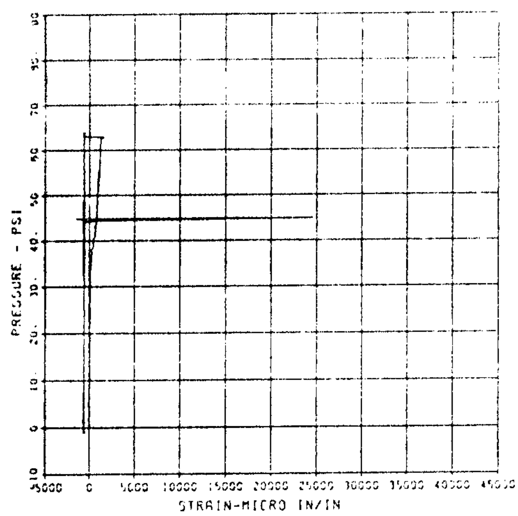

PRINCIPAL STEEL 13
SB-4
MAXIMUM 1207.7515 SIGMA CAL 1.4512 CAL VAL 11450.0
CHANNEL NO. 11 5755 1
05/13/94 R0424

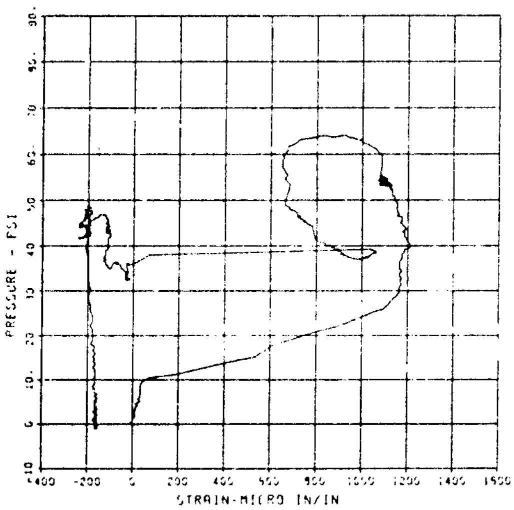

PRINCIPAL STEEL 13
ST-5
MAXIMUM -14350.4494 SIGMA CAL 1.5600 CAL VAL 9550.0
CHANNEL NO. 12 5755 1
05/13/94 R0424

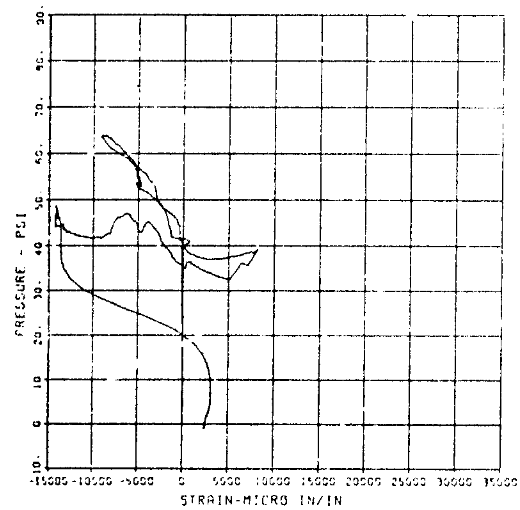

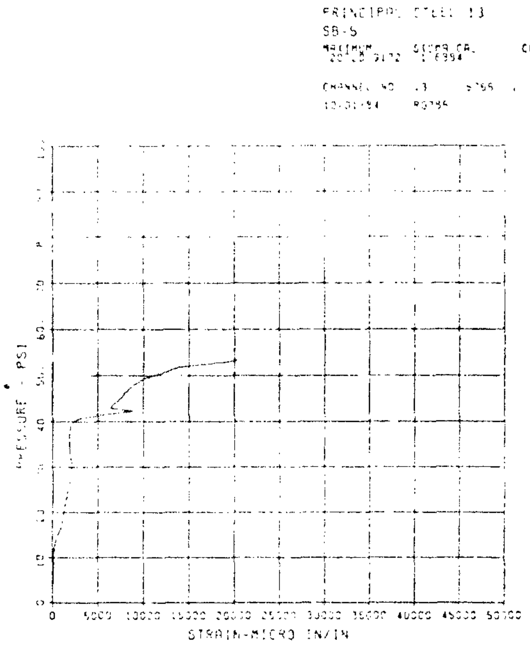
PRINCIPAL STEEL 13
SB-5
PRESSURE - PSI
STRAIN-MICRO IN/IN

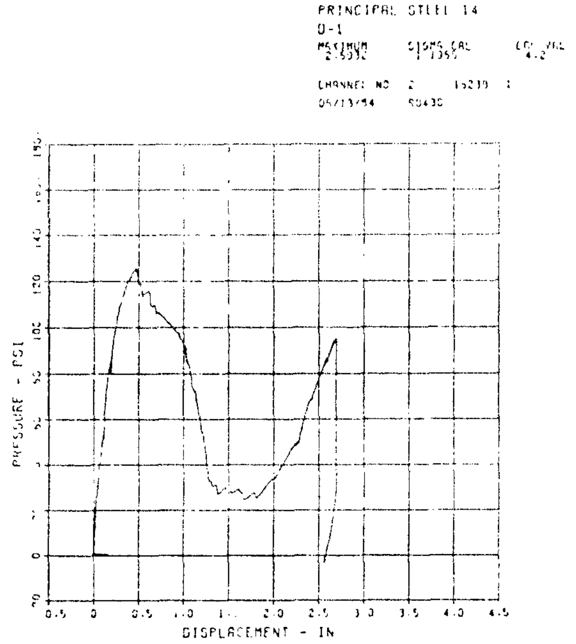
PRINCIPAL STEEL 14
D-1
MAXIMUM
SIGMA CAL
CHANNEL NO 2
05/13/84
PRESSURE - PSI
DISPLACEMENT - IN

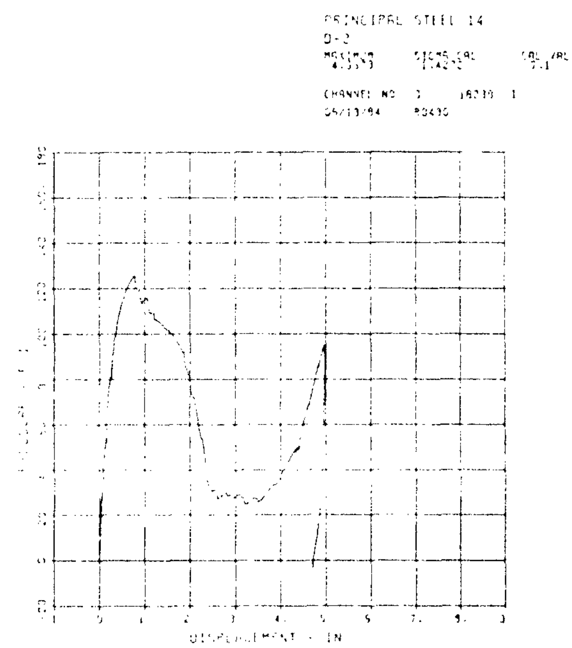
PRINCIPAL STEEL 14
D-2
CHANNEL NO
05/13/84

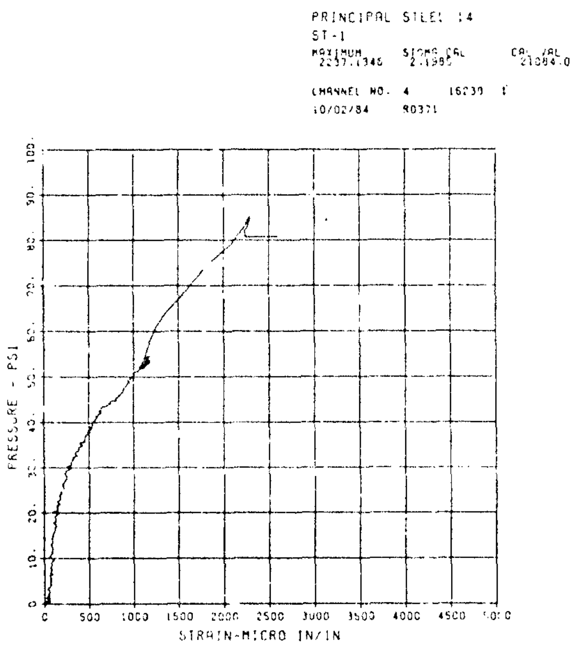
PRINCIPAL STEEL 14
ST-1
MAXIMUM
2237.1346
SIGMA CAL
CAL VAL
21084.0
CHANNEL NO. 4 16239
10/02/84 80371
PRESSURE - PSI
STRAIN-MICRO IN/IN

PRINCIPAL STEEL 14
SB-1
MAXIMUM 20080 CAKI SIGMA CAL 1.3015 CAL VAL 17089.0
CHANNEL NO 5 16239 1
10/02/14 R0371

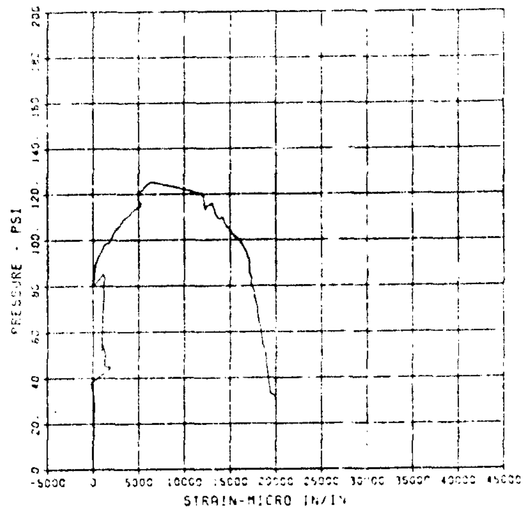

PRINCIPAL STEEL 14
ST-2
MAXIMUM 1236.7355 SIGMA CAL 1.3439 CAL VAL 1493.0
CHANNEL NO. 6 16239 1
05/13/94 R0430

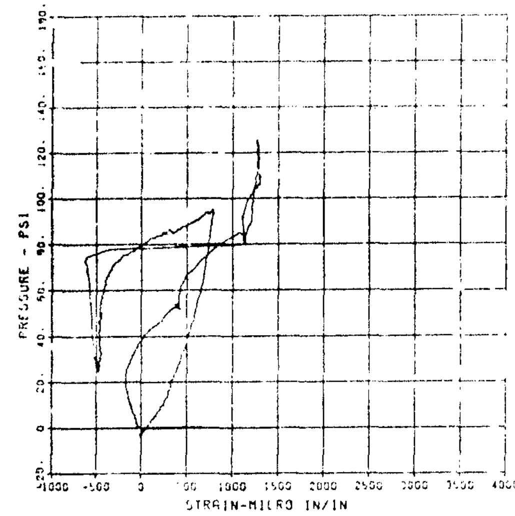

PRINCIPAL STEEL 14
SF-2
MAXIMUM 22435.3457 SIGMA CAL 1.3137 CAL VAL 11493.0
CHANNEL NO. 7 16239 1
05/13/94 R0430

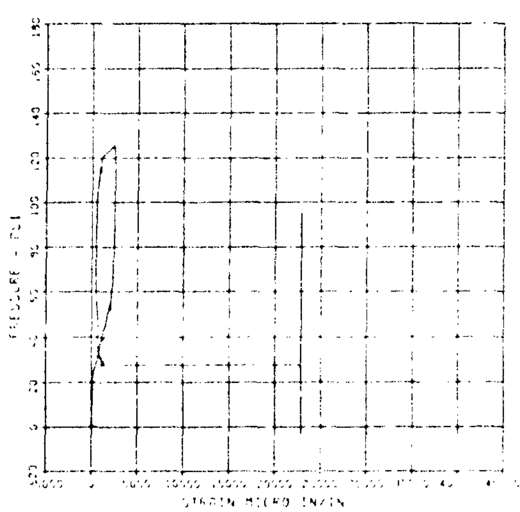

PRINCIPAL STEEL 14
ST-3
MAXIMUM 11217.8192 SIGMA CAL 1.31.2 CAL VAL 979.0
CHANNEL NO 9 19239 1
05/13/94 R0430

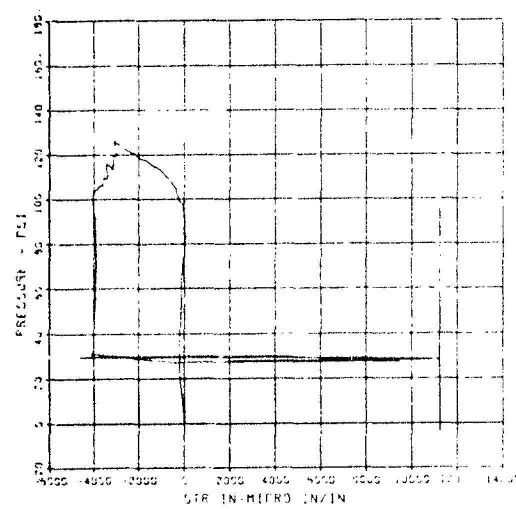

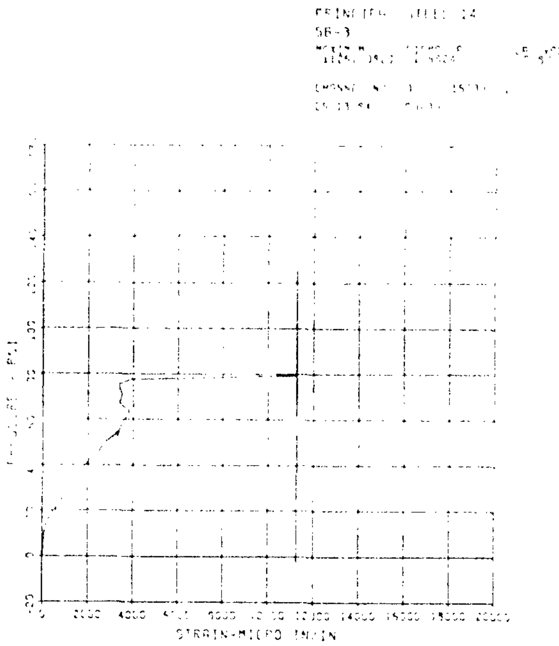
STRAIN-MICRO IN/IN

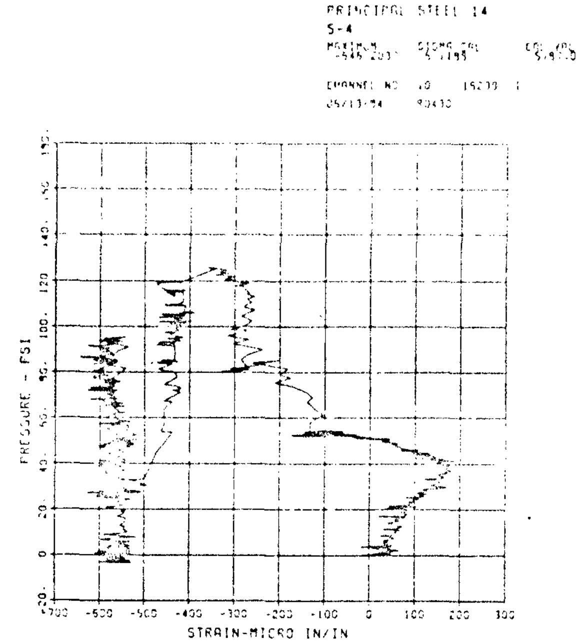
PRINCIPAL STEEL 14
S-4
PRESSURE - PSI
STRAIN-MICRO IN/IN

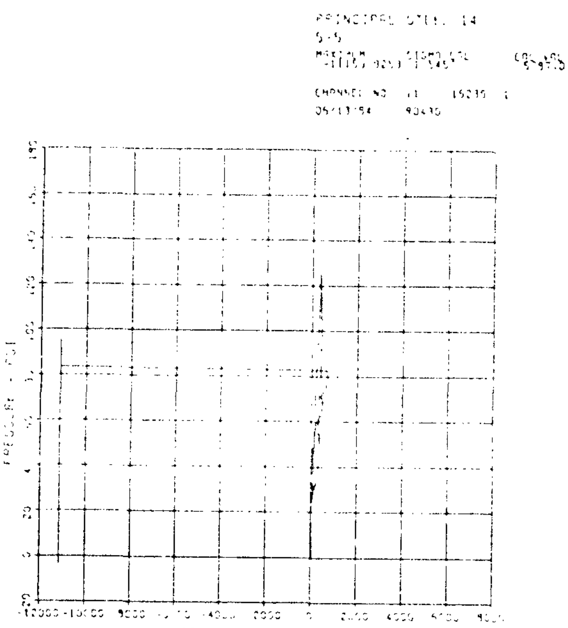
PRINCIPAL STEEL 14
S-5
STRAIN-MICRO IN-IN

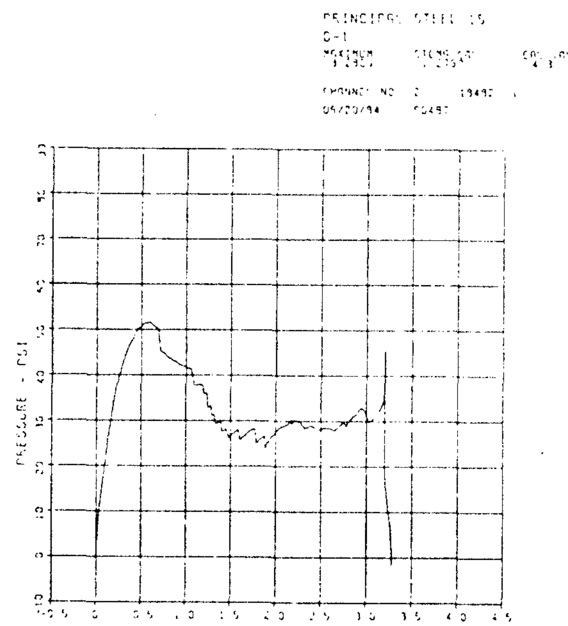
PRINCIPAL STEEL 15
D-1
PRESSURE - PSI
DISPLACEMENT - IN

PRINCIPAL STEEL 15
D-2
MAXIMUM 5.3799 SIGMA CAL 2.4929 CAL VAL
CHANNEL NO 3 19492 1
06/20/94 R0497

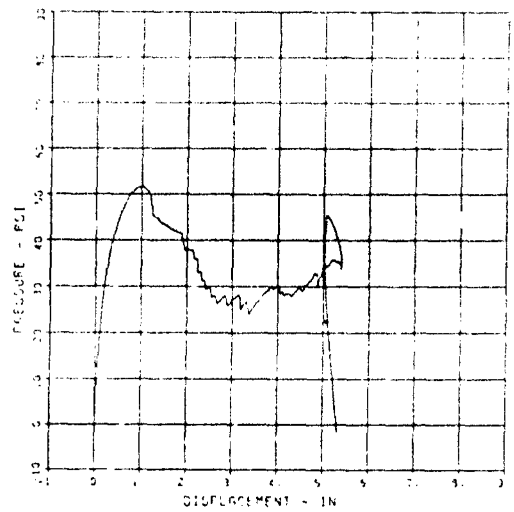

PRINCIPAL STEEL 15
ST-1
MAXIMUM 14019.9793 SIGMA CAL 2.1131 CAL VAL 7100.0
CHANNEL NO 4 19492 1
06/20/94 R0497

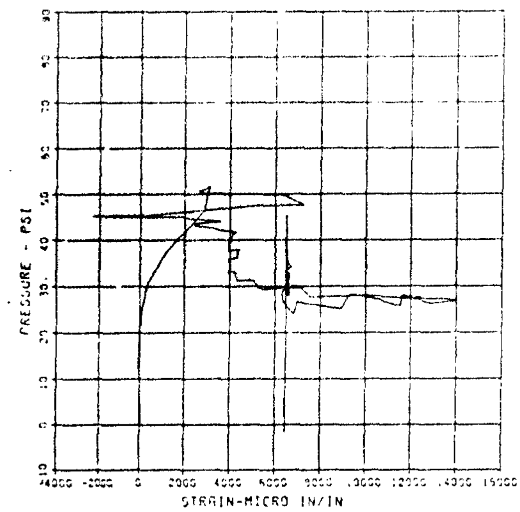

PRINCIPAL STEEL 15
SB-1
MAXIMUM 2293.6932 SIGMA CAL 1.1392 CAL VAL 11500.0
CHANNEL NO 5 19492 1
06/20/94 R0497

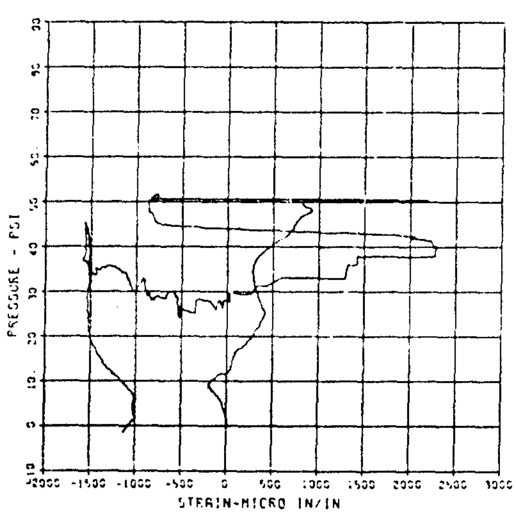

PRINCIPAL STEEL 15
ST-2
MAXIMUM 3905.7763 SIGMA CAL 1.2423 CAL VAL 11500.0
CHANNEL NO 9 19492 1
06/20/94 R0497

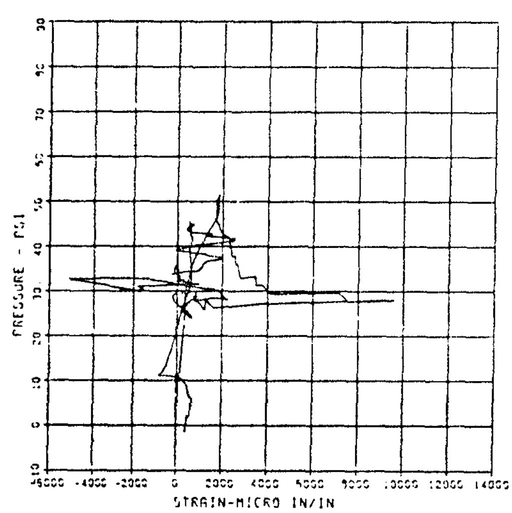

PRINCIPAL STEEL 15
SB-2
MAXIMUM SIGMA CAL CAL VAL

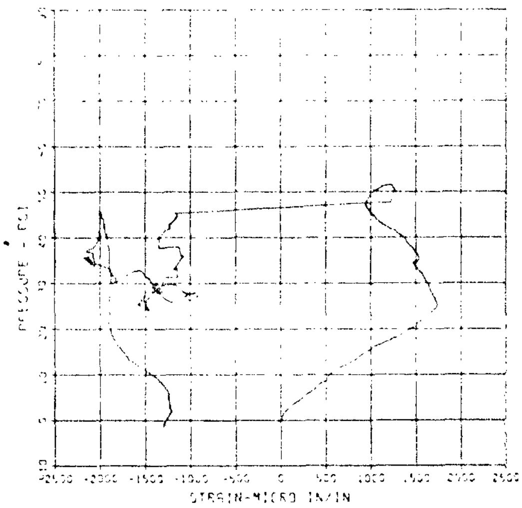

PRINCIPAL STEEL 15
ST-3
MAXIMUM SIGMA CAL CAL VAL
CHANNEL NO 5 19492 1
05/20/94 R0497

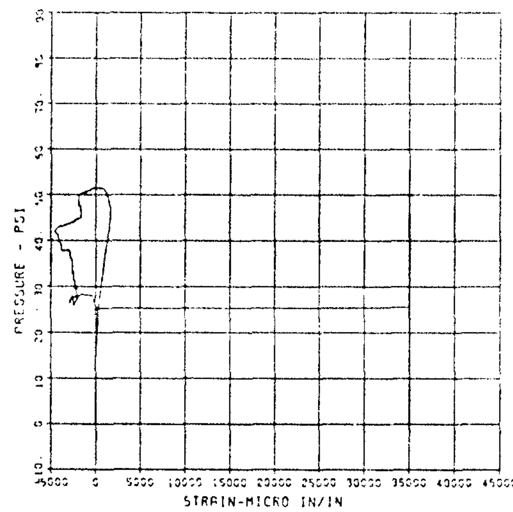

PRINCIPAL STEEL 15
SB-3
MAXIMUM 25114.5971 SIGMA CAL 1.9355 CAL VAL 17100.0
CHANNEL NO. 9 18492 1
10/16/84 R0495

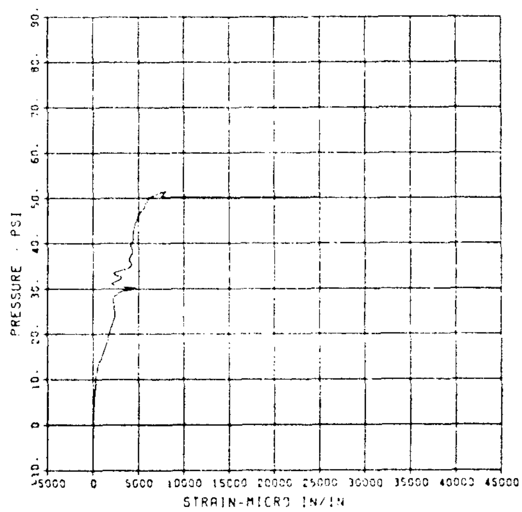

PRINCIPAL STEEL 15
S-4
MAXIMUM SIGMA CAL CAL VAL
CHANNEL NO 10 19492 1
05/20/94 R0497

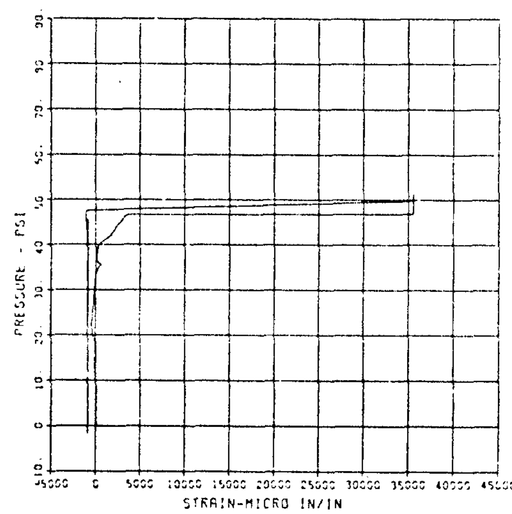

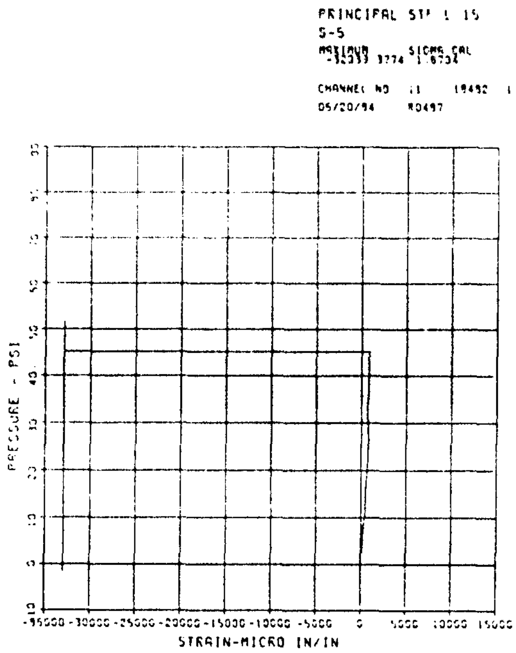
PRINCIPAL
S-5
CHANNEL NO
05/20/94
PRESSURE - PSI
STRAIN-MICRO IN/IN

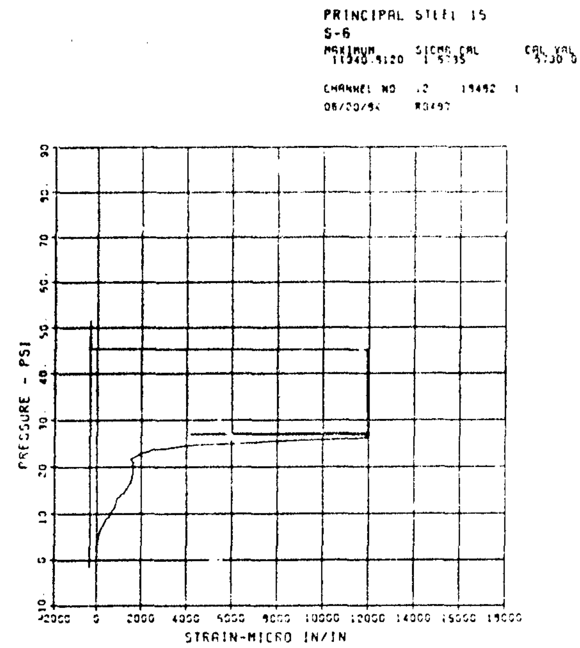
PRINCIPAL
S-6
MAXIMUM
SIGMA CAL
CAL VAL
CHANNEL NO
PRESSURE - PSI
STRAIN-MICRO IN/IN

APPENDIX B

CALCULATION OF CAPACITY IN COMPRESSIVE MEMBRANE REGION

Park's Equations: (See Figures B.1, B.2, and B.3)

$$c' = \frac{h}{2} - \frac{\delta}{4} - \frac{\beta \ell^2}{4\delta}\left(\varepsilon + \frac{2t}{\ell}\right) + \left(\frac{T' - T - C_s' + C_s}{1.7f_c'\beta_1}\right)$$

$$c = \frac{h}{2} - \frac{\delta}{4} - \frac{\beta \ell^2}{4\delta}\left(\varepsilon + \frac{2t}{\ell}\right) - \left(\frac{T' - T - C_s' + C_s}{1.7f_c'\beta_1}\right)$$

Membrane force:

$$N_u = C_c + C_s - T = 0.85f_c'\beta_1 c + C_s - T$$

Moments:

$$M_u = 0.85f_c'\beta_1 c(0.5h - 0.5\beta_1 c) + C_s(0.5h - d') + T(d - 0.5h)$$

$$M_u' = 0.85f_c'\beta_1 c'(0.5h - 0.5\beta_1 c') + C_s'(0.5h - d') + T'(d - 0.5h)$$

Solving for resistance, w , using the virtual work method:

$$\frac{w\ell^2}{8} = M_u' + M_u - N_u s$$

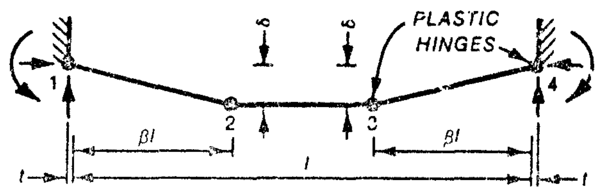

Figure B.1. Plastic hinges of restrained strip.

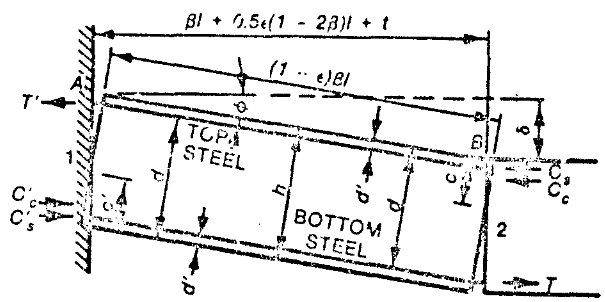

Figure B.2. Portion of strip between Yield Sections 1 and 2.

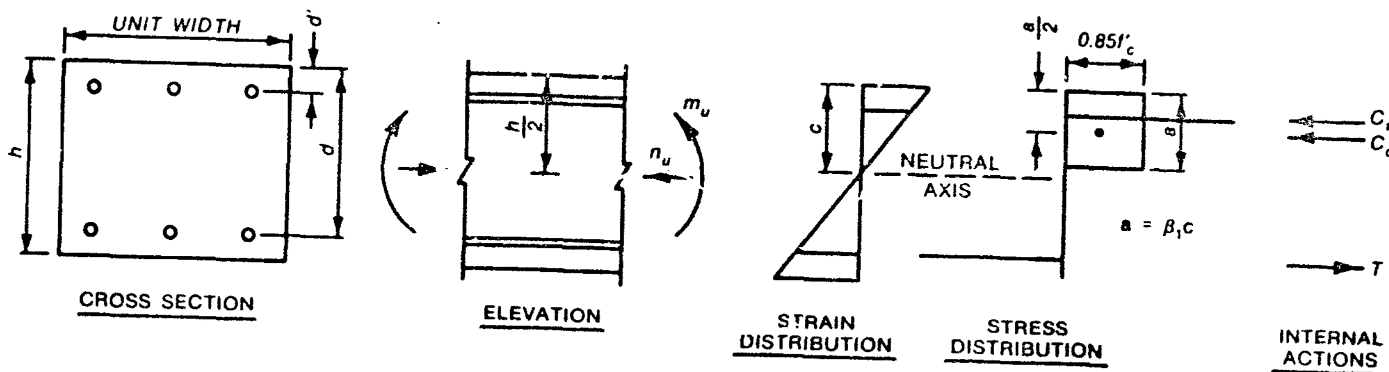

Figure B.3. Conditions at a positive moment yield section.

APPENDIX C

NOTATION

a	Depth of stress block
A_s	Area of tension steel
A'_s	Area of compression steel
c, c'	Distance from compression face of the slab to neutral axis
C_c, C'_c	Concrete compressive force
C_s, C'_s	Force in compression steel
d	Depth from the compression face of the slab to the centroid of the tension steel (effective depth)
d'	Distance from the compression face of the slab to the centroid of the compression steel
f'_c	Compressive strength of concrete
f_y	Yield strength of steel
h	Member thickness
ℓ	Clear span length (Park's notation)
L	Clear span
L/d	Clear span-to-effective depth ratio
L/h	Clear span-to-thickness ratio
M_u	Midspan resisting moment about middepth axis (compressive membrane region)
M'_u	sisting moment at the support about middepth axis (compressive membrane region
N_u	Compressive membrane force
P_B	Ultimate resistance of slab
P_c	Resistance at onset of tensile membrane zone
P_D	Overpressure at incipient collapse
q_{ult}	Ultimate resistance of slab
q_{yl}	Yield-line capacity of slab
t	Support movement
T, T'	Force in Tension steel
T_y/T_x	Ratio of tensile forces in the y and x directions
w	Static collapse load, psi
β	Fraction of clear span length to hinge
β_1	Rectangular stress distribution factor defined by ACI (Reference 14)[1]

[1] References cited in this appendix are included in the References at the end of the main text.

Δ	Midspan deflection
Δ_B	Midspan deflection at ultimate resistance
Δ_c	Midspan deflection at onset of tensile membrane zone
Δ_D	Midspan deflection at incipient collapse
Δ_s	Theoretical deflection at onset of tensile membrane behavior
Δ/L	Ratio of midspan deflection to clear span length
Δ_{ult}	Midspan deflection at ultimate capacity
Δ_{ult}/h	Ratio of deflection at ultimate to slab thickness
ε	Strain
ρ	Tension reinforcement ratio
ρ'	Compression steel ratio

DISTRIBUTION LIST

Director, Federal Emergency Management Agency
ATTN: Mr. Tom Provenzano (25 Cys)
500 C St. SW
Washington, DC 20472

Commander, US Army Engineer District, Wilmington
ATTN: Pat Burns/Library
PO Box 1890
Wilmington, N. C. 28402

Headquarters, Department of Energy
ATTN: Library/G-049 MA-232.2/GTN
Washington, DC 20545

National Bureau of Standards
ATTN: Mr. Samuel Kramer
Dr. Lewis V. Spencer
Washington, DC 20234

Associate Director, Natural Resources and Commercial Services
Office of Science & Technology
ATTN: Mr. Phillip M. Smith
Executive Office Building
Washington, DC 20500

Director, Office of Administration
Program Planning and Control
Department of Housing and Urban Development
ATTN: Mr. Bert Greenglass
Washington, DC 20410

Director, Defense Nuclear Agency
ATTN: SPTD/Mr. Tom Kennedy
STTL/Technical Library
Washington, DC 20305

Director, Defense Intelligence Agency
ATTN: Mr. Carl Wiehle (DB-4C2)
Washington, DC 20301

Assistant Secretary of the Army (R&D)
ATTN: Assistant for Research
Washington, DC 20301

Office, Chief of Engineers, Department of the Army
ATTN: DAEN-RDZ-A
DAEN-ECE-D
Washington, DC 20314

Sandia Corporation
ATTN: Dr. Clarence R. Mehl
Dept. 5230
Box 5800, Sandia Base
Albuquerque, N. Mex. 87115

Director, US Army Engineer Waterways Experiment Station
ATTN: Dr. S. A. Kiger
Mr. Bill Huff
Mr. Stan Woodson
3 cys Library
P. O. Box 631
Vicksburg, Miss. 39180

Defense Technical Information Center
12 cy ATTN: (DTIC-DDAB/Mr. Myer B. Kahn)
Cameron Station
Alexandria, Va. 22314

Commander, US Army Materials and Mechanics Research Center
ATTN: Technical Library
Watertown, Mass. 02172

Command and Control Technical Center
Department of Defense
Room 2E312 Pentagon
Washington, DC 20301

Los Alamos Scientific Laboratory
ATTN: Report Library MS-364
PO Box 1663
Los Alamos, N. Mex. 87544

Director, Ballistic Research Laboratory
ATTN: (DRXBR-TBD/Mr. George Coulter)
Aberdeen Proving Ground, Md. 21005

Commanding Officer, Office of Naval Research
Department of the Navy
Washington DC 20390

Commanding Officer
US Naval Civil Engineering Laboratory
Naval Construction Battalion Center
ATTN: Library (Code L08A)
Port Hueneme, Calif. 93043

Commander, Air Force Weapons Laboratory/SUL
ATTN: Technical Library
Kirtland Air Force Base, N. Mex. 87117

Civil Engineering Center
AF/PRECET
Tyndall AFB, Fla. 32403

University of Florida
Civil Defense Technical Services
College of Engineering
Department of Engineering
Gainesville, Fla. 32601

Technical Reports Library
Kurt F. Wendt Library
College of Engineering
University of Wisconsin
Madison, Wisc. 53706

Agbabian Associates
250 N. Nash Street
El Segundo, Calif. 90245

AT&T Bell Laboratories
ATTN: Mr. E. Witt
Whippany, N. J. 07981

James E. Beck & Associates
4216 Los Palos Avenue
Palo Alto, Calif. 94306

Chamberlain Manufacturing Corp.
GARD, Inc.
7449 N. Natchez Avenue
Niles, Ill. 60648

IIT Research Institute
ATTN: Mr. A. Longinow
10 West 35th Street
Chicago, Ill. 60616

H. L. Murphy Associates
Box 1727
San Mateo, Calif. 94401

RAND Corporation
ATTN: Document Library
1700 Main Street
Santa Monica, Calif. 90401

Research Triangle Institute
ATTN: Mr. Edward L. Hill
PO Box 12194
Research Triangle Park, N. C. 27709

Scientific Services, Inc.
517 East Bayshore Drive
Redwood City, Calif. 94060

US Army Engineer Division, Huntsville
ATTN: Mr. Paul Lahoud (10 cys)
PO Box 1600, West Station
Huntsville, AL 35807

EFFECTS OF REINFORCEMENT CONFIGURATION ON RESERVE CAPACITY OF CONCRETE SLABS, Unclassified, US Army Engineer Waterways Experiment Station, August 1985, 115 pp.

Fifteen one-way reinforced concrete slabs were statically tested under uniform surface pressure either to failure, or to deflections that exceeded 17 to 24 percent of slab clear span. The main objective was to determine principal reinforcement configurations that would enhance tensile membrane behavior at large deflections. Each slab had a clear span of 24 inches and was 2-5/16 inches thick. Grade-60 reinforcement and 4,000-psi concrete were used. The total amount of principal reinforcement was about the same in every test, but the percentages of reinforcement in tension and compression zones were varied. The slabs were supported in a reaction structure and restrained at the supports.

A modified three-hinged mechanism was formed, and rupture of reinforcement prohibited the development of pure tensile membrane behavior in most of the slabs. Posttest analysis applying tensile membrane theory agreed with the experimental tensile membrane slope, when the area of ruptured reinforcement was deleted. Based on these test results, principal reinforcement details were recommended for a blast shelter roof slab design.

EFFECTS OF REINFORCEMENT CONFIGURATION ON RESERVE CAPACITY OF CONCRETE SLABS, Unclassified, US Army Engineer Waterways Experiment Station, August 1985, 115 pp.

Fifteen one-way reinforced concrete slabs were statically tested under uniform surface pressure either to failure, or to deflections that exceeded 17 to 24 percent of slab clear span. The main objective was to determine principal reinforcement configurations that would enhance tensile membrane behavior at large deflections. Each slab had a clear span of 24 inches and was 2-5/16 inches thick. Grade-60 reinforcement and 4,000-psi concrete were used. The total amount of principal reinforcement was about the same in every test, but the percentages of reinforcement in tension and compression zones were varied. The slabs were supported in a reaction structure and restrained at the supports.

A modified three-hinged mechanism was formed, and rupture of reinforcement prohibited the development of pure tensile membrane behavior in most of the slabs. Posttest analysis applying tensile membrane theory agreed with the experimental tensile membrane slope, when the area of ruptured reinforcement was deleted. Based on these test results, principal reinforcement details were recommended for a blast shelter roof slab design.

EFFECTS OF REINFORCEMENT CONFIGURATION ON RESERVE CAPACITY OF CONCRETE SLABS, Unclassified, US Army Engineer Waterways Experiment Station, August 1985, 115 pp.

Fifteen one-way reinforced concrete slabs were statically tested under uniform surface pressure either to failure, or to deflections that exceeded 17 to 24 percent of slab clear span. The main objective was to determine principal reinforcement configurations that would enhance tensile membrane behavior at large deflections. Each slab had a clear span of 24 inches and was 2-5/16 inches thick. Grade-60 reinforcement and 4,000-psi concrete were used. The total amount of principal reinforcement was about the same in every test, but the percentages of reinforcement in tension and compression zones were varied. The slabs were supported in a reaction structure and restrained at the supports.

A modified three-hinged mechanism was formed, and rupture of reinforcement prohibited the development of pure tensile membrane behavior in most of the slabs. Posttest analysis applying tensile membrane theory agreed with the experimental tensile membrane slope, when the area of ruptured reinforcement was deleted. Based on these test results, principal reinforcement details were recommended for a blast shelter roof slab design.

EFFECTS OF REINFORCEMENT CONFIGURATION ON RESERVE CAPACITY OF CONCRETE SLABS, Unclassified, US Army Engineer Waterways Experiment Station, August 1985, 115 pp.

Fifteen one-way reinforced concrete slabs were statically tested under uniform surface pressure either to failure, or to deflections that exceeded 17 to 24 percent of slab clear span. The main objective was to determine principal reinforcement configurations that would enhance tensile membrane behavior at large deflections. Each slab had a clear span of 24 inches and was 2-5/16 inches thick. Grade-60 reinforcement and 4,000-psi concrete were used. The total amount of principal reinforcement was about the same in every test, but the percentages of reinforcement in tension and compression zones were varied. The slabs were supported in a reaction structure and restrained at the supports.

A modified three-hinged mechanism was formed, and rupture of reinforcement prohibited the development of pure tensile membrane behavior in most of the slabs. Posttest analysis applying tensile membrane theory agreed with the experimental tensile membrane slope, when the area of ruptured reinforcement was deleted. Based on these test results, principal reinforcement details were recommended for a blast shelter roof slab design.